

UNCLASSIFIED



AD NUMBER

**AD-486 295**

NEW LIMITATION CHANGE

TO

**DISTRIBUTION STATEMENT - A**

Approved for public release;  
distribution is unlimited

**LIMITATION CODE: 1**

FROM

**No Prior DoD Distr Scty Cntrl St'mt Assigned**

AUTHORITY

AFFDL, Oct 12, 1970.

19990303142

THIS PAGE IS UNCLASSIFIED

AFFDL-TR-65-220

486295

## **MATRIX ANALYSIS METHODS FOR ANISOTROPIC INELASTIC STRUCTURES**

**W. R. JENSEN  
W. E. FÁLBY  
N. PRINCE**

**GRUMMAN AIRCRAFT ENGINEERING CORPORATION**

**TECHNICAL REPORT AFFDL-TR-65-220**

**APRIL 1966**

**AIR FORCE FLIGHT DYNAMICS LABORATORY  
RESEARCH AND TECHNOLOGY DIVISION  
AIR FORCE SYSTEMS COMMAND  
WRIGHT-PATTERSON AIR FORCE BASE, OHIO**

**This document is subject to special export controls and each transmittal to foreign governments or foreign nationals may be made only with prior approval of AFFDL (FDTR), Wright-Patterson Air Force Base, Ohio 45433.**

19990303/42

## NOTICES

When Government drawings, specifications, or other data are used for any purpose other than in connection with a definitely related Government procurement operation, the United States Government thereby incurs no responsibility nor any obligation whatsoever; and the fact that the Government may have formulated, furnished, or in any way supplied the said drawings, specifications, or other data, is not to be regarded by implication or otherwise as in any manner licensing the holder or any other person or corporation, or conveying any rights or permission to manufacture, use, or sell any patented invention that may in any way be related thereto.

Copies of this report should not be returned to the Research and Technology Division unless return is required by security considerations, contractual obligations, or notice on a specific document.

# **MATRIX ANALYSIS METHODS FOR ANISOTROPIC INELASTIC STRUCTURES**

**W. R. JENSEN  
W. E. FALBY  
N. PRINCE**

This document is subject to special export controls and each transmittal to foreign governments or foreign nationals may be made only with prior approval of AFFDL (FDTR), Wright-Patterson Air Force Base, Ohio 45433.

## FOREWORD

This report, prepared by the Grumman Aircraft Engineering Corporation, Bethpage, New York, covers work performed under Air Force Contract AF 33(615)-2260. The contract was sponsored by the Air Force Flight Dynamics Laboratory of the Research and Technology Division, Air Force Systems Command, Wright-Patterson Air Force Base, Ohio. It was accomplished under Project No. 1467, "Structural Analysis Methods," Task 146701, "Stress-Strain Analysis Methods for Structures Exposed to Creep Environment." The work was administered by Mr. Laszlo Berke, *FDTR*, Project Engineer. The report covers work conducted from January 1965 to October 1965. The manuscript was released by the authors in February 1966 for publication as an *RTD* Technical Report.

The investigation was supervised by Dr. Warner Lansing, Chief of Structural Mechanics. The computer programming was carried out by Mr. Albert Davidson. Some preliminary elastic analysis data were automatically generated by the *ASTRAL*, Automated STRuctural AnaLysis program developed by Mr. Philip Mason.

The work of Dr. T. J. Mentel on the evaluation of procedures for carrying out inelastic analyses, and on the formulation of the biaxial stress procedure is also acknowledged. His "Instability Analysis of the Constant Stress and Constant Strain Methods" is reproduced from Reference 6 in Appendix III.

Acknowledgements are made to Drs. Gabriel Isakson and Harry Armen of the Grumman Research Department for their suggestions and review of certain portions of this work.

All computations were carried out at the Grumman Computing Center.

This technical report has been reviewed and is approved.



FRANCIS J. JANIK, JR.  
Chief, Theoretical Mechanics Branch  
Structures Division

## ABSTRACT

Most aerospace structural materials exhibit some degree of anisotropic strain hardening. During the past few years, several methods have appeared in the literature for introducing inelastic isotropic material behavior effects into existing matrix analysis procedures using the incremental theory of plasticity. A review is presented of these methods and a step-by-step routine known as the "constant strain" method is selected for the development of an anisotropic inelastic procedure.

A simple truss with one redundant is used to indicate the basic ideas of the approach. Then the procedure is generalized to the more important case of biaxially stressed structures. Nodal stresses are evaluated step-wise for increasing load through the use of an influence coefficient equation. The inelastic (plastic and creep) strains at one load level are used as initial strains at the subsequent level to account for nonlinear effects. The anisotropic behavior is considered by using a proposed extension of Hu's strain hardening theory.

Several analyses of an aluminum alloy (2024-T4) shear lag structure, which has been tested previously for the Air Force, are carried out, first assuming isotropic and then anisotropic material properties. The correlation between test results and those predicted by isotropic theory is reasonably good. The anisotropic analysis gives predicted results which are in slightly more consistent agreement with the test data.

The procedure is also modified to give an isotropic deformation theory solution, which produces numerical results in a much shorter computer time than required for the incremental theory solution. In the case of the shear lag structure investigated, the results by the two theories are in very close agreement.

Creep test results of an 1100-F aluminum shear lag structure are also available. An analysis of this structure by the proposed incremental method is carried out and its predictions too are in reasonably good agreement with the test data. The 1100-F material is very nearly isotropic and no testing of structures exhibiting anisotropic creep is known to have been performed. Hence the anisotropic creep capability of the proposed method cannot be checked out against tests at this time. A sample calculation is nevertheless carried out for a hypothetical material having this characteristic.

The approach presented, which is simple in concept and execution, is found to be a reasonably good phenomenological model of an exceedingly complex physical problem. The accompanying digital computer program is believed to be very versatile, and well suited for the inclusion of any other types of material nonlinearity that may be of interest.

## TABLE OF CONTENTS

SECTION		PAGE
I	INTRODUCTION	1
II	INELASTIC MATRIX METHODS	3
	A. Formulation	3
	B. Example Problem	4
	C. Step-by-Step Methods	6
	D. Constant Stress Method	6
	E. Constant Strain Method	7
III	ISOTROPIC ELASTIC-PLASTIC ANALYSES	8
	A. Biaxial Theory	8
	B. Determination of Calculation Step Size	11
	C. Description of Shear Lag Structure	11
	D. Elastic Shear Lag Structure Analysis	12
	E. Flow Theory Shear Lag Structure Analysis	12
	F. Deformation Theory Analysis	13
IV	ISOTROPIC ELASTIC-PLASTIC-CREEP ANALYSIS	15
	A. Introduction to Creep Theory	15
	B. Creep Theory Details	15
	C. Description of Structure and Tests	16
	D. Results of Creep Shear Lag Analysis	17
V	ANISOTROPIC ELASTIC-PLASTIC ANALYSIS	19
	A. Anisotropy in Structures	19
	B. Hu's Strain Hardening Theory	19
	C. Extension of Hu's Theory	22
	D. Anisotropic Theory Details	23
	E. Rotation of Axes of Anisotropy	24
	F. Anisotropic Analysis of Shear Lag Structure	25
	G. Discussion of Results	27
VI	ANISOTROPIC ELASTIC-PLASTIC-CREEP ANALYSIS	29
	A. Anisotropic Creep Theory	29
	B. Sample Problem	29
VII	CONCLUSIONS	31
VIII	FIGURES	33

# TABLE OF CONTENTS (continued)

APPENDIX		PAGE
I	ELASTIC ANALYSIS OF SHEAR LAG STRUCTURE	61
	A. Idealization of Shear Lag Structure	61
	B. Force Method	61
	C. Stiffness Method	61
	D. Comparison of Elastic Results and Perspective	62
II	POISSON'S RATIO EFFECT	63
III	INSTABILITY ANALYSIS OF THE CONSTANT STRESS AND CONSTANT STRAIN METHODS	65
IV	ROTATION OF AXES OF ANISOTROPY	72
V	INELASTIC MATRIX COMPUTER PROGRAM	75
	A. Program Description	75
	B. Symbols and Format of Data Cards	77
	C. Anisotropic Parameter Matrices	81
	D. Restart Procedure	81
	E. Time Estimates	81
	F. Sample Data Form	82
	G. Flow Charts	83
	H. Fortran Program	92
VI	STRESS DISTRIBUTIONS DUE TO UNIT INITIAL STRAINS	115
	A. Force Method	115
	B. Stiffness Method	119
	REFERENCES	123



# LIST OF ILLUSTRATIONS

FIGURE	TITLE	PAGE
1	Truss Structure	34
2	Constant Stress Method	34
3	Constant Strain Method	34
4	Results of Constant Stress Method for Bar No. 3 of Truss	35
5	Results of Constant Strain Method for Bar No. 3 of Truss	35
6	Shear-Lag Specimen Designated SLS1 - From Air Force Report No. RTD-TDR-63-4032; 2024-T4 Aluminum Alloy (1100-F Specimen Similar)	36
7	Stiffness Method Idealization	36
8	Force Method Idealization	36
9	Typical Elements of Force Idealization	37
10	Typical Elements of Stiffness Idealization	37
11	2024-T4 Aluminum Alloy Stress-Strain Data and Curve R02M	38
12	Comparison of Predicted Effective Stress-Strain Relationship with R02M at (0, 0) for Various Load Increments	38
13	Instrumentation of 2024-T4 Aluminum Alloy Specimen	39
14	Elastic Strains Along x-Axis for $P = 1 \text{ lb}$	40
15	Elastic Strains Along $x = 0.8125 \text{ in.}$ for $P = 1 \text{ lb}$	40
16	Strains Along x-Axis for $P = 11,600 \text{ lb}$ and $\Delta P = 5 \text{ lb}$	41
17	Strains Along $x = 0.8125 \text{ in.}$ for $P = 11,600 \text{ lb}$ and $\Delta P = 5 \text{ lb}$	41
18	Strains Along x-Axis for $P = 14,600 \text{ lb}$ and $\Delta P = 5 \text{ lb}$	42
19	Strains Along $x = 0.8125 \text{ in.}$ for $P = 14,600 \text{ lb}$ and $\Delta P = 5 \text{ lb}$	42
20	Strains Along x-Axis for $P = 16,760 \text{ lb}$ , and $\Delta P = 5 \text{ lb}$	43
21	Strains Along $x = 0.8125 \text{ in.}$ for $P = 16,760 \text{ lb}$ and $\Delta P = 5 \text{ lb}$	43

# LIST OF ILLUSTRATIONS (continued)

FIGURE	TITLE	PAGE
22	Elastic-Plastic Strains at (0, 0) for Several Assumed Stress-Strain Curves	44
23	The Strain Hardening Rule	45
24	1100-F Aluminum Time-Dependent Behavior and Fitted Curves (Reference 7)	46
25	1100-F Aluminum Stress-Strain Data at Room Temperature and at 206°C, for Time $t = 0.00$	47
26	Location of Strain Gages on 1100-F Specimen (Reference 7)	47
27	Strains Along x-Axis for $P = 1600$ lb and $t = 0.06$ hr	48
28	Strains Along $x = 1$ in. for $P = 1600$ lb and $t = 0.06$ hr	48
29	Strains Along x-Axis for $P = 2020$ lb and $t = 1.10$ hr	49
30	Strains Along $x = 1$ in. for $P = 2020$ lb and $t = 1.10$ hr	49
31	Strains Along x-Axis for $P = 2020$ lb and $t = 3.0$ hr	50
32	Strains Along $x = 1$ in. for $P = 2020$ lb and $t = 3.0$ hr	50
33	Effective Stress vs Strain at Center Node	51
34	Total (Elastic, Plastic and Creep) Strains at Center of Specimen (Gage 1) for $P = 1600$ lb to Time 1 hr, then $P = 2020$ lb to Time 3 hr	52
35	Total (Elastic, Plastic and Creep) Strains at (1.0 in., 3.0 in.) (Gage 8) for $P = 1600$ lb to Time 1 hr, then $P = 2020$ lb to Time 3 hr	53
36	Typical Uniaxial Stress vs Plastic Work, $w$ , Plot	54
37	Assumed Effective Stress ( $y-y$ ) Curve, Calculated $x-x$ Curves and Test Data	55
38	Node Strains at (0, 0) - Isotropic and Anisotropic Analysis	56

# LIST OF ILLUSTRATIONS (continued)

FIGURE	TITLE	PAGE
39	Strains Along x-Axis for P = 16,760 lb - Isotropic and Anisotropic Analyses	57
40	Strains Along x = 0.8125 in. for P = 16,760 lb - Isotropic and Anisotropic Analyses	57
41	Strains Along x-Axis for P = 2020 lb and t = 3.0 hr - Isotropic and Anisotropic Analyses	58
42	Strains Along x = 1 in. for P = 2020 lb and t = 3.0 hr - Isotropic and Anisotropic Analyses	58
43	Elastic Stress Distribution Along x-Axis	59
44	Elastic Stress Distribution Along x = 0.8125 in.	60

# SYMBOLS

$[ ]$	Rectangular matrix
$\{ \}$	Column matrix
$q_1$	Member load, any load acting directly on a member
$\sigma_u$	$u^{th}$ ordinary stress component (normal or shear) at a node point
$\sigma_{3N-2}, \sigma_{3N-1}, \sigma_{3N}$	The normal stress components and shear stress component at node N - another designation for $\sigma_u$
$\bar{\sigma}_N$	Effective stress at node N
$\bar{\sigma}_*^N$	Relaxed effective stress at node N
$\sigma_0$	Reference stress in Ramberg-Osgood Equation
$\Gamma_{um}$	$u^{th}$ stress component in linear redundant structure due to the $m^{th}$ unit applied load
$\Gamma_{uv}$	$u^{th}$ stress component in linear redundant structure due to the $v^{th}$ unit initial strain
$\Gamma_{im}$	$i^{th}$ member load in the redundant structure due to $m^{th}$ applied load
$\Gamma_{ij}$	$i^{th}$ member load in the redundant structure caused by a unit initial strain at the $j^{th}$ member load
$P_m$	$m^{th}$ applied load
$\epsilon_v$	$v^{th}$ component of initial strain
$\epsilon(p)_v$	$v^{th}$ component of plastic strain
$\epsilon(c)_v$	$v^{th}$ component of creep strain
$\bar{\epsilon}(p)_N$	Effective plastic strain at node N
$\bar{\epsilon}(c)_N$	Effective creep strain at node N
$\epsilon$	Total (elastic, plastic, and creep) strain component
$\epsilon_{xy}$	Engineering shear strain
$\xi$	Error
$E$	Young's modulus

$T$	Temperature
$t^*$	Equivalent time at start of creep cycle calculation
$\Delta t$	Cycle duration (elapsed time)
$\alpha, \beta, \gamma$	Material constants in creep strain equation
$\alpha_{ij}$	Subscripted anisotropic parameters
$\Delta$	Increment (prefix)
$n, \theta$	Nonlinear parameters in Ramberg-Osgood equation
$k$	Cycle designation, superscript
$N$	Nodal index
$u, v$	Nodal stress component or strain component index, related to the nodal index as indicated in equation
$Y_{ij}$	Simple directional characteristic stress
$\sigma_{xx}, \sigma_{yy}$	Uniaxial stress in the x-x, y-y direction
$\epsilon_{xx}, \epsilon_{yy}$	Plastic strain in the x-x, y-y direction due to uniaxial x-x, y-y stress
$\sigma_{xy}$	Shear stress in x-y plane
$\epsilon_{xy}$	Shear strain in x-y plane

## SECTION I

### INTRODUCTION

With the introduction of high-speed, large-capacity, digital computers, a number of investigators (References 1,4,7) have adapted essentially linear matrix analysis methods to the solution of redundant structures where nonlinear material plasticity and creep properties are considered. These methods have been either iterative or non-iterative step-by-step numerical procedures.

The present work is an effort to explore, revise, and extend the matrix method of analysis in order to apply it to a range of practical aerospace structural problems exhibiting inelastic isotropic or inelastic anisotropic material behavior. Thus, the intent is to concentrate upon methods which are able to predict inelastic strain distributions in irregular idealized structures in a biaxial stress state where materials exhibit strain hardening and creep properties representative of those employed in aerospace construction.

A discussion of complete load reversal, although desirable for plastic fatigue studies, is not included because the theoretical foundation for such a procedure is apparently not yet fully developed. The present formulation of elastic, plastic and creep loading, followed by elastic unloading, while restrictive, is nevertheless of practical interest.

Of the proposed analytical methods, one by Denke (Reference 1) has developed naturally from the matrix force method of analysis and consists of including nonlinear plastic and creep terms in the equations for the gaps at those cuts which are required to make the structure statically determinate. The redundant forces, required to close the gaps and make the structure continuous, are obtained by solving these nonlinear equations by a Newton-Raphson procedure.

A second method reported by Kobayashi and Weikel (Reference 2) has been developed from the direct stiffness method. Here, forces occurring as a consequence of the inelastic effects are included in the nodal force equations. The nodal displacements (or displacement rates, where creep is considered) obtained by solving these equations impose equilibrium at the nodes under the action of internal loads, surface tractions, and prescribed displacements.

When the inelastic effects are accounted for by a flow (or incremental) theory, the deformation is an accumulation of increments each governed by the prevailing stress. Thus, when either of the methods just described is used, one must obtain (for the governing equations) a series of solutions, with one solution corresponding to each load increment. This requires a considerable amount of computer time even for medium-sized analyses.

The approach recommended here, in addition to being conceptually simple, does not require repeated matrix inversions. It was developed from that proposed by R. Gallagher, J. Padlog and others at Bell Aerospace (References 3,4). Input data, as in the case with these other nonlinear analyses, are generated by an elastic analysis; however, for this approach, either the matrix force method or direct stiffness method can be used. The problem, formulated in terms of standard influence coefficients for applied load and initial strain, is reduced from a nonlinear to a linear one by using those strains obtained at the previous load level to approximate the current inelastic strains.

Development of the anisotropic analysis is based on an extension of the proposed anisotropic theory of Hu, Reference 11. The constant-anisotropic-coefficient assumption of Hu is replaced by one in which the coefficients are allowed to vary with the level of stress. The formulation is then a simple modification of the isotropic procedure. It is also shown that anisotropic creep can be included in a manner similar to the isotropic creep.

## SECTION II

### INELASTIC MATRIX METHODS

#### A. Formulation

An inelastic structural analysis can be carried out in two steps. The first is the standard elastic solution where internal stresses and accompanying strains are related through Hooke's law. The second step, the modification of this elastic system to include inelastic strains, is analogous to a procedure for including superimposed thermal strains. The inelastic strains are defined as the differences between the total strains and the elastic strains and are generally functions of the final stresses, not those of the linear, elastic state.

The simple, pin-jointed, single-redundant truss, pictured in Figure (1), illustrates the basic notions more clearly. All bars are considered to be elastic, except the vertical diagonal which can become plastic and has a stress-strain relation represented by the curve shown in Figure (2). The applied load  $P$  is large enough to cause member 3 to become plastic.

A solution might be obtained by first simply ignoring plastic strain in member 3 and assuming all members elastic. The resulting stress would then be of magnitude  $\sigma$ . The actual stress for member 3, of lower magnitude due to plastic yielding, is designated  $\sigma^{(k)}$  and the associated inelastic strain  $\epsilon^{(k)}$  in Figure (2). These stresses and strains are related in the following equation.

$$\sigma^{(k)} = \sigma + \Gamma \epsilon^{(k)} \quad (1)$$

where:

- $\sigma^{(k)}$  is the actual final stress
- $\sigma$  is the elastic stress
- $\epsilon^{(k)}$  the inelastic strain
- $\Gamma$  the redundant elastic stress for a unit value of initial strain

To be more specific  $\Gamma$  is equal to the redundant stress in member 3 corresponding to a unit initial strain in member 3. Note that  $\Gamma$  must be negative to cause a reduction of stress in the diagonal member.

An important feature to be observed about Equation 1 is that, since the inelastic strain  $\epsilon^{(k)}$  is a nonlinear function of the final stress  $\sigma^{(k)}$ , this equation is really a nonlinear relation to be solved



for  $\sigma^{(k)}$ . This characteristic will always be present in the analyses to be discussed in this report.

Equation 1 can be generalized to provide stresses in all members of the structure and provide for inelastic strains in all members for a variety of applied loads. This basic influence coefficient equation\* is as follows:

$$\{\sigma_u\} = [\Gamma_{um}]\{P_m\} + [\Gamma_{uv}]\{\epsilon_v\} \quad (2)$$

The  $\sigma_u$ 's are the ordinary stress components at the various node points of the structure. An element of  $[\Gamma_{um}]$  gives the  $u^{\text{th}}$  stress in the linear redundant structure due to a unit  $m^{\text{th}}$  applied load, and  $\{P_m\}$  represents the actual applied loads. Also, an element of  $[\Gamma_{uv}]$  gives the  $u^{\text{th}}$  stress component in the linear redundant structure due to a unit initial strain at the  $v^{\text{th}}$  stress location in the unloaded, statically determinate structure. Finally, an element of  $\{\epsilon_v\}$  represents the actual initial strain at the  $v^{\text{th}}$  stress location.

The problem is now reduced in essence to the determination of the inelastic strains to use as the initial strains  $\{\epsilon_v\}$  in Equation 2.

For a structure in a load-temperature-time environment, this task can be rather formidable, because  $\{\epsilon_v\}$  is a function of local temperature and time, as well as the local stress history.

#### B. Example Problem

Continuing our study of the simple truss example of Figure (1), we now allow all members to go plastic. The exact results for the deformation and stresses in the truss, for nonlinear properties, are easily obtained by direct numerical solution of the equations, and hence will be used without development.

The step-by-step finite element method for determining the stresses  $\{\sigma_u\}$  and strains  $\{\epsilon_v\}$  involves the use of Equation 2 and a nonlinear stress-strain relation. This relation will be assumed to be a piecewise linear approximation of the Ramberg-Osgood stress-strain relation.

$$\epsilon = \frac{\sigma}{E} + \epsilon$$

---

\*The derivation of matrices  $[\Gamma_{um}]$  and  $[\Gamma_{uv}]$  is given in Appendix VI.

where  $\epsilon$  denotes the inelastic (or plastic) strains and is given by

$$\epsilon = \frac{3}{7} \left( \frac{\sigma}{\sigma_0} \right)^{\theta-1}$$

and where

$\epsilon$  = total strain

$\sigma$  = member stress

$E$  = Young's modulus

$\sigma_0$  = reference stress (stress at secant modulus of  $0.7E$ )

$\theta$  = nonlinear parameter

The first step, in applying the finite element method, is to obtain the influence coefficient matrices  $[\Gamma_{um}]$  and  $[\Gamma_{uv}]$  for the linear, redundant structure. This requires specification of the geometry of the structure and the (linear) material properties of the individual structural elements. The geometry of the example truss problem is given in Figure (1). The material is assumed to be an aluminum alloy with the following constants.

$$E = 10^7 \text{ psi}, \sigma_0 = 10^5 \text{ psi}, \theta = 10$$

The approximate stress-strain curve used matches the Ramberg-Osgood values at 2000 psi stress intervals.

In this case, we find

$$[\Gamma_{um}] = \begin{bmatrix} .207 \\ -.293 \\ .707 \end{bmatrix}, [\Gamma_{uv}] = 10^7 \times \begin{bmatrix} -.414 & .207 & .207 \\ .586 & -.293 & -.293 \\ .586 & -.293 & -.293 \end{bmatrix}$$

for the case of the single applied load  $P$ .

### C. Step-by-Step Methods

References 3 and 4 present what appears to be the simplest possible approach to this problem from a computational standpoint.\* A non iterative step-by-step calculation is performed in which all quantities including the initial strains  $\epsilon_v$  are incremented and then assumed to remain constant in the ensuing load interval. The inherent difficulty in this approach is to establish the connection between successive steps. Two methods, both of which involve the initial strains from the prior step to predict quantities in the current step are suggested. It is anticipated that by controlling the size of the interval one may achieve any degree of accuracy.

The development herein is discussed only in the detail necessary to analyze the redundant truss of Figure (1) being loaded for the first time into the plastic range. Generalization to biaxial plasticity and creep phenomena are discussed in the succeeding sections.

The step-by-step procedure for solving the problem is introduced by rewriting Equation 2 in the form

$$\{\sigma_u^{(k)}\} = [\Gamma_{um}] \{P_m^{(k)}\} + [\Gamma_{uv}] \{\epsilon_v^{(k-1)}\} \quad (3)$$

where

k is the cycle designation

This can be regarded as the fundamental equation for the non-iterative, step-by-step methods. The idea in formulating this equation, as indicated by the cycle designating superscript is that the initial strains of the previous cycle can be used to approximate the initial strains of the current cycle. The strains of the previous cycle may be incorporated in several ways, two of which constitute the constant stress and the constant strain methods of analysis.

### D. Constant Stress Method

As indicated previously, in the step-by-step procedure considered here, one enters the  $k^{\text{th}}$  cycle with applied loads  $\{P_m^{(k)}\}$  and initial strains  $\{\epsilon_v^{(k-1)}\}$ , the latter evaluated during the preceding cycle.

---

\*These methods make use of devices previously used by others to solve inelastic problems; for example, S. S. Manson at the Lewis Research Laboratory, NASA, Cleveland, Ohio, has previously carried out inelastic analyses of turbine discs involving somewhat similar techniques (Reference 5).

The first operation of the current cycle is to determine  $\{\sigma_u^{(k)}\}$  from Equation 3 by direct substitution. The second operation is a determination of  $\{\epsilon_v^{(k)}\}$  for use in the next cycle. The constant stress method does this in the most obvious way, by reading from the given stress-strain curve the plastic strains  $\{\epsilon_v^{(k)}\}$  corresponding to the  $\sigma_u^{(k)}$ 's (the reason for the name "constant stress" is thus apparent). The operation is indicated schematically in Figure (2).

The results of the application of this method to the example truss problem are shown in Figure (4), where the stress in the vertical member (Bar #3) has been plotted versus load. These results display a striking defect of the method due to the development of a sudden and catastrophic divergence, whose onset depends upon step size. This dependence is such that any attempt to improve accuracy by reducing step size only hastens the occurrence of divergence. An explanation of this behavior is given in Appendix III. Because of this defect, the constant stress method in this form must be eliminated from consideration as an acceptable method for general use.

#### E. Constant Strain Method

The first operation of the constant strain method is exactly the same as the first operation of the constant stress method;  $\sigma_u^{(k)}$  is evaluated by direct substitution in Equation 3. Thereafter, one determines  $\epsilon_v^{(k)}$  for use in the next cycle as follows. Referring to Figure (3), for each member, point A is determined with stress-strain coordinates  $\sigma_u^{(k)}$  and  $\sigma_u^{(k)}/E + \epsilon_v^{(k-1)}$ . A relaxed stress  $\sigma_u^{*(k)}$  is now calculated with the same total strain, corresponding to point B on the given stress-strain curve. Note that here the total strain, rather than stress, remains unchanged--hence the name "constant strain" method. The required initial strain  $\epsilon_v^{(k)}$  is the inelastic strain  $\epsilon^{(k)}$  corresponding to the relaxed stress, as indicated on Figure (3).

The results of applying the constant strain method to the truss problem, for the three step sizes 5000, 500 and 50 lb., are shown in Figure (5). The accuracy, for a given step size, is not as good as that of the constant stress method, but the analysis is now free of any instability. The constant strain method is therefore selected for further use herein. The discussion of the step size and of a method of monitoring it is left for a later section.

### SECTION III

#### ISOTROPIC ELASTIC-PLASTIC ANALYSIS

##### A. Biaxial Theory

Having presented the simple truss example of the step-by-step procedure, we proceed now to the case of more practical interest -- a biaxially stressed structure. The new procedure is identical to the one already discussed for the simple truss with one exception. Because of the biaxial stress we can no longer work directly from the stress-strain curve to obtain the plastic strains for use in Equation 3; instead, we must employ the well-known concept of an "effective" stress-strain relationship in conjunction with a von Mises type yield condition and the associated incremental flow relations.

The biaxial theory is described by a summary of the steps to be used as a guide for a detailed description which follows. The constant strain method used here is a step-by-step procedure which, after incrementing the applied load, can be applied in four parts:

1. Obtain the stress components at each node using the basic Equation 3 by assuming the initial strains from the previous load level.
2. Using these stresses, calculate an effective stress at each node.
3. Assume that the effective stress-strain relation for the material, modified by including the elastic strain, corresponds to data measured in a simple uniaxial tension test. Using this, calculate the effective strain corresponding to the effective stress.
4. Using the incremental flow relations, determine the inelastic strain increments. The proportionality constant in these equations is the ratio of the effective strain increment to the effective stress.

At this point in the calculation, the applied load can be incremented again and the cycle repeated.

When calculating the ordinary stresses  $\{\sigma_u^{(k)}\}$  for the  $k^{\text{th}}$  load level using Equation 3 (Step 1), it is convenient to re-identify these stresses by means of a new subscript N, as follows:

$$\begin{Bmatrix} \vdots \\ \sigma_u^{(k)} \\ \vdots \end{Bmatrix} = \begin{Bmatrix} \vdots \\ \sigma_{3N-2}^{(k)} \\ \sigma_{3N-1}^{(k)} \\ \sigma_{3N}^{(k)} \\ \vdots \end{Bmatrix} \quad (4)$$

The stresses are thus arranged in groups of three components (two normal and one shear) at each node point N.

We now calculate the corresponding effective stresses  $\bar{\sigma}_N^{(k)}$  for each of the nodes from the von Mises type formula (Step 2)

$$\bar{\sigma}_N^{(k)} = \left[ \left( \sigma_{3N-2}^{(k)} \right)^2 - \left( \sigma_{3N-2}^{(k)} \right) \left( \sigma_{3N-1}^{(k)} \right) + \left( \sigma_{3N-1}^{(k)} \right)^2 + 3 \left( \sigma_{3N}^{(k)} \right)^2 \right]^{\frac{1}{2}} \quad (5)$$

Note that by this definition  $\bar{\sigma}_N^{(k)}$  must be positive and is proportional to the octahedral shear stress. This formula together with the stress-strain data constitutes the strain hardening criterion.

We now go to the tensile stress-strain curve (which is also the  $\bar{\sigma}$  vs  $\bar{\epsilon}/E + \bar{\epsilon}(p)$  curve) for the material of interest and, using the constant strain method, read from it the corresponding effective plastic strain  $\bar{\epsilon}(p)_N^{(k)}$ . This operation (Step 3) is identical to that previously described for the uniaxial case on page 7.

In accordance with the flow theory of plasticity, the increment in the effective strain  $\Delta \bar{\epsilon}(p)_N^{(k)}$  over that of the preceding interval must be calculated (Step 4). The increment will be either positive or zero, depending upon whether plastic loading or elastic unloading (or reloading) is taking place. Thus,

$$\Delta \bar{\epsilon}(p)_N^{(k)} = \bar{\epsilon}(p)_N^{(k)} - \bar{\epsilon}(p)_N^{(k-1)} \quad (6a)$$

when  $\bar{\sigma}_N^{(k)}$  is greater than any previous  $\bar{\sigma}_N$  (inelastic strain increasing)

$$\Delta \bar{\epsilon}(p)_N^{(k)} = 0 \quad (6b)$$

when  $\bar{\sigma}_N^{(k)}$  is smaller than a previous  $\bar{\sigma}_N$  (elastic unloading or reloading, inelastic strain constant)

The increments in the ordinary plastic strain components may now be obtained using a Prandtl-Reuss incremental relationship.

$$\begin{aligned} \Delta \epsilon(p)_{3N-2}^{(k)} &= \frac{\Delta \bar{\epsilon}(p)_N^{(k)}}{\bar{\sigma}_N^{(k)}} \left[ \sigma_{3N-2}^{(k)} - 1/2 \sigma_{3N-1}^{(k)} \right] \\ \Delta \epsilon(p)_{3N-1}^{(k)} &= \frac{\Delta \bar{\epsilon}(p)_N^{(k)}}{\bar{\sigma}_N^{(k)}} \left[ \sigma_{3N-1}^{(k)} - 1/2 \sigma_{3N-2}^{(k)} \right] \\ \Delta \epsilon(p)_{3N}^{(k)} &= \frac{\Delta \bar{\epsilon}(p)_N^{(k)}}{\bar{\sigma}_N^{(k)}} \left[ 3\sigma_{3N}^{(k)} \right] \end{aligned} \quad (7)$$

The total, ordinary plastic strain components are obtained by addition,

$$\begin{Bmatrix} \vdots \\ \epsilon(p)_{3N-2}^{(k)} \\ \epsilon(p)_{3N-1}^{(k)} \\ \epsilon(p)_{3N}^{(k)} \\ \vdots \end{Bmatrix} = \begin{Bmatrix} \vdots \\ \epsilon(p)_{3N-2}^{(k-1)} \\ \epsilon(p)_{3N-1}^{(k-1)} \\ \epsilon(p)_{3N}^{(k-1)} \\ \vdots \end{Bmatrix} + \begin{Bmatrix} \vdots \\ \Delta \epsilon(p)_{3N-2}^{(k)} \\ \Delta \epsilon(p)_{3N-1}^{(k)} \\ \Delta \epsilon(p)_{3N}^{(k)} \\ \vdots \end{Bmatrix} \quad (8)$$

These components together with the new applied loads  $p_m^{(k+1)}$  may be substituted in Equation 3 to obtain  $\sigma_u^{(k+1)}$  in the next load cycle.

### B. Determination of Calculation Step Size

It should be noted that, according to the constant strain method, every predicted value of effective strain  $\bar{\epsilon}(p)_N^{(k)}$  together with its accompanying value of effective stress  $\bar{\sigma}_N^{(k)}$  constitutes an approximation to a point on the actual effective stress-strain curve. The excellence of the approximation is directly related to the loading increment, as is shown in the truss results Figure (5). Thus it is only necessary to monitor this agreement for one or more of the critically loaded nodes to determine whether the step size is satisfactory. This is illustrated below in connection with the shear lag structure investigation.

### C. Description of Shear Lag Structure

Several very useful tests have been performed for the Air Force upon shear lag structures (Reference 7). The structure, loaded as shown in Figure (6), is an integrally machined part of 2024-T4 aluminum alloy stiffened along the loading (y) axis. The stiffener is tapered in thickness from each end towards the center of the structure.

This structure was chosen originally because it is simple to work with and well adapted to analysis by both matrix methods when appropriate idealizations are employed. When tension forces are applied to the ends of the stiffener, high stress gradients are induced in a manner analogous to those encountered in aircraft structures.

The material properties essential to this analysis were obtained from tension tests reported in Reference 7. These tests were performed on coupons, machined from the parent plate, in the longitudinal or x-direction and the transverse or y-direction of Figure (6). The data resulting from these tests, Figure (11), indicate the presence of a considerable degree of anisotropy. In the present study, three piecewise linear representations of stress-strain curves were fitted to these points; two, RO1 and RO2, in Figure (11), are equivalent to Ramberg-Osgood curves used in Reference 7; the third, RO2M, is a Grumman modification. The modulus of elasticity of all the curves is taken as  $10.3 \times 10^6$  psi. Note also that the maximum strains recorded are of the order of 0.010 in/in, whereas the maximum strains reached in the shear lag tests are around 0.020 in/in. Thus there is some doubt as to whether the idealized curve correctly represents the test material in this high strain region.

The locations of the strain gages for the test of the stiffened plate are shown in Figure (13). The plate was loaded by applying tension to the stiffener in steps of 1000 pounds to 6000 pounds, gage readings being taken at each step. It was then unloaded in steps of 1500 pounds to zero, and finally progressively loaded to failure. Buckling occurred at a load of 23,000 pounds and fracture at 25,800 pounds. Data from this test are plotted on Figures (14) through (22).



#### D. Elastic Shear Lag Structure Analysis

The idealizations of the upper right quadrant of the shear lag structure for a direct stiffness and a force method analysis are shown in Figures (7) and (8) respectively. A typical element of the force method analysis, Figure (9), consists of conventional bars and rectangular shear panels. Many previous idealizations have omitted the Poisson's Ratio effect. The present idealization, however, incorporates this effect in the manner described in Appendix II.

The basic element of the stiffness approach consists of a cluster of four "Turner triangles" (References 8,9) to form a rectangle as shown in Figure (10). The manner of obtaining the stresses is discussed in Appendix I.

An elastic analysis under a unit applied load was performed by both the force and the stiffness methods. These results are compared in Appendix I.

The inelastic analysis can be made using either of the two approaches (stiffness or force method). For the present investigation, only the force method is used.

#### E. Flow Theory Shear Lag Structure Analysis

The inelastic analysis was carried out using the Fortran 2 program listed in Appendix V. This program is capable of carrying out isotropic or anisotropic, plastic or creep flow theory analyses. The flow charts and instructions for preparation and submission of data are also included in Appendix V.

Before comparing the analytical and test results, let us look at a plot of the tensile stress-strain curve, R02M, and compare it with the predicted effective stress-strain relationship for various step sizes. Such a comparison is found in Figure (12) for the node corresponding to the center of the specimen which is the point of highest strain in the structure. It can be seen there that for a step size of  $\Delta P = 500$  lb., the agreement is rather poor. For  $\Delta P = 50$  lb. the agreement is much better, while for  $\Delta P = 5$  lb., the predicted value lies directly on the stress-strain curve. The IBM 7094 computer time for this best result and a maximum load of  $P = 16,760$  lb. is approximately 20 minutes.

The predicted strain distributions are shown in Figures (14) through (21), together with the corresponding test values, along the two strain gage lines. In these plots, the calculated results are linearly interpolated values between node points. Figures (14) and (15) give elastic results; the agreement with test data is seen to be rather good, giving the necessary confidence in the accuracy of the basic influence coefficient matrices. It is observed also that the specimen achieves its basic purpose of displaying a pronounced shear lag effect with the highest strain occurring at the central node, as expected.

As the applied load increases through 7070 lbs., the strains at the central node become plastic. During the tests, the strain gages continued to function through an applied load level of 14,600 lb.; beyond this point the x-gage failed to record. The y-gage failed also above a load level of 16,760 lb., which, consequently, is the highest level considered in the comparison of test and analysis even though the plate did not buckle until  $P = 23,000$  lb.

The proportional limit for the test specimen material occurs at a strain of approximately .004 in/in, as shown in Figure (11). Bearing this in mind during an examination of Figures (16) through (21), it is seen that plastic behavior is primarily confined to a fairly small region around the central node, and we thus have a case of contained plasticity. The analysis predicts a very pronounced strain redistribution extending somewhat beyond this region. This is indicated by a comparison of the plastic results with extrapolated elastic results shown as dotted curves on Figures (20) and (21).

As for agreement with test values, the analysis substantially underpredicts the strain gage readings where plasticity is most pronounced. Since the elastic results agree so much better, one must assume that the difficulty lies somewhere in the plasticity part of the correlation. It was mentioned previously that the idealization of the stress-strain curve R02M of Figure (11) was open to question at the high strain end because of the absence of test points. Accordingly, an additional run was made for a revised curve extending horizontally beyond the last indicated test point. The plastic strains at the critical central node are increased approximately 10% by so doing. This represents an appreciable closing of the gap, but the gap nevertheless remains.

Calculations were also made based upon the previously mentioned stress-strain curves R01 and R02 of Figure (11). The results for the central node are shown on Figure (22). As might be expected, they depart appreciably from the R02M predictions.

#### F. Deformation Theory Analysis

Solutions by a deformation theory have traditionally been considered to be more easily obtainable than flow theory solutions. This is, of course, because only the stresses at the final applied load level need be considered, rather than the stress histories developed during loading. It is therefore of interest to determine whether similar benefits are attainable in the case of the finite element analyses currently being considered.

Once again, a solution of Equation 3 is required, this time such that the initial strains  $\epsilon_v$  satisfy the deformation theory of plasticity. This can be accomplished as follows. Equation 3, the " $k^{\text{th}}$  cycle" stress equation of the preceding section, can be used intact if it is understood that  $P_m^{(k)}$  is the peak load at which the results are required and does not change from one cycle to another as before. We must iterate to a solution in order to obtain a satisfactory approximation to the plastic strains.

The intra-cycle procedure employed for the determination of the equivalent strain for the  $k^{\text{th}}$  cycle is the same as before, namely the constant strain method. At this point, however, the equivalent strain itself, not its increment, is resolved into the node plastic strains by utilizing an engineering adaptation of the incremental relations, Equations 7, thus:

$$\begin{aligned}\epsilon_{3N-2}^{(p)(k)} &= \frac{\bar{\epsilon}^{(p)}_N^{(k)}}{\bar{\alpha}_N^{(k)}} \left[ \sigma_{3N-2}^{(k)} - 1/2 \sigma_{3N-1}^{(k)} \right] \\ \epsilon_{3N-1}^{(p)(k)} &= \frac{\bar{\epsilon}^{(p)}_N^{(k)}}{\bar{\alpha}_N^{(k)}} \left[ \sigma_{3N-1}^{(k)} - 1/2 \sigma_{3N-2}^{(k)} \right] \\ \epsilon_{3N}^{(p)(k)} &= \frac{\bar{\epsilon}^{(p)}_N^{(k)}}{\bar{\alpha}_N^{(k)}} \left[ 3\sigma_{3N}^{(k)} \right]\end{aligned}\quad (9)$$

These are now available for the stress equation of the next cycle.

Three analyses, one at  $P = 11,600$  lbs., one at  $P = 14,600$  lbs., and one at  $P = 16,760$  lbs. were performed on the shear lag specimen by this deformation theory procedure. The results were practically identical with those shown in Figures (16) to (21). The convergence to each of these results was obtained after less than thirty cycles of iteration. The machine time for each calculation was approximately four minutes.

In the case of solutions like this, where the two analyses give practically identical results, the deformation approach is naturally very attractive because of the greatly reduced machine time. However, the question remains of determining when to expect the results to agree in this manner.

The IBM program presented in Appendix V cannot be used for deformation theory analyses. However, minor changes can be made in the program to permit calculations of this type to be carried out.

SECTION IV  
ISOTROPIC ELASTIC-PLASTIC-CREEP ANALYSIS

A. Introduction to Creep Theory

Strains due to creep constitute an additional form of inelastic strain, and can be handled in a way analogous to that already discussed for bi-axial plasticity by the flow theory. It is only necessary to select a method for evaluating these time-dependent strains based upon the material properties and to add them to the plastic strains prior to insertion in the basic Equation 3.

A familiar relationship used to match the creep behavior in a tensile creep test, performed at constant stress and constant temperature, is (Reference 4):

$$\epsilon(c) = \alpha t^\gamma (e^{\beta \sigma} - 1) \quad (10)$$

in which

$\epsilon(c)$  is the tensile creep strain

$t$  is the elapsed time

$\sigma$  is the constant tensile stress

$\alpha, \beta, \gamma$  are empirical constants for the particular test temperature

For this analysis the assumption is made that there exists an effective creep strain  $\bar{\epsilon}(c)$  in a biaxial situation which can be calculated using Equation 10. In doing this the stress  $\sigma$  is taken to be the von Mises effective stress obtained from Equation 5. The further assumption is made that this effective creep strain can be resolved into nodal creep strains by use of a Prandtl-Reuss type of flow law.

The creep strain calculation must be generalized to situations in which the stresses vary with time. One well-known procedure for doing this, the strain-hardening rule (Reference 4), has been determined to be most appropriate for the present purposes. Its use will be described presently in connection with the  $k^{\text{th}}$  calculation cycle.

B. Creep Theory Details

The calculation cycle follows a sequence similar to that described previously for the isotropic elastic-plastic analysis. An additional step is necessary, just after the plastic strains are obtained, to determine the creep strains. The intra-cycle order of calculation is as follows.

Entering the  $k^{\text{th}}$  cycle with applied loads  $\{P_m(k)\}$ , and with the initial strains, plastic and creep, as calculated during the preceding cycle, the stresses  $\{\sigma_u(k)\}$  are calculated from Equation 3.

The effective stresses  $\{\bar{\sigma}_N(k)\}$  obtained from Equation 5 are used to obtain the effective plastic strains.

The creep strain increments at each node, for a specified time step, are now determined by the strain hardening rule which relates the strain at a node to the corresponding stress and strain for the previous cycle by the introduction of an assumed elapsed time.

Referring to Figure (23), one goes to the constant effective stress-temperature curve  $(\bar{\sigma}^k, T^k)$  relevant to the node and the cycle, and locates upon it the point with ordinate  $\bar{\epsilon}(c)^{(k-1)}$ . The corresponding abscissa, designated  $t^{*(k)}$ , is called the reference time and is generally different from the actual elapsed time at the start of the cycle. The required effective creep strain increment  $\Delta\bar{\epsilon}(c)^{(k)}_N$  is that corresponding to the increase in time from  $t^{*k}$  to  $(t^{*k} + \Delta t^k)$  as shown on Figure (23),  $\Delta t^k$  being the selected calculation time increment.

The increment  $\Delta\bar{\epsilon}(c)^k$  is substituted into the Prandtl-Reuss type incremental relations, Equations 7, together with the stresses indicated there. The creep initial strains are then obtained as in Equation 8.

In summary, the steps in the  $k^{\text{th}}$  calculation take the following order:

- (1) Evaluation of Equation 3 to obtaining the stress components,  $\sigma_u(k)$
- (2) The calculation of effective stress according to Equation 5
- (3) The determination of the node plastic strains
- (4) The determination of the node creep strains
- (5) The addition of the nodal plastic and creep strains to give the initial strains for the next cycle.

### C. Description of Structure and Tests

The description of the shear lag structure to be analyzed in this section and tests for the material properties may be found in Reference 7. The shear lag structure was manufactured from 1100-F aluminum. It was of the same physical dimensions as the structure of Figure (6). The idealization of the upper right quadrant remains unchanged.

Material properties for the creep analysis were obtained from uniaxial strain-time tests for constant tensile stress. The temperature at which these tests were conducted was 206°C, the temperature identical to that of the structural test. The curves for these tests are presented in Figure (24) together with the fitted curves from Equation 10. The constants of the equation were obtained from Reference 7 and are as follows:

$$\alpha = 0.650 \times 10^{-4}$$

$$\gamma = 0.500$$

$$\beta = 0.700 \times 10^{-3} \text{ in}^2/\text{lb}$$

Ordinary tensile stress-strain tests were performed at room temperature on coupons cut from the x and y orientations of the plate material. The data and faired curve are presented in Figure (25). Tensile stress-strain data for 206°C are also plotted here. These data were obtained from the intersections of the test curves on the zero time axis in Figure (24). A piecewise linear representation TC1 was fitted to this latter data.

The location of the strain gages on the structure is given in Figure (26). The shear lag specimen was tested for a total of three hours at 206°C. An initial applied load of 1600 lb. was increased to 2020 lb. at the end of the first hour. It was held constant thereafter to the end of the test.

#### D. Results of Creep Shear Lag Analysis

The predicted strain distributions along the x-axis and along the section  $x = 1$  in. at  $t = 0.06$  hr.,  $t = 1.10$  hr., and  $t = 3.00$  hr. elapsed times, are given in Figures (27) through (32), together with the experimental data of Reference 7. Test data are not available for the y-node strains at the center node, and so this correlation point of critical significance does not exist.

The curve of Figure (33), effective stress versus strain at the central node, exhibits the shapes characteristic to the various regions of the load-time sequence. The initial linear segment, representing elastic loading is followed by the region of the negative curvature representing loading into the plastic range, all at assumed zero time. Thereafter, the applied load remains constant for one hour, during which time there is a stress redistribution in the structure due to creep. This particular node unloads, as evidenced by the reduction in effective stress, although the total strain is growing continuously. The applied load is now increased to 2020 lb. Because of the previous elastic strain recovery, the effective stress at first goes up elastically, and then becomes plastic once more. Once the applied load reaches its final value, redistribution due to creep effects again takes place.

In the initial stages of creep the curve is very sensitive to time increment size and it is necessary to choose exceptionally small time

increments in this region if good accuracy is to be achieved. The time increments employed are as shown in Figure (33).

Considering the simplicity of the expressions employed to describe as complex a phenomenon as creep and the liberal assumptions made in the process, the correlation between analysis and experiment, as evidenced by the preceding graphs and also by Figures (34) and (35), is surprisingly good.

## SECTION V

### ANISOTROPIC ELASTIC-PLASTIC ANALYSIS

#### A. Anisotropy in Structures

Several "expanding yield surface" theories for extending the isotropic plastic theory to provide for anisotropy have become available within the last two decades. Each is based on experimentally determined parameters and, therefore, each is biased in favor of specific test data. The complexity and amount of testing required to obtain these parameters differ considerably. Under these circumstances, no single theory can be completely acceptable, but it is thought that a suitable theory must, at least, be capable of evaluating the type of anisotropy associated with biaxially stressed structures used in flight vehicle design without being unduly complex in application. It would be desirable to have the procedure based on a well-known, accepted theory.

A particular type of anisotropy, the so-called "orthotropic symmetric" type, develops during a cold rolling process where the material is lengthened and thinned with no appreciable change in width. Since cold rolled sheet and plate are frequently used in aerospace structures, this type of anisotropy may be anticipated and is considered here.

A theory proposed by Hill, Reference 10, has been widely accepted as the most straightforward extension of the isotropic theory. The formulation, however, is not very convenient for numerical step-by-step computation. A modification of Hill's theory proposed by Hu, Reference 11, however, is very tractable to formulation into the matrix inelastic program discussed previously in this report. The Hu procedure has two distinct advantages:

- (1) It employs a von Mises type hardening surface, associated flow law and effective stress-strain relationships in appropriate form.
- (2) It requires a minimum of material data: simple uniaxial and shear stress-strain tests on coupons cut in the directions of the orthotropy.

#### B. Hu's Strain Hardening Theory

A summary of Hu's theory is presented to establish its limitations and provide background for the necessary modifications to obtain a more general theory.

The isotropic expressions for effective stress, Equation 5, and associated incremental relations, Equations 7, are modified by means of anisotropic parameters ( $\alpha_{ij}$ ). These are constants in Hu's theory. Here it is more convenient to introduce the 1-1, 2-2, etc., directions instead



of x-x, y-y, etc. The modified expression for the effective stress is

$$\bar{\sigma} = \left[ \alpha_{12}(\sigma_{11} - \sigma_{22})^2 + \alpha_{23}(\sigma_{22} - \sigma_{33})^2 + \alpha_{31}(\sigma_{33} - \sigma_{11})^2 + 3\alpha_{44}\sigma_{12}^2 + 3\alpha_{55}\sigma_{23}^2 + 3\alpha_{66}\sigma_{31}^2 \right]^{\frac{1}{2}} \quad (11)$$

The incremental flow equations are

$$\begin{aligned} d\epsilon_{11} &= \frac{d\bar{\epsilon}}{\bar{\sigma}} \left[ \alpha_{11}\sigma_{11} - \alpha_{12}\sigma_{22} - \alpha_{31}\sigma_{33} \right] \\ d\epsilon_{22} &= \frac{d\bar{\epsilon}}{\bar{\sigma}} \left[ -\alpha_{12}\sigma_{11} + \alpha_{22}\sigma_{22} - \alpha_{23}\sigma_{33} \right] \\ d\epsilon_{33} &= \frac{d\bar{\epsilon}}{\bar{\sigma}} \left[ -\alpha_{31}\sigma_{11} - \alpha_{23}\sigma_{22} + \alpha_{33}\sigma_{33} \right] \\ d\epsilon_{12} &= \frac{d\bar{\epsilon}}{\bar{\sigma}} \left[ 3\alpha_{44}\sigma_{12} \right] \\ d\epsilon_{23} &= \frac{d\bar{\epsilon}}{\bar{\sigma}} \left[ 3\alpha_{55}\sigma_{23} \right] \\ d\epsilon_{31} &= \frac{d\bar{\epsilon}}{\bar{\sigma}} \left[ 3\alpha_{66}\sigma_{31} \right] \end{aligned} \quad (12)$$

Equations 11 and 12 are written for the case where the reference axes are the principal axes of anisotropy.

The anisotropic parameters are determined by means of a total of six, simple, directional, stress-strain tests (i.e., uniaxial and shear tests), where, alternately, all stress components are equal to zero except one. From each of the six tests a characteristic stress, such as an approximate yield stress, is read off. Then substituting each of these results into Equation 11 in succession, we may write

$$\begin{aligned} \alpha_{11} &= \alpha_{12} + \alpha_{31} = \left( \frac{K}{Y_{11}} \right)^2 & \alpha_{44} &= \frac{1}{3} \left( \frac{K}{Y_{12}} \right)^2 \\ \alpha_{22} &= \alpha_{23} + \alpha_{12} = \left( \frac{K}{Y_{22}} \right)^2 & \alpha_{55} &= \frac{1}{3} \left( \frac{K}{Y_{23}} \right)^2 \\ \alpha_{33} &= \alpha_{31} + \alpha_{23} = \left( \frac{K}{Y_{33}} \right)^2 & \alpha_{66} &= \frac{1}{3} \left( \frac{K}{Y_{31}} \right)^2 \end{aligned} \quad (13)$$

where

$K$  = the effective characteristic stress

$Y_{ij}$  = the simple directional characteristic stress

It remains to assume an effective stress-effective strain relationship. Hu shows that it is acceptable to assume the stress-strain data associated with one particular simple tension test as the effective relationship. It can be seen from Equations 13 that this implies setting one  $\alpha_{11}$  equal to unity.

Thus, in particular for  $\alpha_{22} = 1$ , from Equations 11 and 12:

$$\begin{aligned}\bar{\sigma} &= \sigma_{22} \\ d\bar{\epsilon} &= d\epsilon_{22}\end{aligned}\tag{14}$$

Now consider Equation 12 for simple stress-strain tests in the other directions. Then

$$\begin{aligned}d\epsilon_{11} &= \alpha_{11}\sigma_{11}\frac{d\bar{\epsilon}}{\bar{\sigma}} \\ d\epsilon_{33} &= \alpha_{33}\sigma_{33}\frac{d\bar{\epsilon}}{\bar{\sigma}} \\ d\epsilon_{12} &= 3\alpha_{44}\sigma_{12}\frac{d\bar{\epsilon}}{\bar{\sigma}} \\ d\epsilon_{23} &= 3\alpha_{55}\sigma_{23}\frac{d\bar{\epsilon}}{\bar{\sigma}} \\ d\epsilon_{31} &= 3\alpha_{66}\sigma_{31}\frac{d\bar{\epsilon}}{\bar{\sigma}}\end{aligned}\tag{15}$$

or

$$\frac{d\bar{\epsilon}}{\bar{\sigma}} = \frac{1}{\alpha_{11}} \frac{d\epsilon_{11}}{\sigma_{11}} = \frac{1}{\alpha_{33}} \frac{d\epsilon_{33}}{\sigma_{33}} = \frac{1}{3\alpha_{44}} \frac{d\epsilon_{12}}{\sigma_{12}} = \frac{1}{3\alpha_{55}} \frac{d\epsilon_{23}}{\sigma_{23}} = \frac{1}{3\alpha_{66}} \frac{d\epsilon_{31}}{\sigma_{31}}$$

These equations say that, with the anisotropic parameters constant for strain hardening, the simple, stress-incremental strain relations must be proportional to the effective stress-incremental strain relationship. The implication is that the integrated forms of Equations 15, that is, the simple, directional stress strain curves, are thus prescribed. These may or may not be a reasonable fit to the test data for the material of interest. Obviously, only when the fit is good can one hope for Hu's theory to give acceptable results for all types of loading.

Based upon the Hu theory, it becomes relatively easy to obtain anisotropic solutions using the previously developed isotropic inelastic procedure and corresponding digital computer program. It is only necessary to substitute the appropriate anisotropic constants for their

isotropic counterparts, for which  $\alpha_{11} \dots \alpha_{66} = 1$ ,  $\alpha_{12} = \alpha_{23} = \alpha_{31} = \frac{1}{2}$ .

### C. Extension of Hu's Theory

It is in the determination of the parameters that an extension to Hu's theory is made. Except for the special case pointed out in the preceding section, these parameters should not be constant for a strain hardening material, but should be variables dependent upon stress level. The objective, obviously, is to determine the variation in a manner that allows for all of the simple, directional stress-strain curves to be correctly reproduced. This can be accomplished by a consideration of plastic work.

In the current approach, one continues with the assumption of the existence of an effective stress-strain relationship. Then the basic notion is that the anisotropic parameters are determined such that, for equal amounts of plastic work done during simple directional stress strain tests in all directions, the effective stress level reached will be identical.

Accordingly, for a tensile specimen in the 1-1 direction, one calculates the plastic work  $w$  performed during a uniaxial test by the formula

$$w = \int \alpha_{11} d\epsilon_{11} = \int \bar{\sigma} d\bar{\epsilon} \quad (16)$$

Let the corresponding maximum stress reached be identified by the superscript (I), i.e.  $\sigma_{11}^I$ . For a similar test in the 2-2 direction, and for which the amount of plastic work performed is identical, the corresponding maximum stress reached is  $\sigma_{22}^I$ . Since the amounts of work done in the two cases are the same,  $\sigma_{11}^I$  and  $\sigma_{22}^I$  correspond to the same effective stress  $\bar{\sigma}^I$ . By means of Equation 11 we have

$$(\bar{\sigma}^I)^2 = \alpha_{11} (\sigma_{11}^I)^2 = \alpha_{22} (\sigma_{22}^I)^2 \quad (17)$$

This expression constitutes a relationship defining  $\alpha_{11}$  and  $\alpha_{22}$  as functions of  $\bar{\sigma}$ . Similar relationships can clearly be found for the other  $\alpha_{ij}$ 's. Thereafter, the  $\alpha_{ij}$ 's can be determined as functions of  $\bar{\sigma}$  by recourse to the  $\alpha$  definitions of Equations 13.

It is convenient to again select the 2-2 direction stress-strain curve as the one defining the effective stress-strain relationship. This results in  $\alpha_{22}$  being equal to unity once more.

The actual evaluation of the other  $\alpha$ 's as functions of  $\bar{\sigma}$  follows easily. Figure (36) indicates schematically how the plastic work done in each simple directional stress-strain test can be plotted as a function of stress. Then for a given amount of plastic work, and reading off the corresponding stresses  $\sigma_{11}^I$  and  $\sigma_{22}^I$  for example, by Equation 17 one finds that

$$\alpha_{11} = \frac{\left(\sigma_{22}^I\right)^2}{\left(\sigma_{11}^I\right)^2} \quad (18)$$

Using this and similar relationships in the other directions, curves representing all of the  $\alpha$ 's as functions of  $\bar{\sigma}$  may be constructed. The incorporation of this information in the step-by-step calculation procedure is discussed in the next section.

#### D. Anisotropic Theory Details

The detailed step-by-step calculation procedure to be followed in the case of anisotropic material in a biaxially stressed structure is very similar to that previously discussed for isotropic materials. Accordingly, only the differences will be stressed.

As before, one starts the  $k^{\text{th}}$  calculation cycle by evaluating  $\{\sigma_u^{(k)}\}$  by means of Equation 3. This operation employs the initial strains of the preceding cycle  $\{\epsilon_v(p)^{(k-1)}\}$ .

The next operation is to evaluate the effective stresses at each of the nodes,  $\bar{\sigma}_N^{(k)}$ , by Equation 11, modified for the biaxial case to

$$\begin{aligned} \bar{\sigma}_N^{(k)} = & \left[ \alpha_{11}^{(k-1)} \left( \sigma_{3N-2}^{(k)} \right)^2 - 2\alpha_{12}^{(k-1)} \left( \sigma_{3N-2}^{(k)} \right) \left( \sigma_{3N-1}^{(k)} \right) + \left( \sigma_{3N-1}^{(k)} \right)^2 \right. \\ & \left. + 3\alpha_{44}^{(k-1)} \left( \sigma_{3N}^{(k)} \right)^2 \right]^{\frac{1}{2}} \quad (19) \end{aligned}$$

We continue here our assumption that the 2-2 direction has been selected as that in which the effective stress-strain relationship is defined; hence  $\alpha_{22} = 1$ .

Note that if the Hu theory is being used, the  $\alpha_{ij}$ 's are all known constants. If the modified theory is being employed, the variable  $\alpha_{ij}$ 's are those that have been evaluated during the preceding cycle, (k-1). This is in keeping with the overall nature of the analysis as a step-by-step procedure.

Having determined the  $\bar{\epsilon}_N^{(k)}$ 's, one can now go to the curves representing the  $\alpha_{ij}$ 's as functions of  $\bar{\epsilon}$  to evaluate  $\alpha_{11}^{(k)}$ ,  $\alpha_{12}^{(k)}$  and  $\alpha_{44}^{(k)}$ . After having also determined  $\bar{\epsilon}_N(p)^{(k)}$  and  $\Delta\bar{\epsilon}_N(p)^{(k)}$  as before by the constant strain method, these quantities may be substituted into a finite equivalent of Equations 12 specialized for the biaxial case, to yield

$$\begin{aligned}\Delta\epsilon(p)_{3N-2}^{(k)} &= \frac{\Delta\bar{\epsilon}(p)_N^{(k)}}{\bar{\alpha}_N^{(k)}} \left[ \alpha_{11}^{(k)} \sigma_{3N-2}^{(k)} - \alpha_{12}^{(k)} \sigma_{3N-1}^{(k)} \right] \\ \Delta\epsilon(p)_{3N-1}^{(k)} &= \frac{\Delta\bar{\epsilon}(p)_N^{(k)}}{\bar{\alpha}_N^{(k)}} \left[ \sigma_{3N-1}^{(k)} - \alpha_{12}^{(k)} \sigma_{3N-2}^{(k)} \right] \\ \Delta\epsilon(p)_{3N}^{(k)} &= \frac{\Delta\bar{\epsilon}(p)_N^{(k)}}{\bar{\alpha}_N^{(k)}} \left[ 3\alpha_{44}^{(k)} \sigma_{3N}^{(k)} \right]\end{aligned}\tag{20}$$

From these, the strain components  $\epsilon(p)_{3N-2}^{(k)}$ ,  $\epsilon(p)_{3N-1}^{(k)}$  and  $\epsilon(p)_{3N}^{(k)}$  are obtained by addition, as before, using Equation 8.

After incrementing the applied load the sequence can now be repeated for the next load cycle.

#### E. Rotation of Axes of Anisotropy

Anisotropic symmetry may occur in a structure for which it is convenient to choose coordinate axes that are rotated from the orthogonal axes of anisotropy. The corresponding expressions for the incremental flow equations and effective stress equations are derived in Appendix IV. The derivation is limited to the case of biaxial stress where the 3-3 and z-z axes coincide. A method of obtaining the shear anisotropic coefficients is also indicated.

#### F. Anisotropic Analysis of Shear Lag Structure

It has been pointed out earlier that the 2024-T4 aluminum alloy of the shear lag structure tested for the Air Force (Reference 7) displayed considerable anisotropy as shown in Figure (11). The structure had been analyzed for isotropic strain hardening based upon the curve R02M in this figure, and the results discussed in Section III. A corresponding anisotropic strain hardening analysis has also been carried out, employing first the Hu theory and then the proposed extension.

Material stress-strain data is available along two of the axes of anisotropy, the rolling or x-x (1-1) direction, and the long transverse or y-y (2-2) direction. This data has been plotted and discussed in connection with Figure (11); it is replotted for convenience in Figure (37).

The additional required, but missing, test data is (a) tensile stress-strain data in the short transverse or z-z (3-3) direction and (b) shear stress-strain data in the x-y plane. A reasonable assumption to make for engineering purposes for (a) is that the long and short transverse properties are identical; this is made in the analyses to follow. In the case of (b), the missing shear data, the following is done. First, a shear stress-strain curve is obtained based upon the tensile curve in the rolling direction, together with the assumption that the material is isotropic and governed by the incremental theory of Section III -- specifically, Equations 5 and 7. Next, a similar shear stress-strain curve based upon the tensile curve in the long transverse direction is obtained. Finally, a faired-in average of these two curves is taken to represent the missing shear stress-strain relation.

In order to apply the Hu theory, one must first select four characteristic stresses to represent the directional stress-strain curves, as discussed in Section V-B. These are the quantities  $Y_{11}$ ,  $Y_{22}$ ,  $Y_{33}$  and  $Y_{12}$  of Equations 13. We arbitrarily choose the proportional limits from the four curves just discussed for these values; they are

$$Y_{11} = 51 \text{ ksi}$$

$$Y_{22} = 32 \text{ ksi}$$

$$Y_{33} = 51 \text{ ksi}$$

$$Y_{12} = 22 \text{ ksi}$$

Since the simple directional stress-strain curve in the 2-2 direction, i.e. R02M, is selected for the effective stress relationship, the effective stress characteristic value K is also 32 ksi. Substituting these values in Equations 13, one can solve for the necessary anisotropic parameters. This information is all that is required to carry out an analysis of the shear lag structure by the Hu theory.

As pointed out previously, once the anisotropic parameters  $\alpha_{11}$ ,  $\alpha_{22}$ ,  $\alpha_{12}$  and  $\alpha_{44}$  have been specified and one of the stress-strain curves chosen as the effective stress-strain curve, the remaining simple direc-

tional stress-strain curves are prescribed. Let us now examine the consequences of our current parameter selection. Since only test data in the 1-1 and 2-2 directions are available, we shall concentrate on these. For this special case, Equations 11 and 12 can be easily manipulated to yield

$$\bar{\sigma} = \sqrt{\alpha_{11}} \sigma_{11}$$

$$\frac{d\epsilon_{11}}{d\sigma_{11}} = \alpha_{11} \frac{d\bar{\epsilon}}{d\bar{\sigma}} \quad (21)$$

Using these expressions, one can construct a  $\sigma_{11}$  stress-strain curve.

Such a curve is shown on Figure (37). As can be seen, the fit with the 1-1 test data is very poor. Apparently, one could do better by arbitrarily choosing for the 1-1 characteristic value  $Y_{11}$  a much lower value than 51 ksi -- perhaps in the neighborhood of 35 ksi. Nevertheless, it is clear that in this case it would still be impossible to get a really good fit because of the fundamentally different shapes of the two stress-strain curves, especially in the region of their knees. It will turn out that, in the case of the shear lag structure, this selection is not critical, because of the fact that stresses in the 1-1 direction are very low, compared to those in the 2-2 direction.

In order to carry out an analysis of the shear lag structure based upon the extension to the Hu theory, one must first evaluate the plastic work done in each of the simple directional stress-strain tests as a function of the applicable stress. Using this information in the manner discussed previously, one can then obtain the anisotropic parameters as functions of effective stress. This has been done, assuming that it is sufficiently accurate to represent the curves by a small number of connected straight line segments. The key values of the resulting  $\alpha$ 's are given in the accompanying table. Corresponding total strains  $\bar{\epsilon}$  ( $= \bar{\sigma}/E + \bar{\epsilon}$ ) are also listed.

$\bar{\sigma}$	$\bar{\epsilon}$	$\alpha_{11} = 2\alpha_{12}$	$\alpha_{22}$	$\alpha_{44}$
32000	.00310	0.394	1.000	0.697
37000	.00378	.510	1.000	.755
40000	.00435	.590	1.000	.795
43000	.00509	.660	1.000	.833
46000	.00622	.742	1.000	.871
48000	.00734	.809	1.000	.905
49000	.00800	.835	1.000	.918
51000	.00980	.892	1.000	.945
54000	.03800	.930	1.000	.965

In the preceding table, the reduction in number of independent anisotropic parameters is a consequence of the assumptions which had to be made for the missing stress-strain curves.

The value of unity for  $\alpha_{22}$  is in accordance with our continued selection of the tensile stress-strain curve R02M in the y-y or 2-2 direction as the basis for our effective stress-strain relationship.

It might be reiterated that, because of the manner in which the  $\alpha$ 's are derived in this case, all of the simple directional stress-strain curves are matched as closely as desired.

Using first the anisotropic parameters selected as described for the Hu theory, and then for its extension, the shear lag structure has been analyzed. The results are presented in the next section.

#### G. Discussion of Results

Some of the highlights of the two anisotropic analyses are presented in Figures (38) through (40). Corresponding results obtained previously and based upon isotropic theory are also included for comparison.

Figure (38) refers to the central node of the shear lag structure and shows the variation of the total strains in the x and y directions with increasing applied load. The isotropic result is replotted from Figure (22) -- specifically those curves based upon the effective stress-strain curve R02M.

It can be seen from Figure (38) that the most flexible analysis predictions, that is, those for which the total strains are the largest, are obtained by the isotropic analysis. The analysis based upon the extension to the Hu theory is somewhat less flexible, while the Hu theory results are the stiffest. Also, the differences between the three analyses are less in the y direction than in the x direction.

These observations are clearly in agreement with the nature of the material stress-strain relations upon which the analyses are based. In all three cases, we are assuming that the y-y curves are identical, that is, all are represented by R02M. Referring to Figure (37), in the case of the isotropic analysis, we are also assuming, in effect, that the x-x stress-strain curve is identical to the y-y curve R02M. The x-x curve for the extension to the Hu theory is seen to be somewhat stiffer than R02M, while the x-x curve for the Hu theory is by far the stiffest of the three.

Comparing the analyses with the test data, all three analyses substantially underpredict the test points in the high applied load regime, and more so in the y than in the x direction. It is interesting to note however, that while the anisotropic analyses make these differences even greater, they do have the virtue of making the comparison more consistent as between the x and y directions. Thus it would appear that the



anisotropic nature of the 2024-T4 material does influence the strain distribution in the shear lag structure, and that the anisotropic analyses can detect this tendency.

Figures (39) and (40) show the strain distributions along the two strain gage lines of the test structure. In addition to the isotropic predicted results, replotted from Figures (20) and (21), anisotropic results based upon the extension to the Hu theory are presented. They indicate that while the differences are not dramatic, they do in fact exist.

## SECTION VI

### ANISOTROPIC ELASTIC-PLASTIC-CREEP ANALYSIS

#### A. Anisotropic Creep Theory

The application of matrix analysis procedures to problems involving anisotropic creep is at present academic. Neither meaningful analytical research nor appropriate test data has been found. Therefore the procedure presented here for anisotropic creep is a simple extension of that already described in previous sections. Accordingly, only the difference and additional assumptions are discussed.

Strains due to anisotropic creep can be handled in a way similar to those due to isotropic creep. The step-by-step procedure has only to be modified for the anisotropic behavior by substituting Equations 19 and 20 for Equations 5 and 7 respectively in the manner described for time independent plastic anisotropy in Section V-D. The additional assumptions implied by this simple extension are the following:

- (1) The anisotropic parameters calculated from zero time simple directional tests (by either Hu theory or the proposed extension) are valid for anisotropic creep.
- (2) The effective creep strain equation, Equation 10, remains valid and the empirical constants ( $\alpha, \beta, \gamma$ ) are determined for the tensile creep test in the assumed effective stress-strain direction.

Because testing of structures exhibiting anisotropic creep has apparently not been done, the anisotropic creep procedure cannot be checked out against tests at this time. However, the results of a sample calculation are presented for a hypothetical material having this characteristic.

#### B. Sample Problem

The 1100-F aluminum shear lag specimen, already analyzed for isotropic creep, is used for an anisotropic creep analysis making the following assumptions:

- (1) All the uniaxial data (Figure 25) employed in the isotropic creep analysis is assumed to refer to the y-y (2-2) effective direction of the anisotropic creep analysis.
- (2) The plastic anisotropic parameters (extension of Hu's theory) for the effective stress-strain curve of the 2024-T4 aluminum alloy material for successive levels of stress, 32 ksi, 37 ksi, 40 ksi, etc., are arbitrarily chosen for the stress levels, 2 ksi, 3 ksi, 4 ksi, etc., of the 1100-F aluminum effective stress-strain curve TC1 (Figure 25). Thus:

$\bar{\sigma}$	$\bar{\epsilon}$	$\alpha_{11} = 2\alpha_{12}$	$\alpha_{22}$	$\alpha_{44}$
2000	.000222	0.394	1.000	0.697
3000	.000359	.510	1.000	.755
4000	.000540	.590	1.000	.795
5000	.000815	.660	1.000	.833
6000	.001256	.742	1.000	.871
7000	.001967	.809	1.000	.905
8000	.003038	.835	1.000	.918
10000	.007110	.892	1.000	.945

This means that the uniaxial x-x (1-1) predicted stress-strain curve and the shear x-y stress-strain curve are arbitrarily stiffer than the corresponding isotropic curves.

The node strains obtained, using the anisotropic assumptions for load  $P = 2020$  lbs at time  $t = 3$  hrs, are presented for the x-axis and along  $x = 1$  in. in Figures (41) and (42) respectively.

In general, the anisotropic results appear to be stiffer than those for the isotropic case, and this is especially true for the vertical gage line, where the anisotropic shear strains are of the order of  $3/4$  of the isotropic values. This should be expected, due to the fact that the anisotropic parameters used are all less than, or at the most equal to, their isotropic equivalents.

## SECTION VII

### CONCLUSION

The linear, matrix structural analysis methods currently in general use throughout the aerospace industry have recently been extended to include structures loaded into the inelastic material behavior regime. However, very little published information is available correlating predicted results with the test data.

The current report recommends a simple analytical approach to such problems. It is based upon the concept of initial strains in combination with a suitable matrix of influence coefficients, obtained by standard linear matrix structural analysis methods. The initial strains are those associated with plasticity and creep.

Some particularly useful tests of aluminum and aluminum alloy shear lag structures have been performed previously for the Air Force. These structures have been analyzed by the recommended method, and the resulting agreement (for both the plasticity and the creep tests) is considered to be very encouraging. On the other hand, additional testing must be carried out and correlations with analysis made before the method can be considered as fully evaluated.

In the meantime, the writers believe that sufficient confidence in the method has been established that it may now be used in practical engineering applications. For example, it should be immediately useful in such problems as predicting inelastic strain distributions around stress raisers in simple structural components.

As for the influence of anisotropy, it has been shown that this material property can be readily accommodated in the recommended procedure. Calculations made for the 2024-T4 shear lag structure indicate that, in this case at least, anisotropy plays a minor but discernable role in determining the strain distributions. This evidence is inconclusive, because in this particular test, while the material itself is decidedly anisotropic, the stresses normal to the direction of the applied loads are quite small.

It is recommended that in cases where doubt exists as to the importance of anisotropy, it be included in the analysis. Certainly in such examples as the shear lag structure, the additional complexity in the use of the computer program is very slight.

There is one very important restriction implicit in the method proposed in this report. Essentially, this method applies only to a structure in which the material is initially in the virgin state, and thereafter experiences only continually-increasing applied loads until failure occurs. This limitation can actually be relaxed to the extent that elastic unloading followed by reloading can also be accommodated, but

completely reversed loading is specifically excluded. For the latter case, a different plasticity theory is needed. It is important that a technique for handling such problems be developed because of the need for such applications in fatigue work. Efforts toward removing this restriction are currently under way under government contract.

Other than the preceding, the largest remaining obstacle to complete inelastic analysis of practical aerospace structures is believed to be the dearth of appropriate material property data, and constitutive laws to describe them.

SECTION VIII

FIGURES

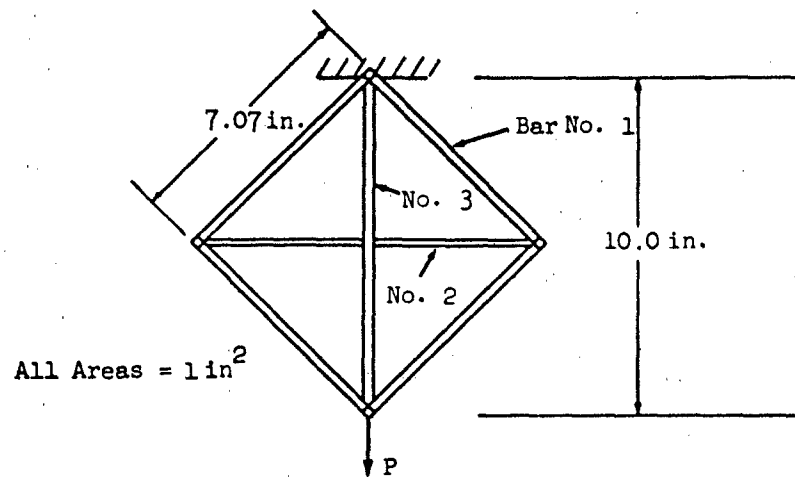


Fig. 1 Truss Structure

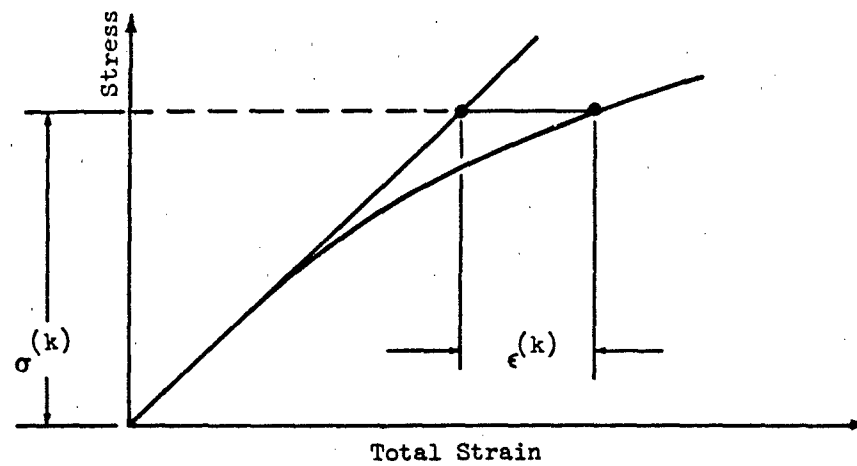


Fig. 2 Constant Stress Method

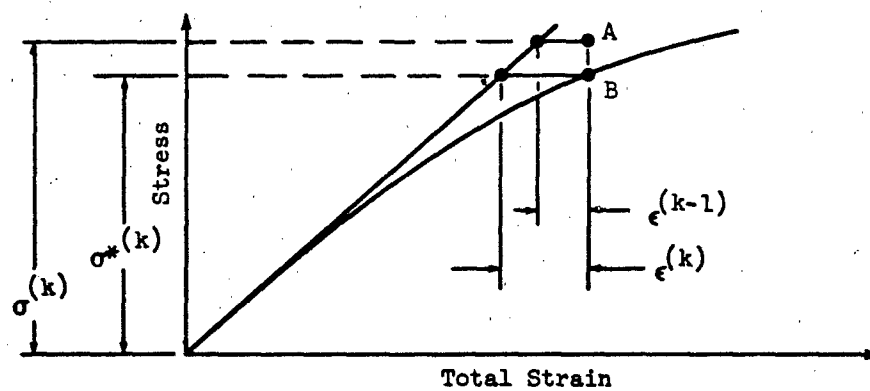


Fig. 3 Constant Strain Method

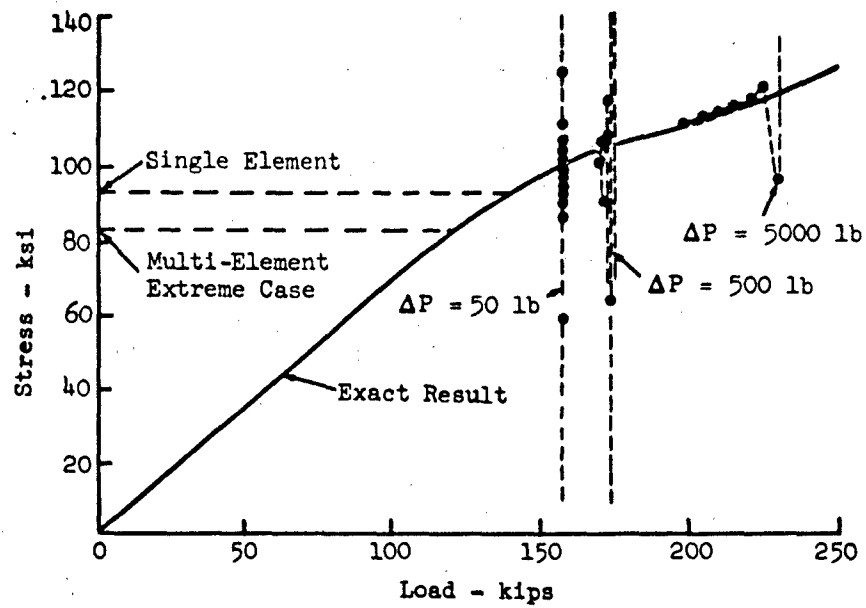


Fig. 4 Results of Constant Stress Method for Bar No. 3 of Truss

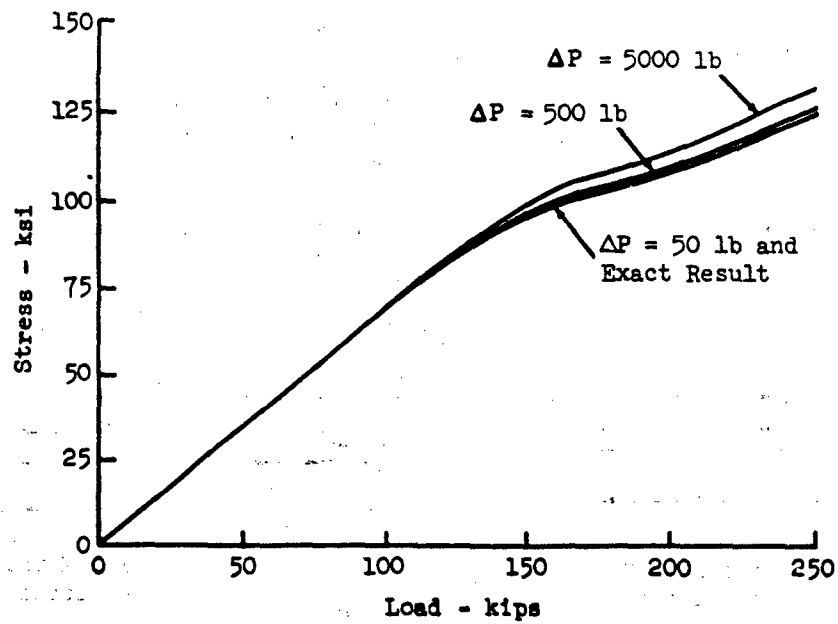


Fig. 5 Results of Constant Strain Method for Bar No. 3 of Truss



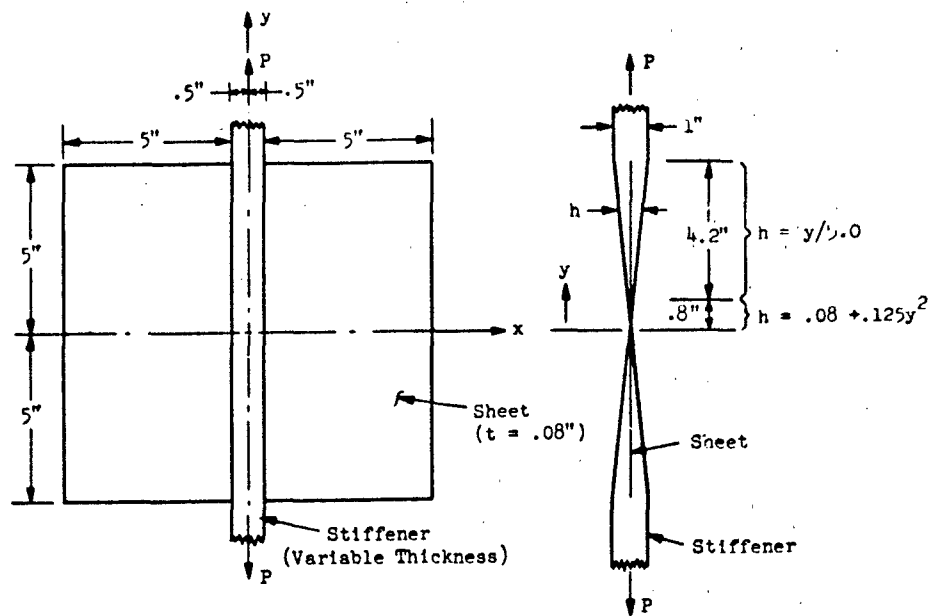


Fig. 6 Shear-Lag Specimen Designated SIS1 - From  
Air Force Report No. RTD-TDR-63-4032;  
2024-T4 Aluminum Alloy (1100-F Specimen Similar)

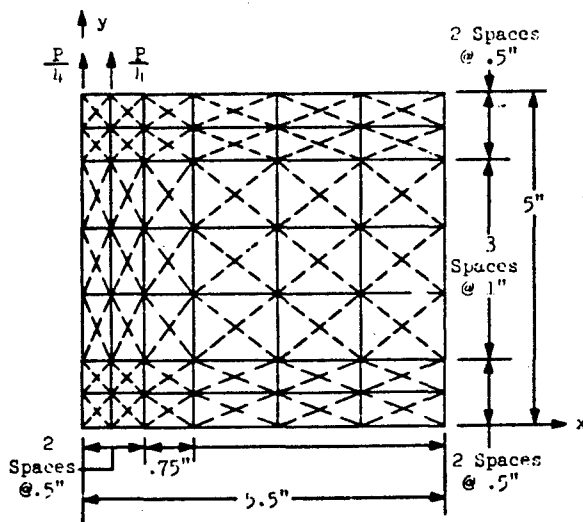


Fig. 7 Stiffness Method  
Idealization

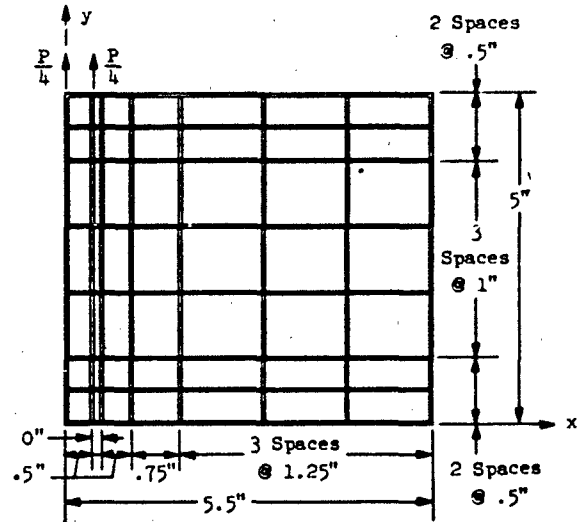


Fig. 8 Force Method  
Idealization

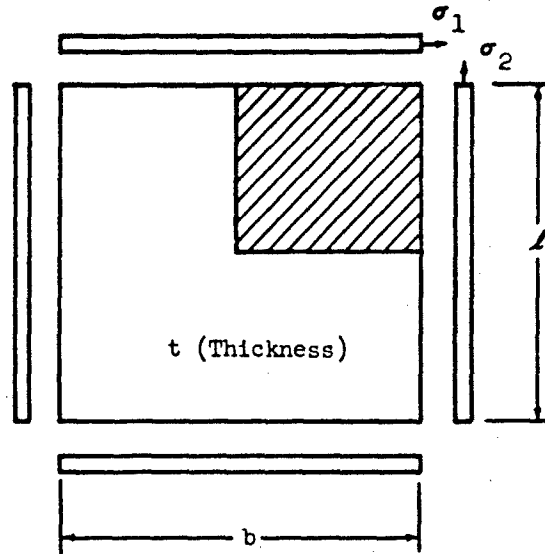


Fig. 9 Typical Elements of Force Idealization

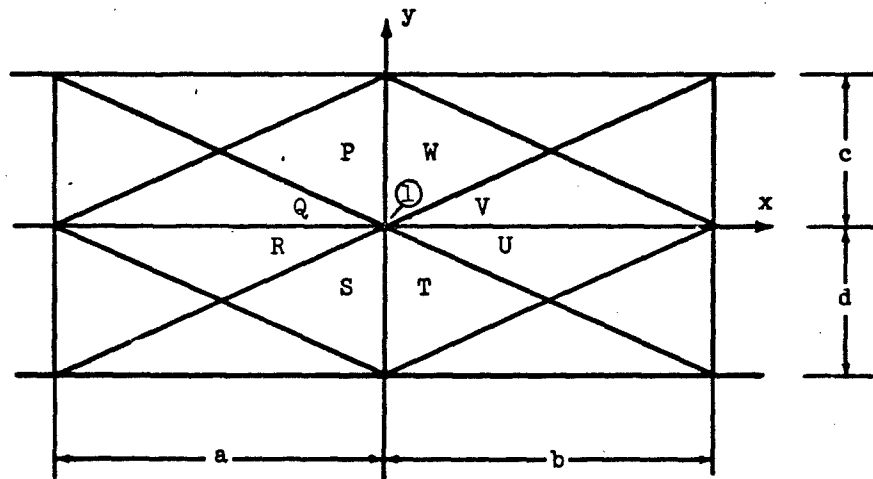


Fig. 10 Typical Elements of Stiffness Idealization

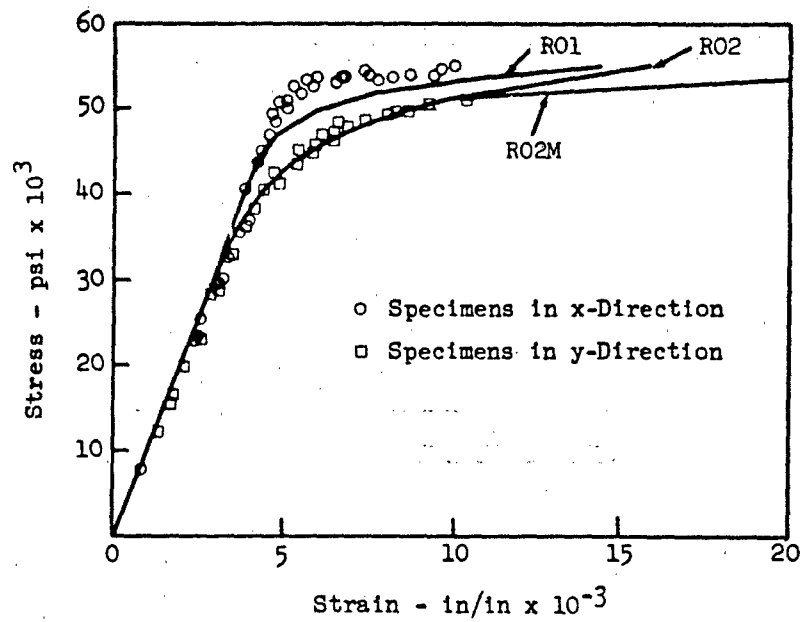


Fig. 11 2024-T4 Aluminum Alloy Stress-Strain Data and Curve R02M

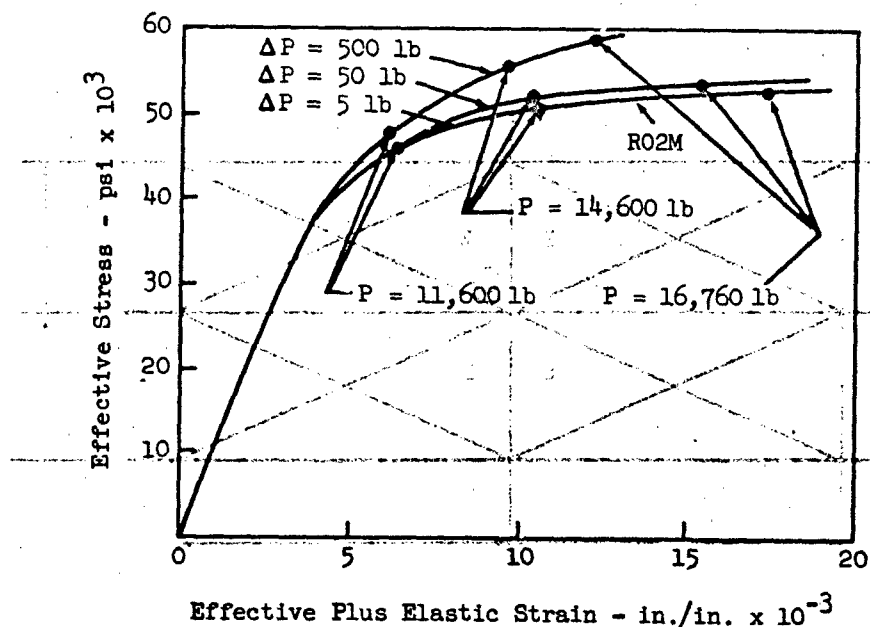
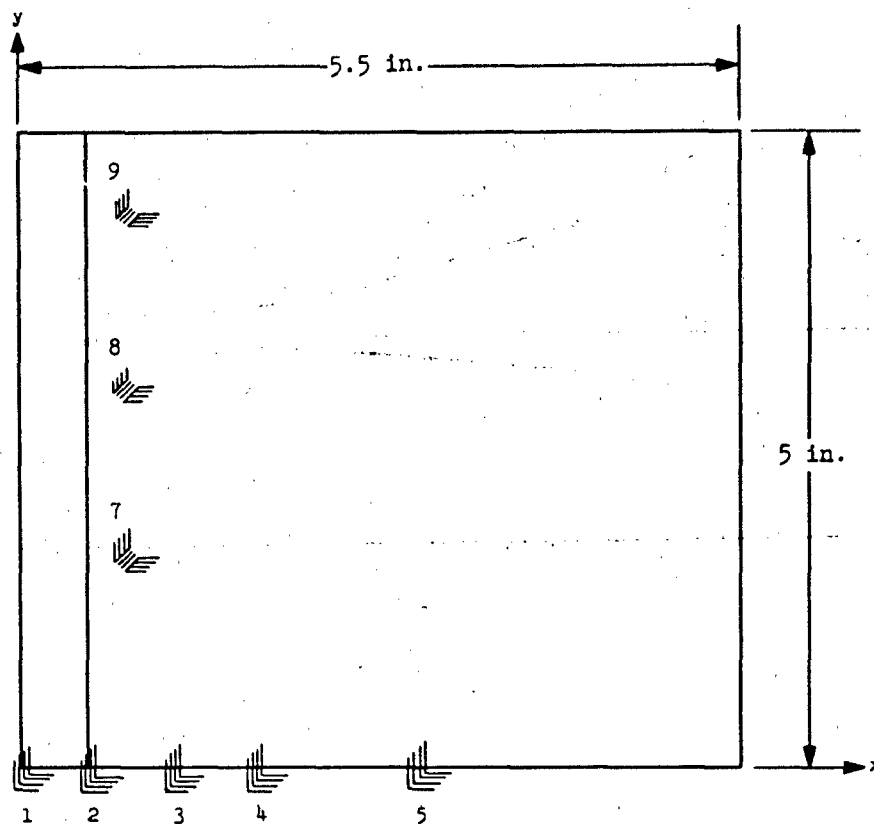


Fig. 12 Comparison of Predicted Effective Stress-Strain Relationship with R02M at (0, 0) for Various Load Increments



Gage Nos.		Co-ordinates		Gage Nos.		Co-ordinates	
Front	Back	x in.	y in.	Front	Back	x in.	y in.
1	11	0.0	0.0	6	16	-1.125	0.0
2	12	0.5	0.0	7	17	0.8125	1.5625
3	13	1.125	0.0	8	18	0.8125	2.8125
4	14	1.750	0.0	9	19	0.8125	4.0625
5	15	3.000	0.0				

Fig. 13 Instrumentation of 2024-T4 Aluminum Alloy Specimen

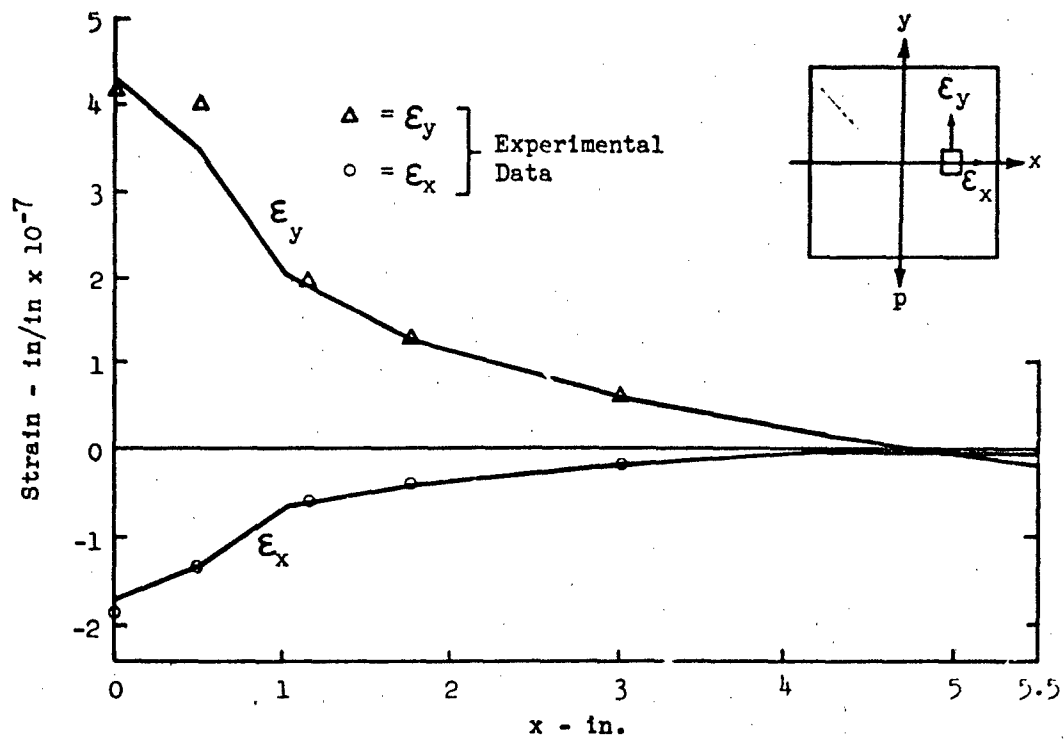


Fig. 14 Elastic Strains Along x-Axis for  $P = 1$  lb

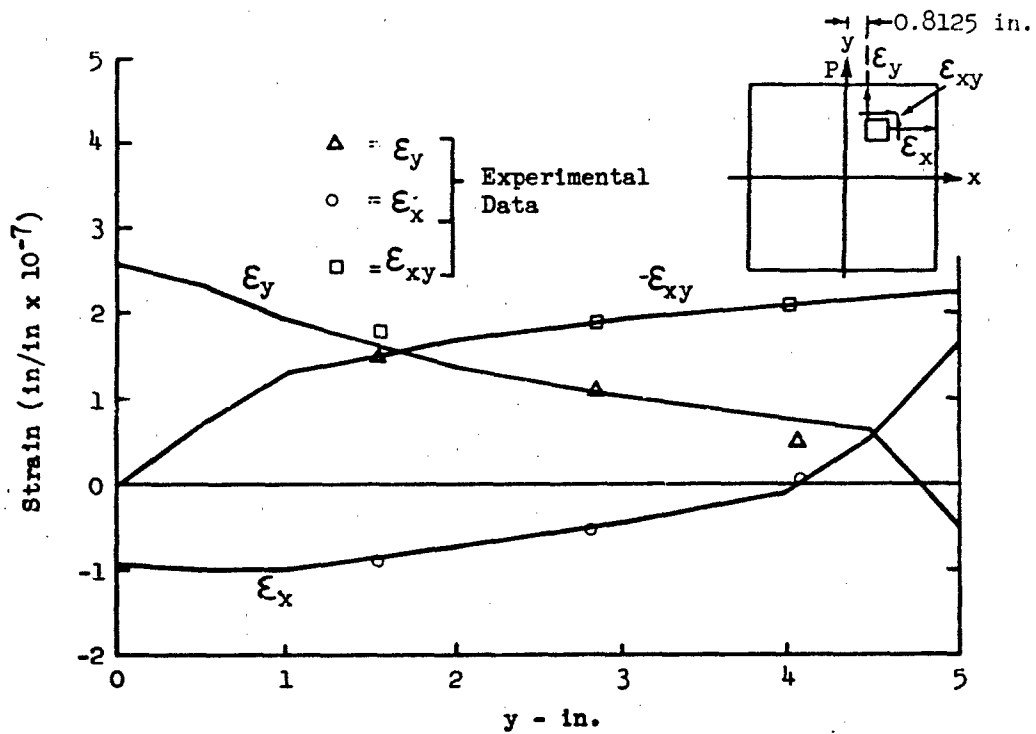


Fig. 15 Elastic Strains Along  $x = 0.8125$  in. for  $P = 1$  lb

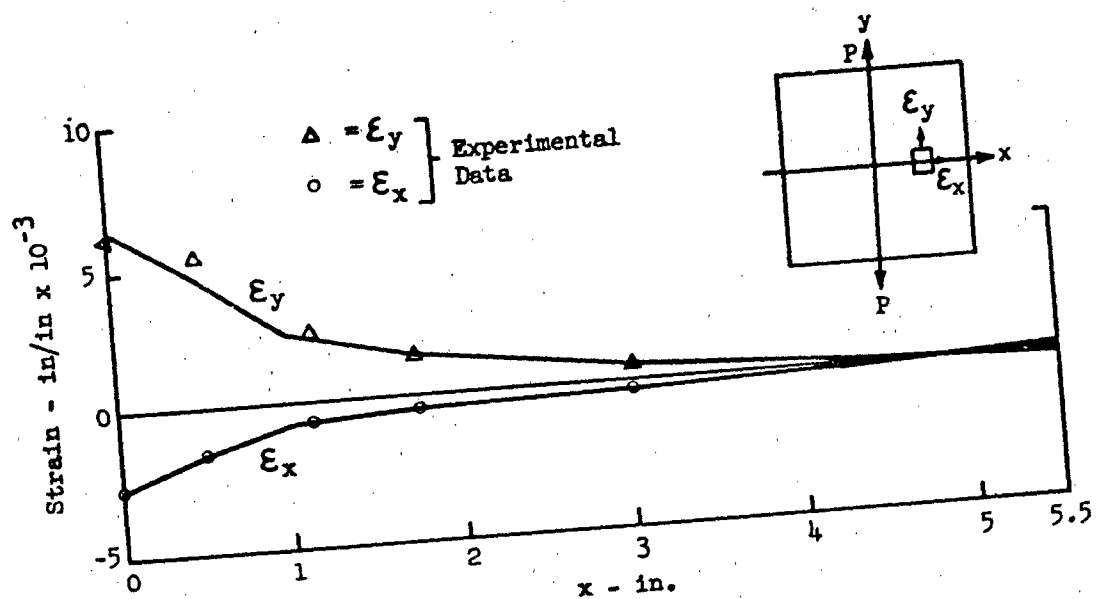


Fig. 16 Strains Along x-Axis for  $P = 11,600$  lb and  $\Delta P = 5$  lb

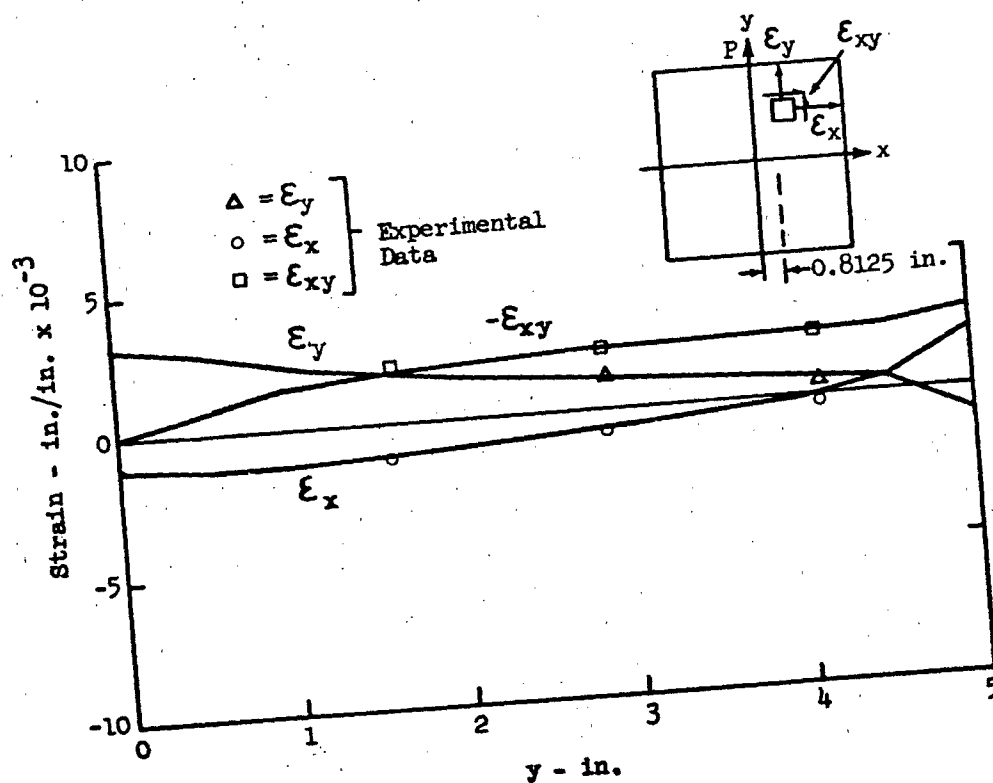


Fig. 17 Strains Along  $x = 0.8125$  in. for  $P = 11,600$  lb and  $\Delta P = 5$  lb

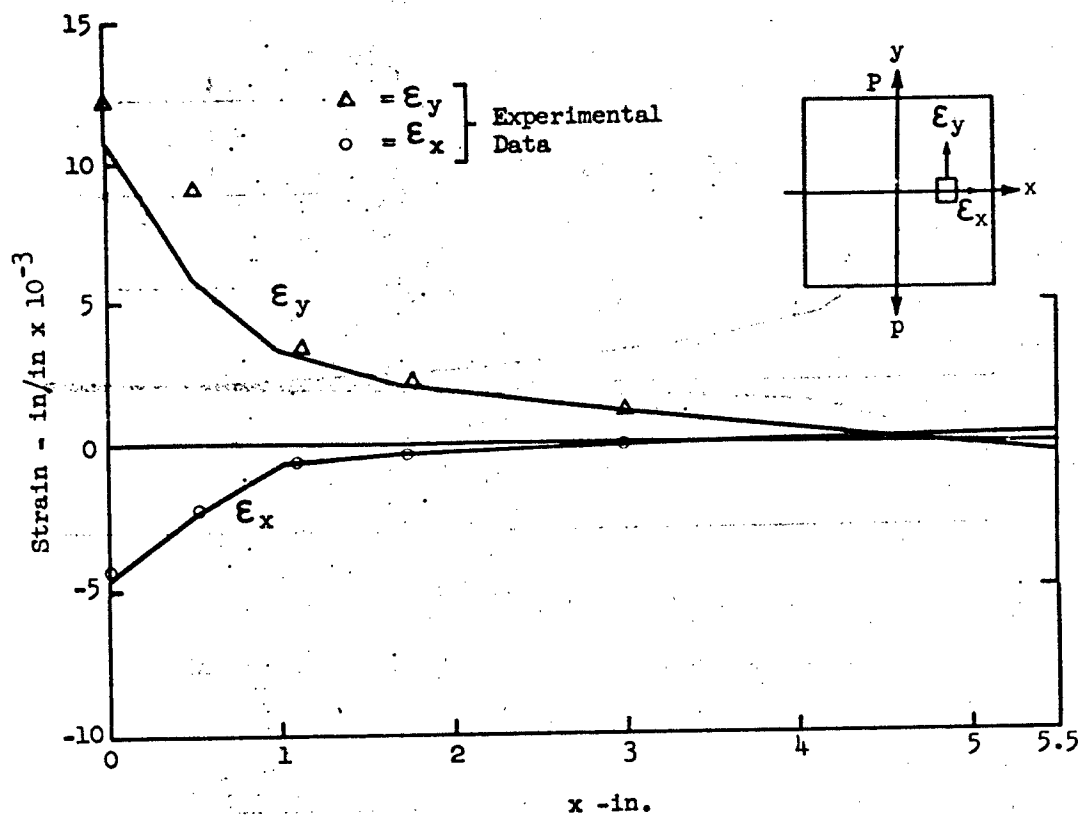


Fig. 18 Strains Along x-Axis for  $P = 14,600$  lb and  $\Delta P = 5$  lb

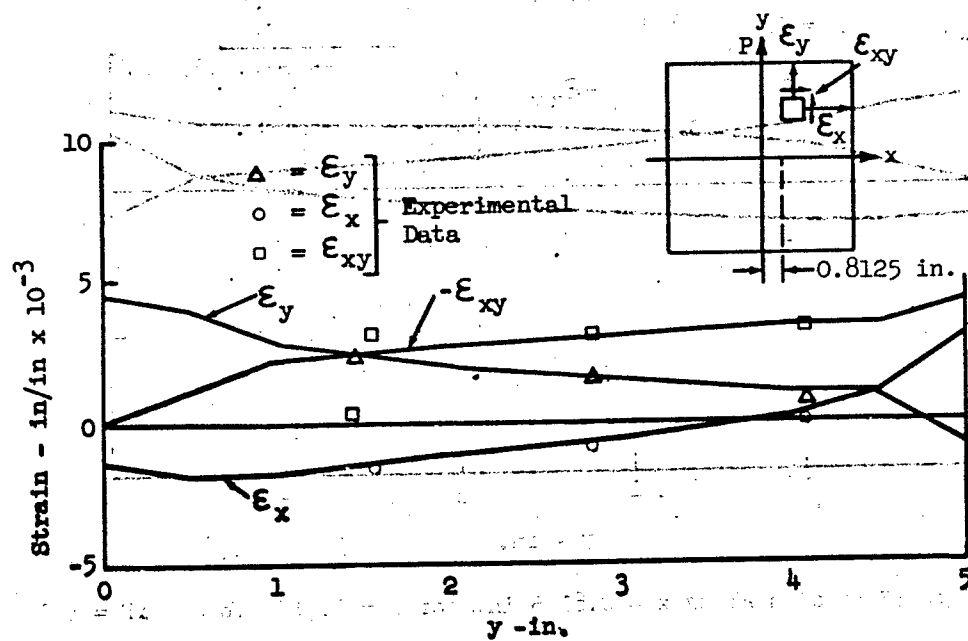


Fig. 19 Strains Along  $x = 0.8125$  in. for  $P = 14,600$  lb and  $\Delta P = 5$  lb

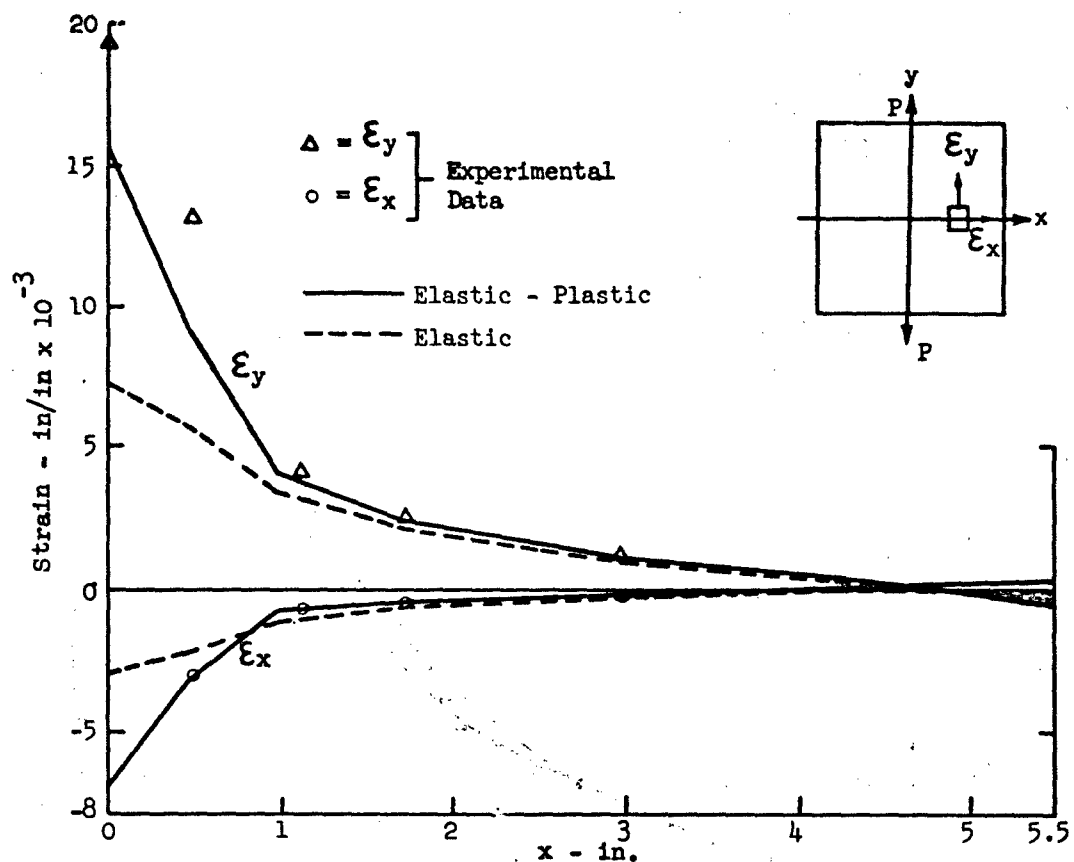


Fig. 20 Strains Along x-Axis for  $P = 16,760 \text{ lb}$ , and  $\Delta P = 5 \text{ lb}$

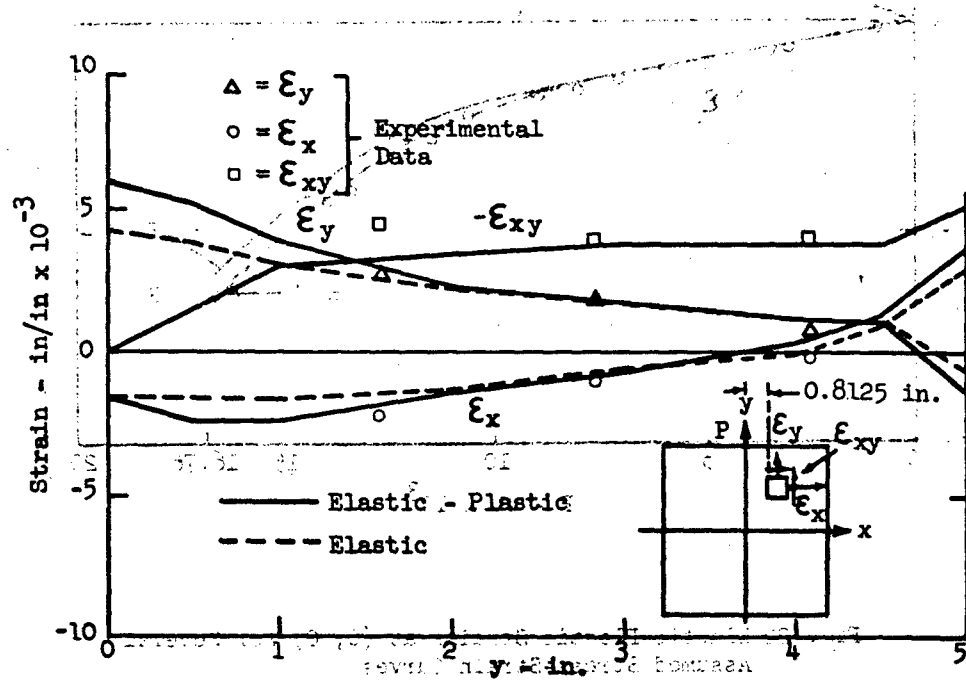


Fig. 21 Strains Along  $x = 0.8125 \text{ in.}$  for  $P = 16,760 \text{ lb}$  and  $\Delta P = 5 \text{ lb}$



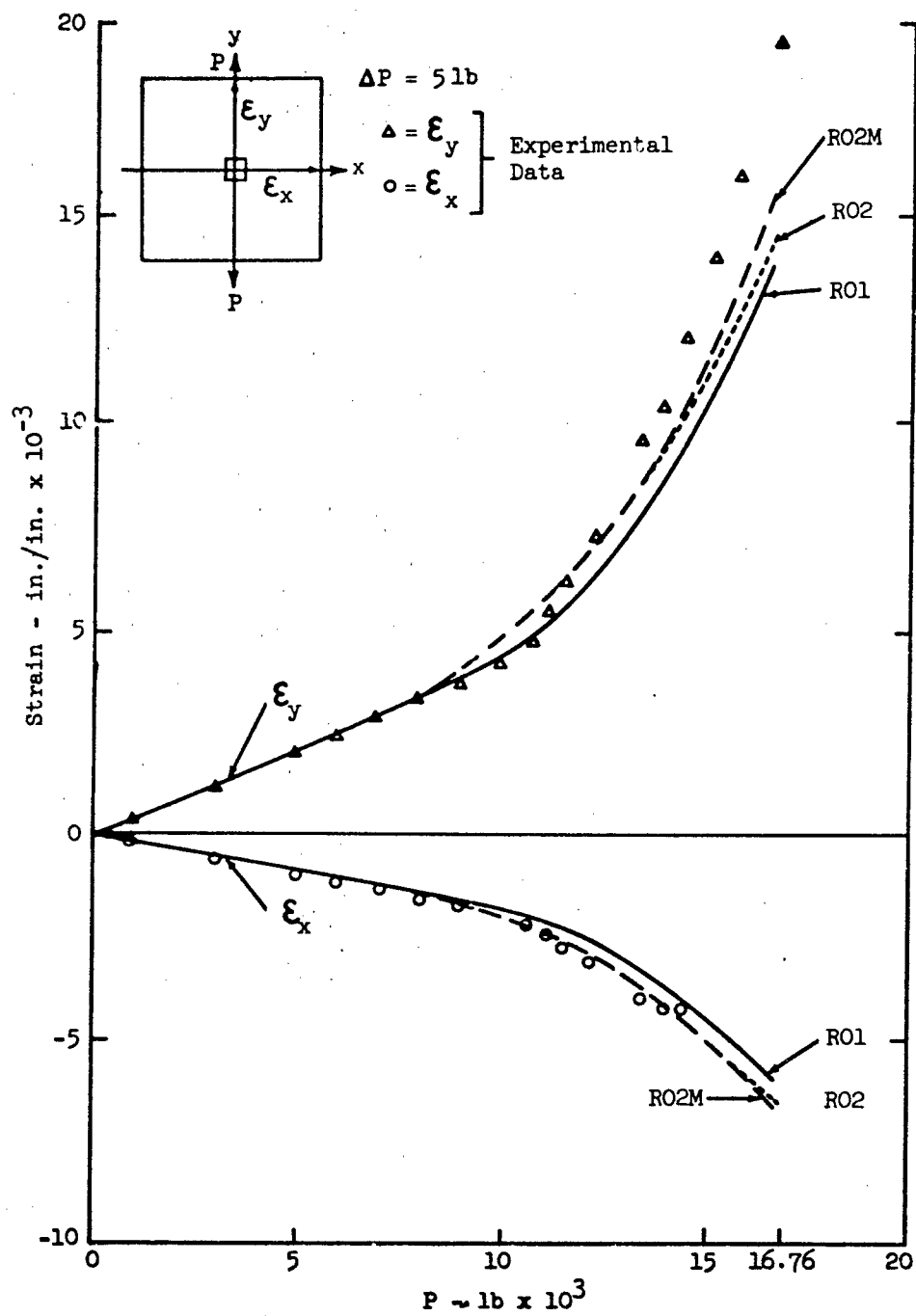


Fig. 22 Elastic-Plastic Strains at (0, 0) for Several Assumed Stress-Strain Curves

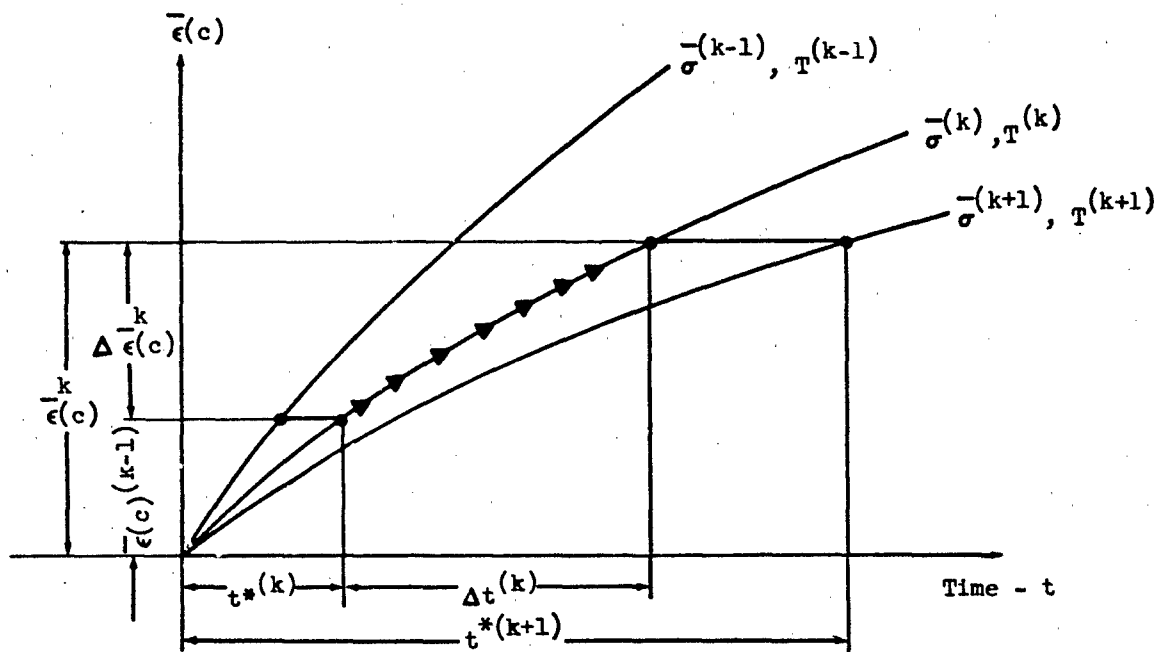


Fig. 23 The Strain Hardening Rule

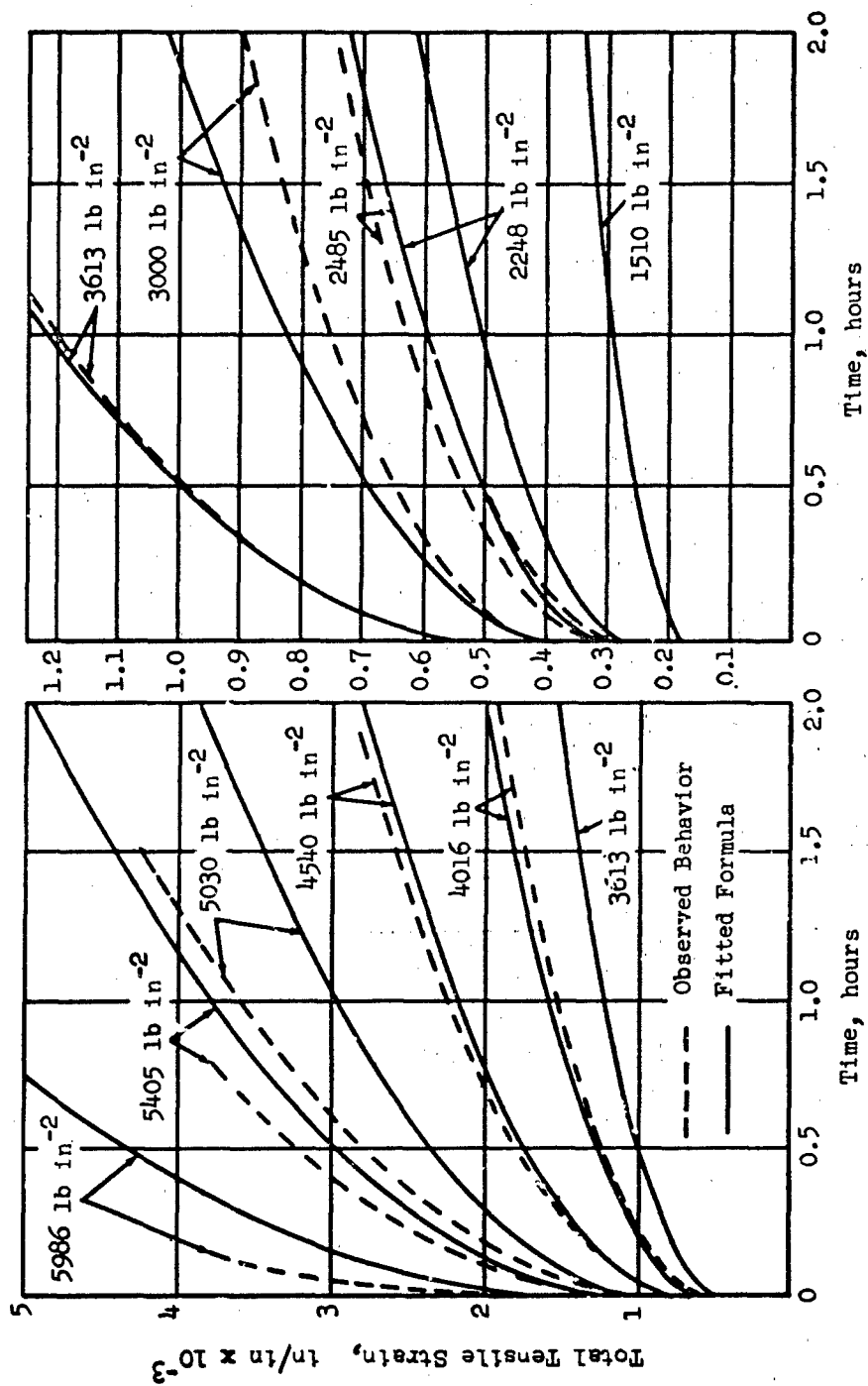


Fig. 24 1100-F Aluminum Time-Dependent Behavior and Fitted Curves (Ref. 7)

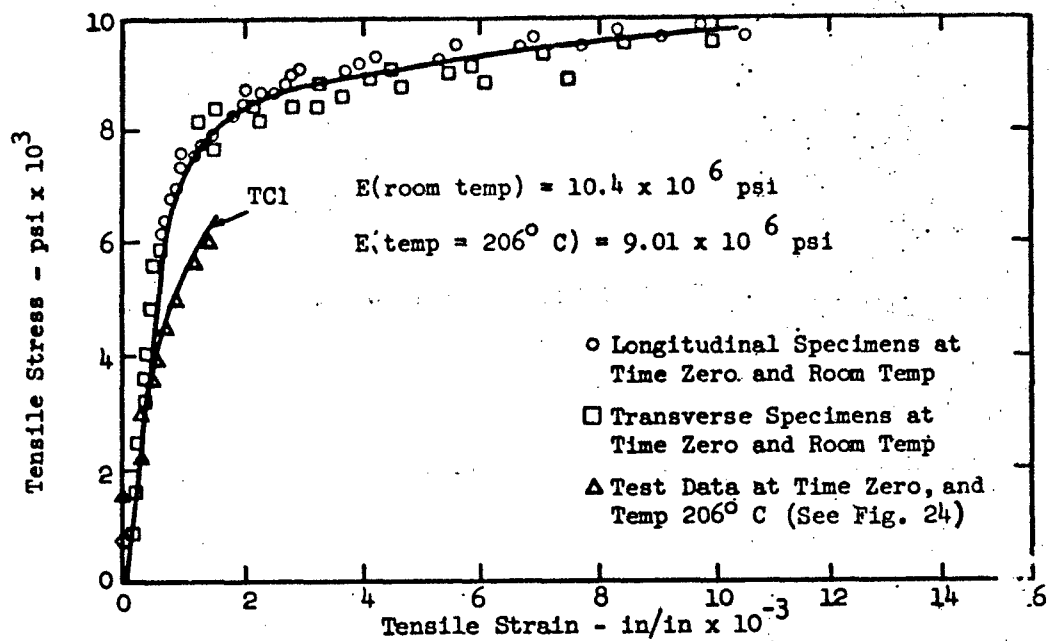


Fig. 25 1100-F Aluminum Stress-Strain Data at Room Temperature and at  $206^\circ \text{C}$ , for Time  $t = 0.00$

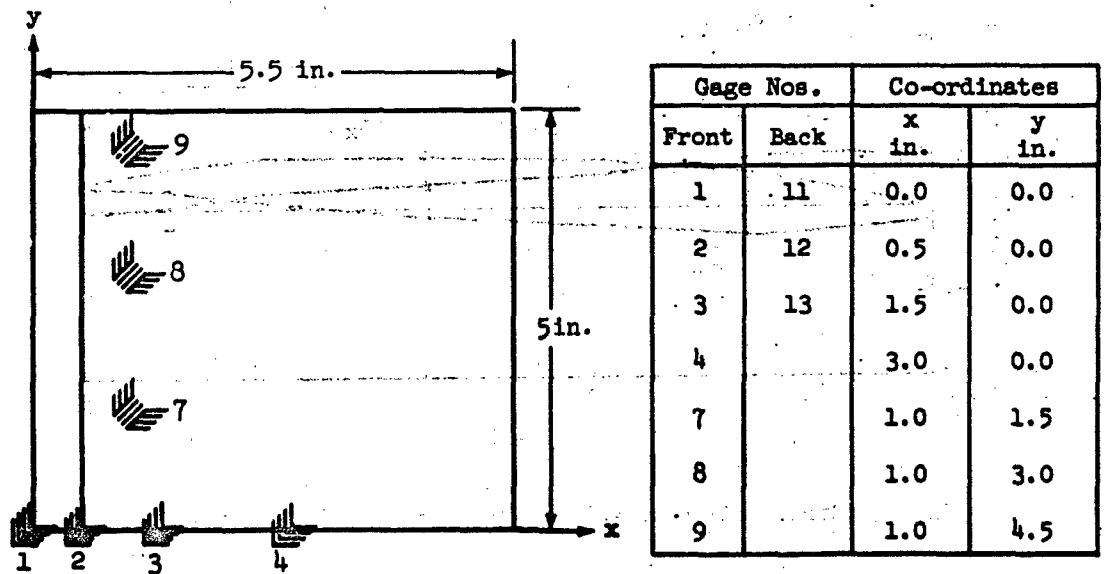


Fig. 26 Location of Strain Gages on 1100-F Specimen (Ref. 7)

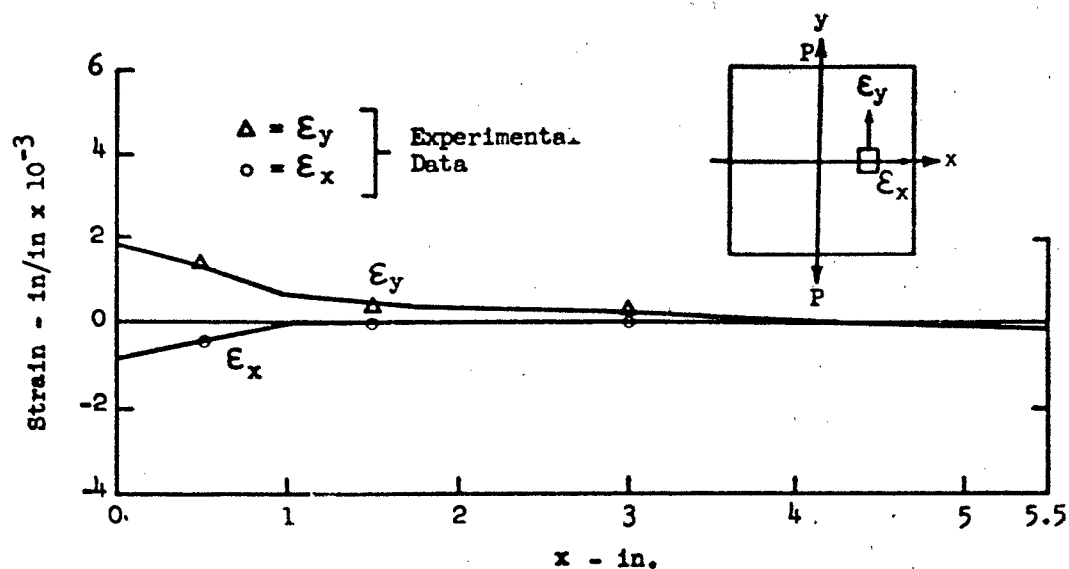


Fig. 27 Strains Along x-Axis for  $P = 1600 \text{ lb}$  and  $t = 0.06 \text{ hr}$

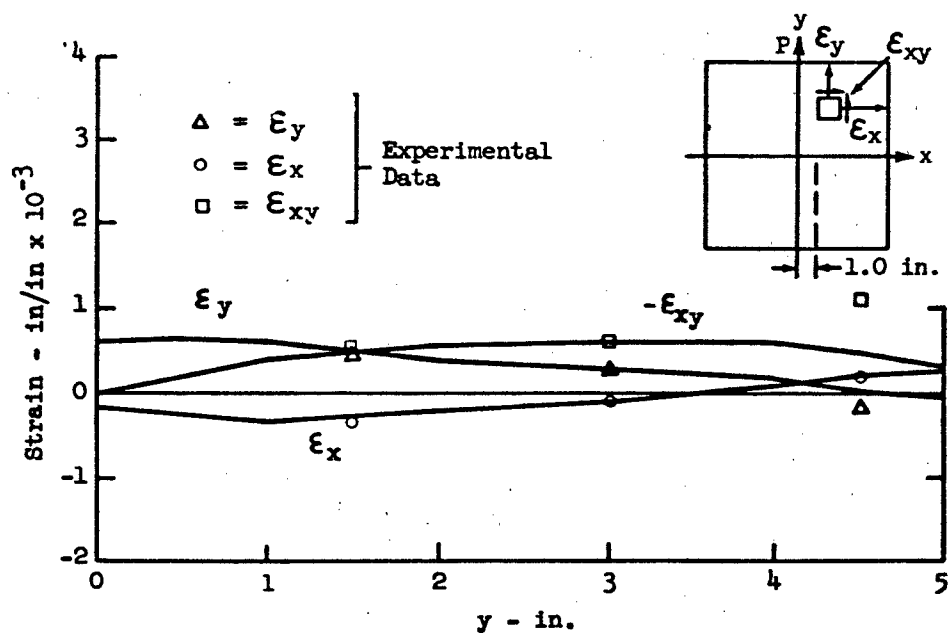


Fig. 28 Strains Along  $x = 1 \text{ in.}$  for  $P = 1600 \text{ lb}$  and  $t = 0.06 \text{ hr}$

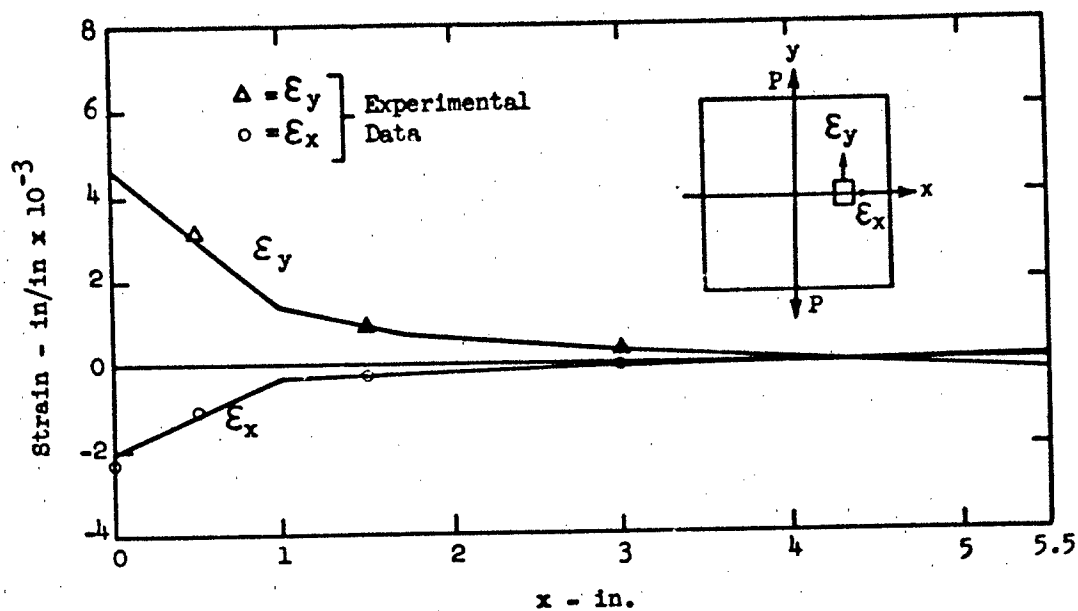


Fig. 29 Strains Along x-Axis for  $P = 2020$  lb and  $t = 1.10$  hr

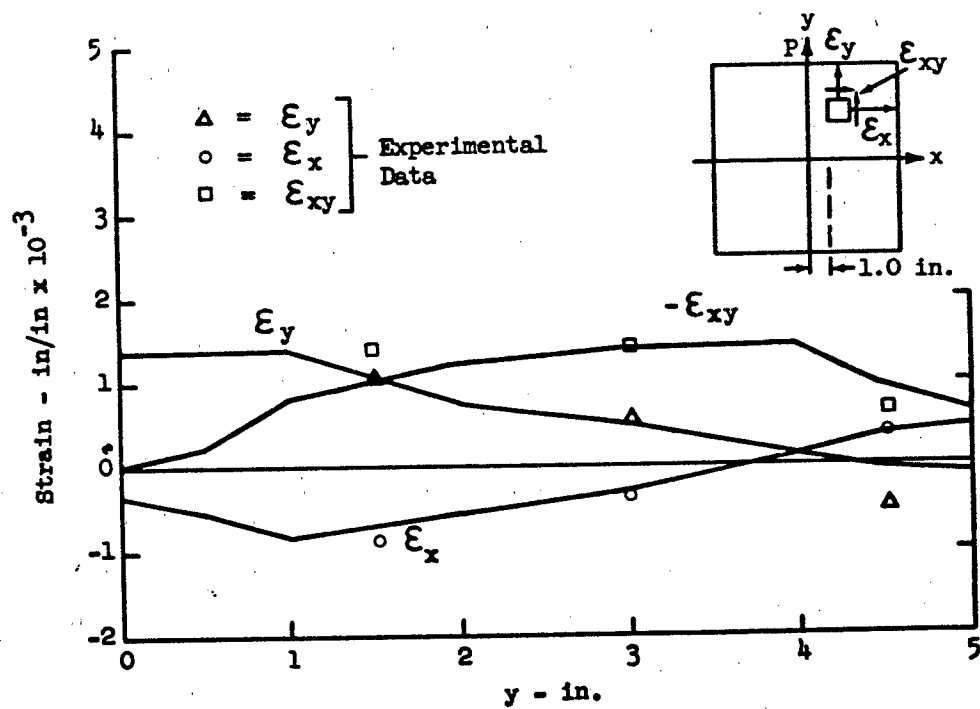


Fig. 30 Strains Along  $x = 1$  in. for  $P = 2020$  lb and  $t = 1.10$  hr

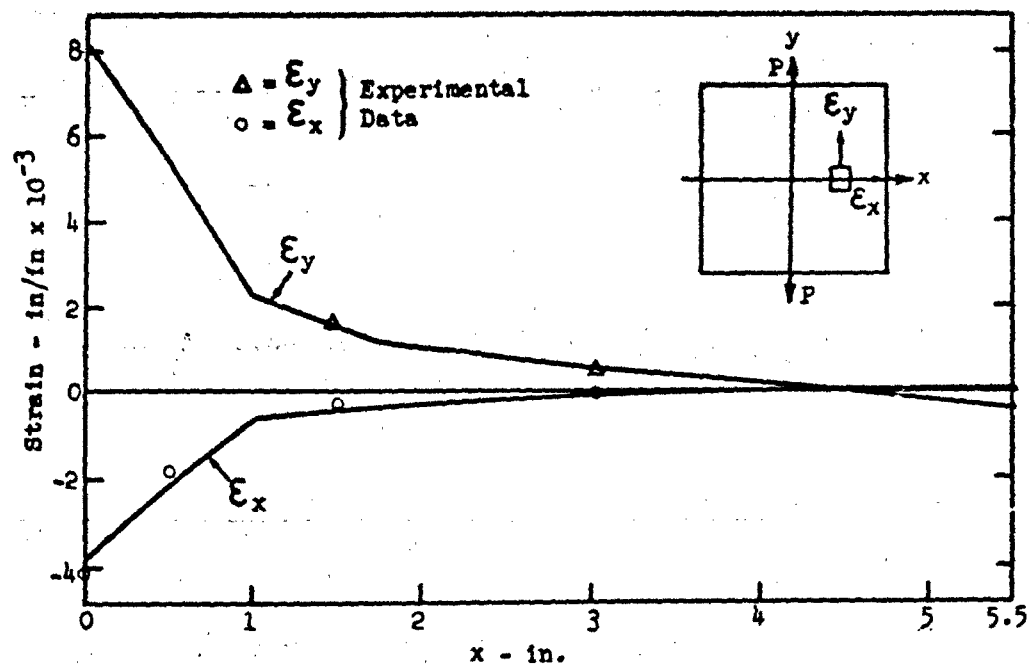


Fig. 31 Strains Along x-Axis for  $P = 2020 \text{ lb}$  and  $t = 3.0 \text{ hr}$

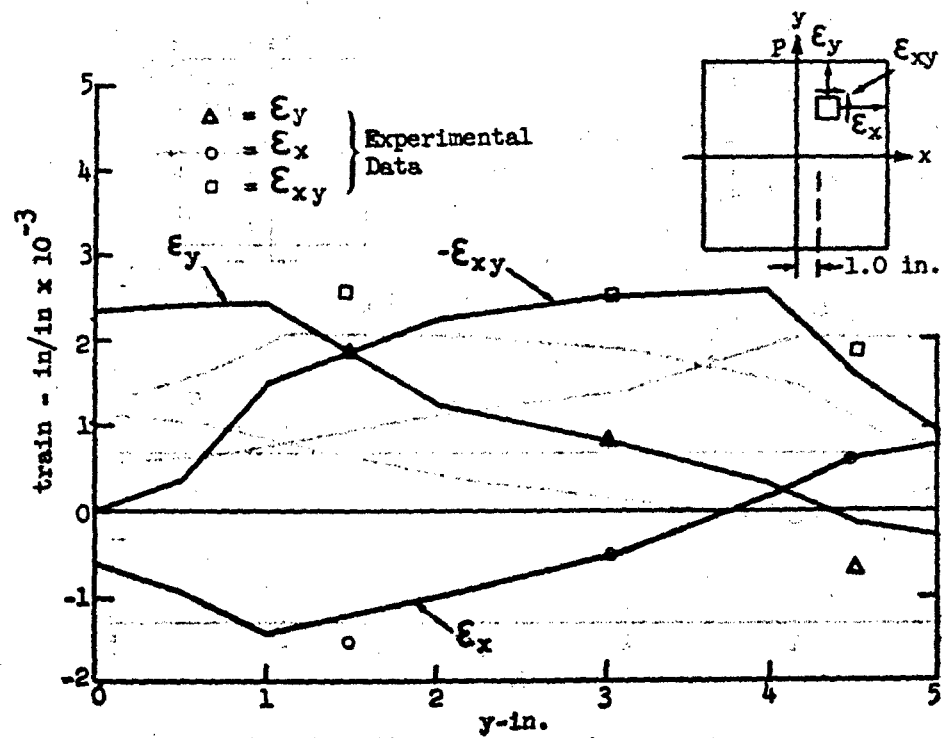


Fig. 32 Strains Along  $x = 1 \text{ in.}$  for  $P = 2020 \text{ lb}$  and  $t = 3.0 \text{ hr}$

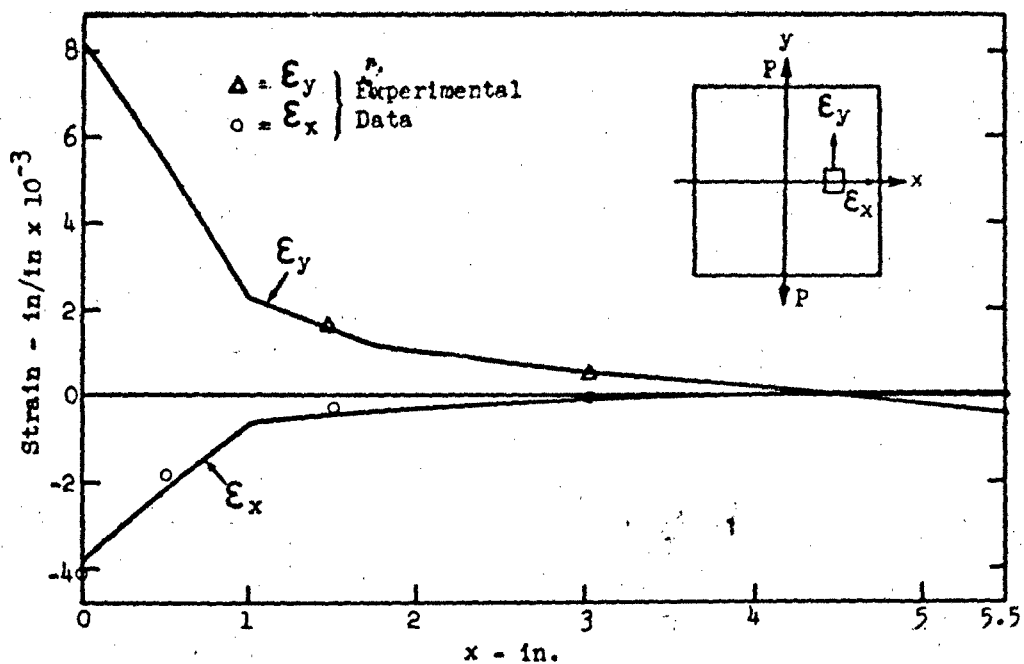


Fig. 31 Strains Along x-Axis for  $P = 2020$  lb and  $t = 3.0$  hr

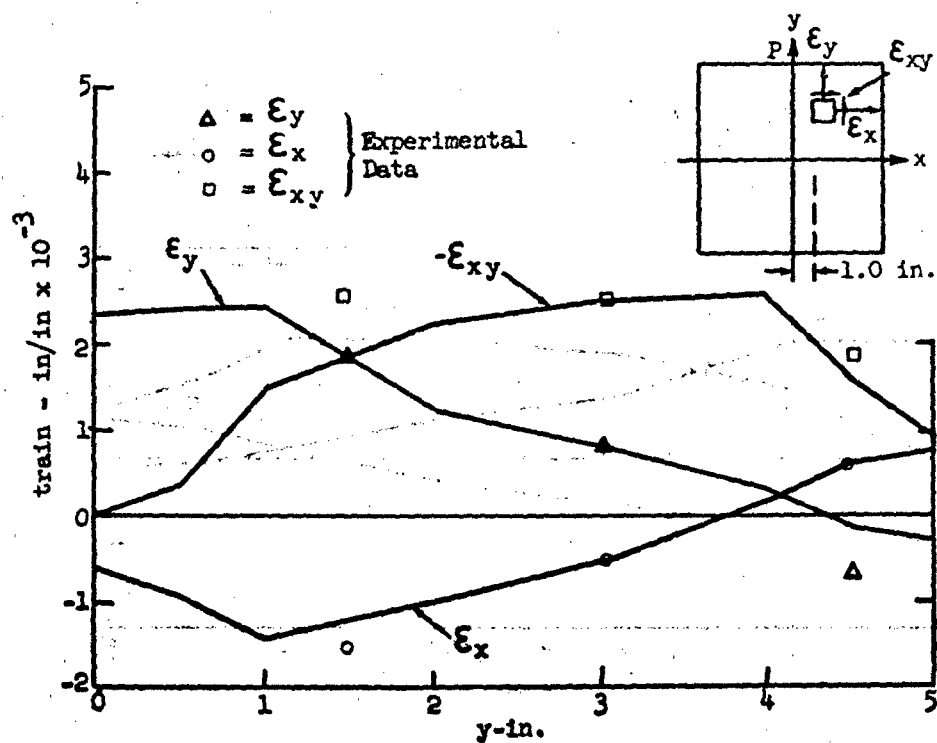


Fig. 32 Strains Along  $x = 1$  in. for  $P = 2020$  lb and  $t = 3.0$  hr



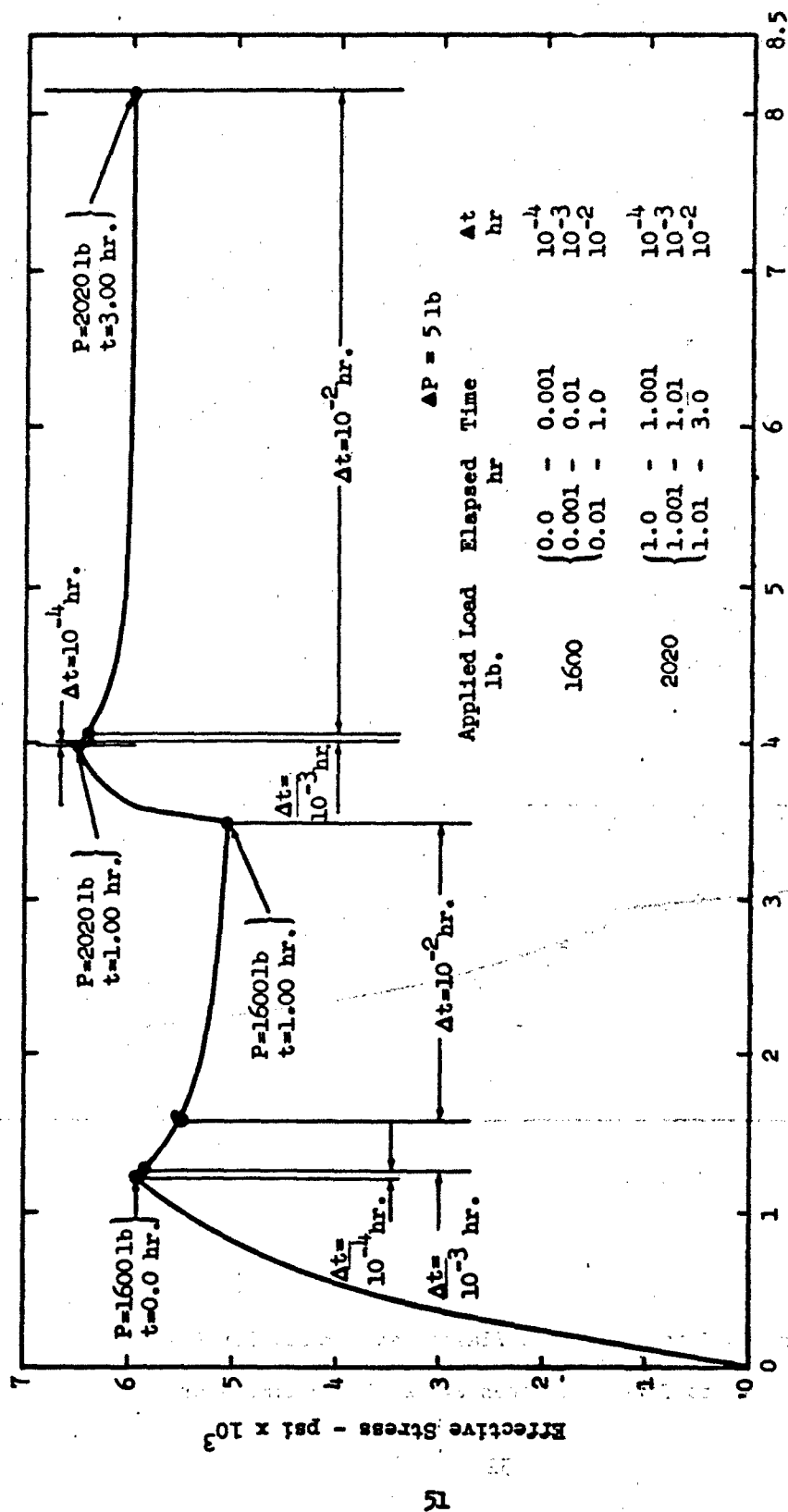


Fig. 33 Effective Stress vs Strain at Center Node

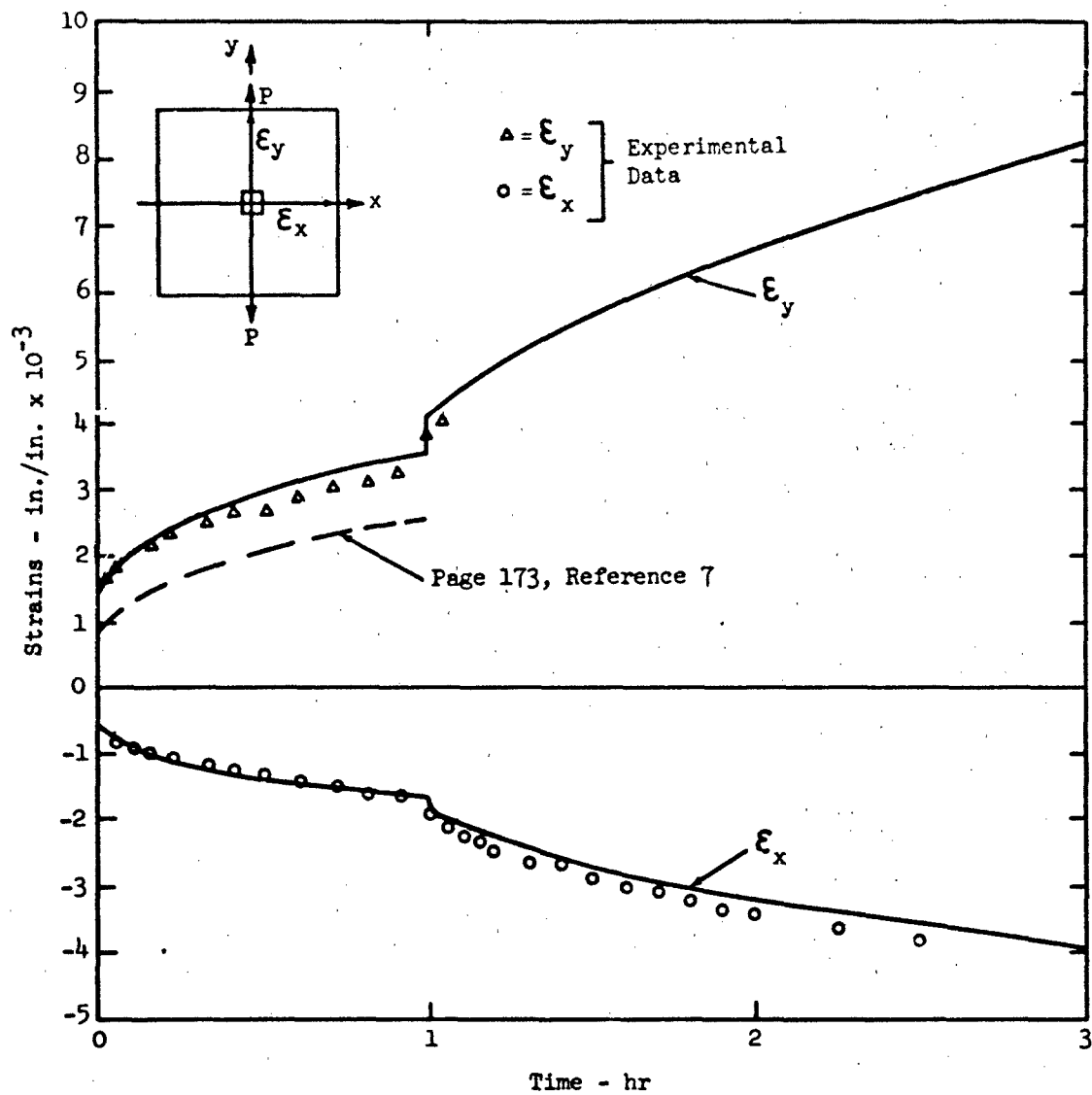


Fig. 34 Total (Elastic, Plastic and Creep) Strains at Center of Specimen (Gage 1) for P=1600 lb to Time 1 hr, then P=2020 lb to Time 3 hr

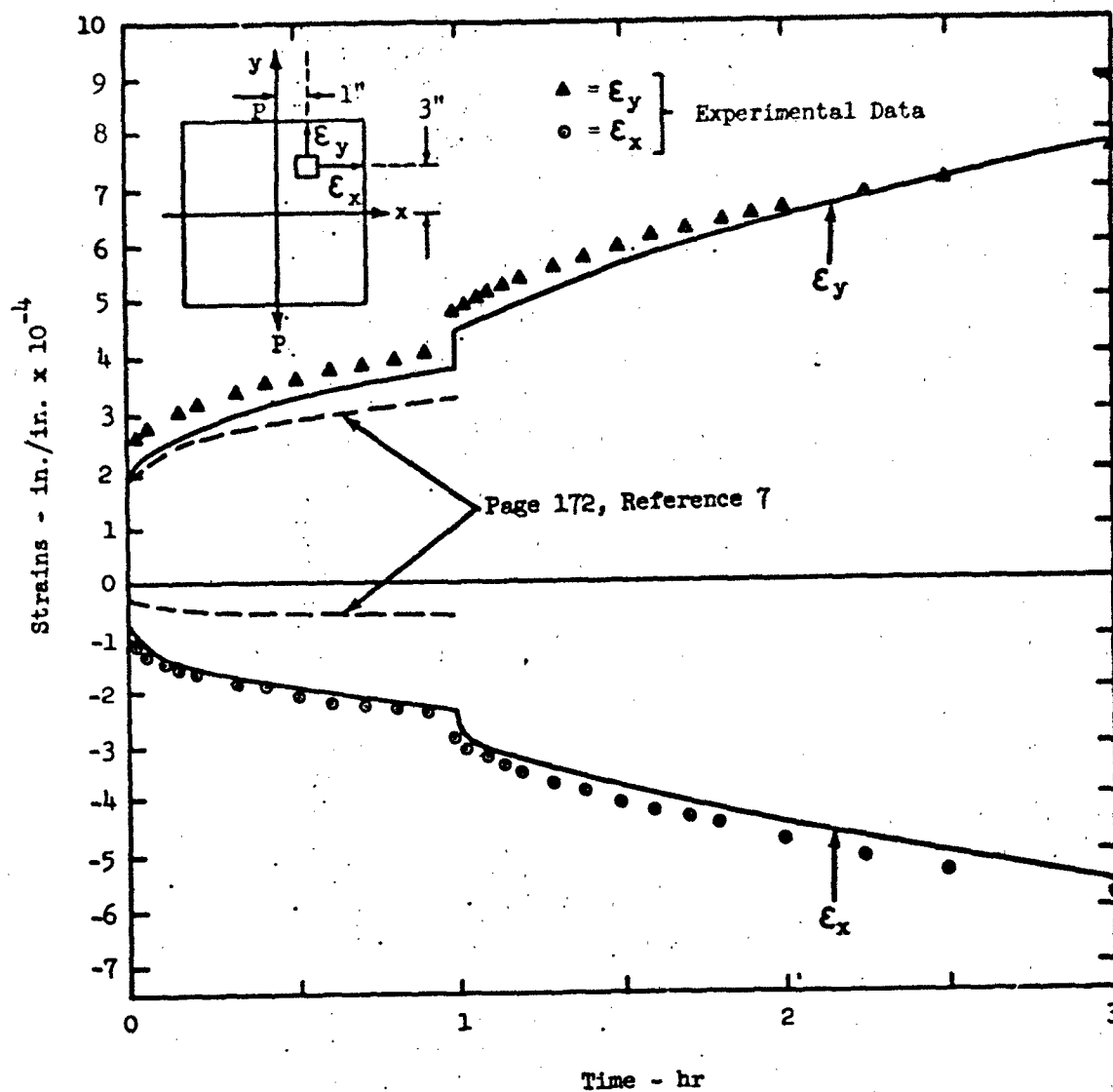


Fig. 35 Total (Elastic, Plastic and Creep) Strains at (1.0 in., 3.0 in.) (Gage 8) for  $P = 1600$  lb to time 1 hr, then  $P = 2020$  lb to time 3 hr

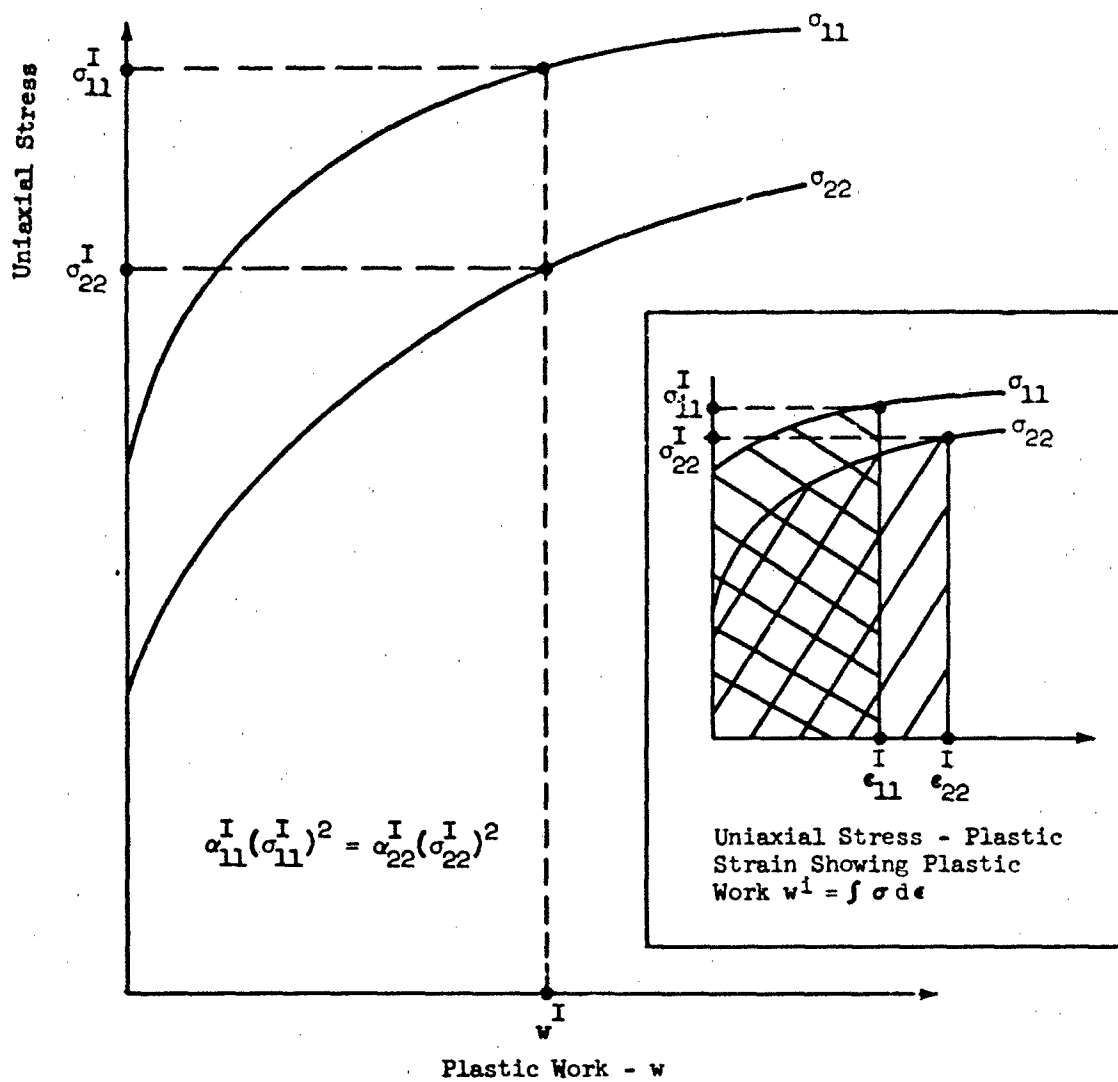


Figure 36 Typical Uniaxial Stress vs Plastic Work, w, Plot.

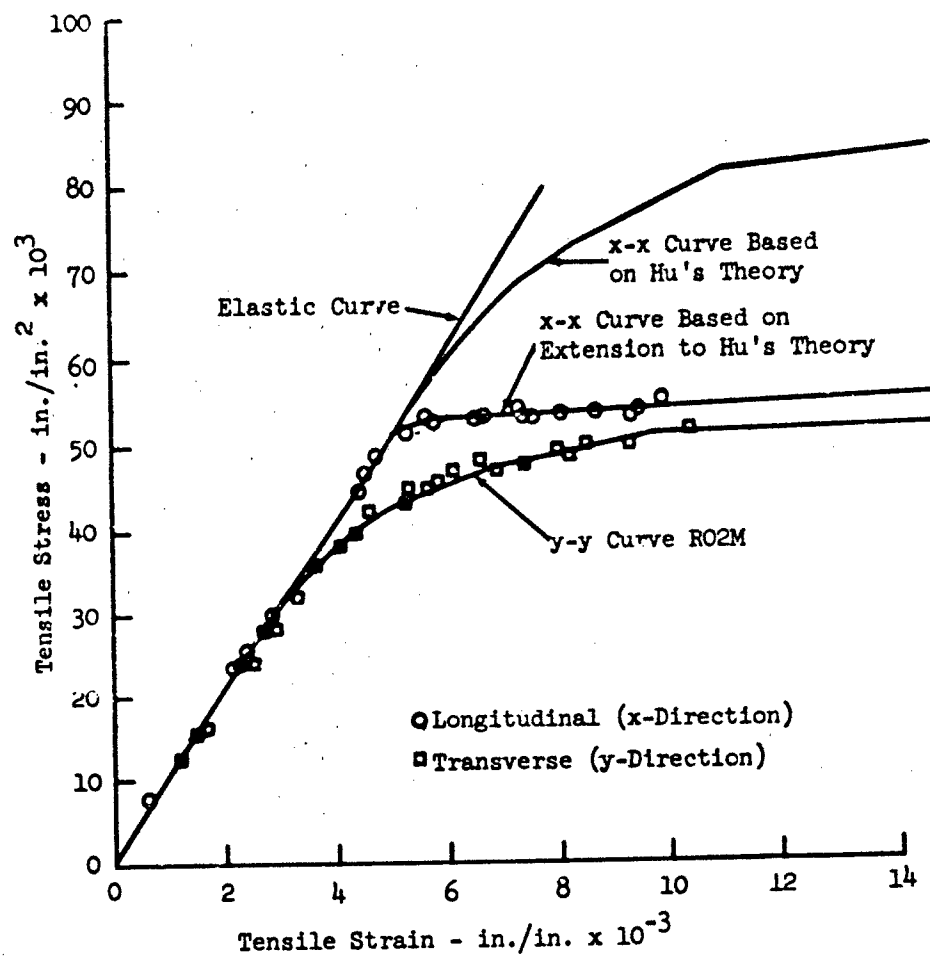


Fig. 37 Assumed Effective Stress (y-y) Curve,  
Calculated x-x Curves and Test Data

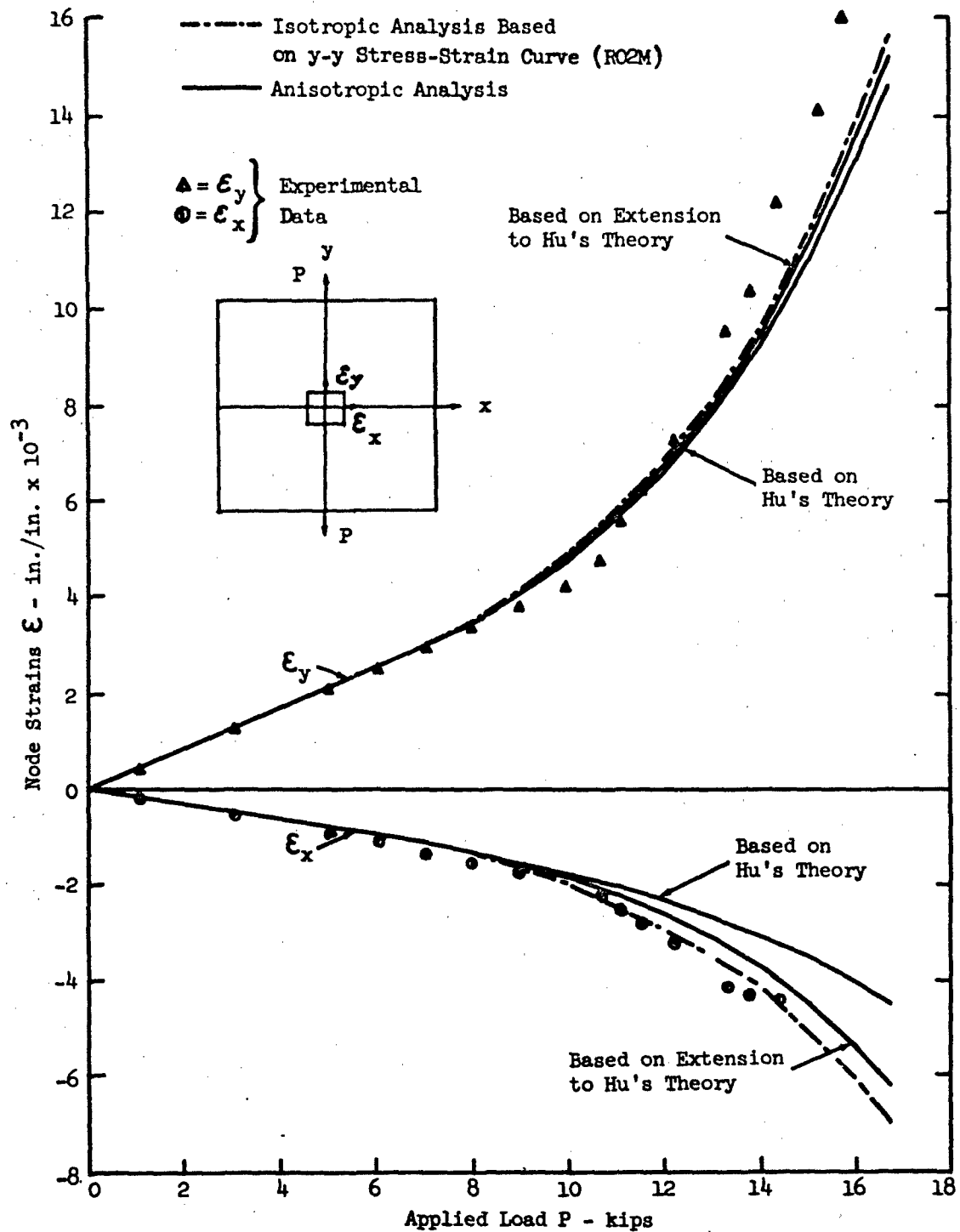


Fig. 38 Node Strains at (0, 0) - Isotropic and Anisotropic Analysis

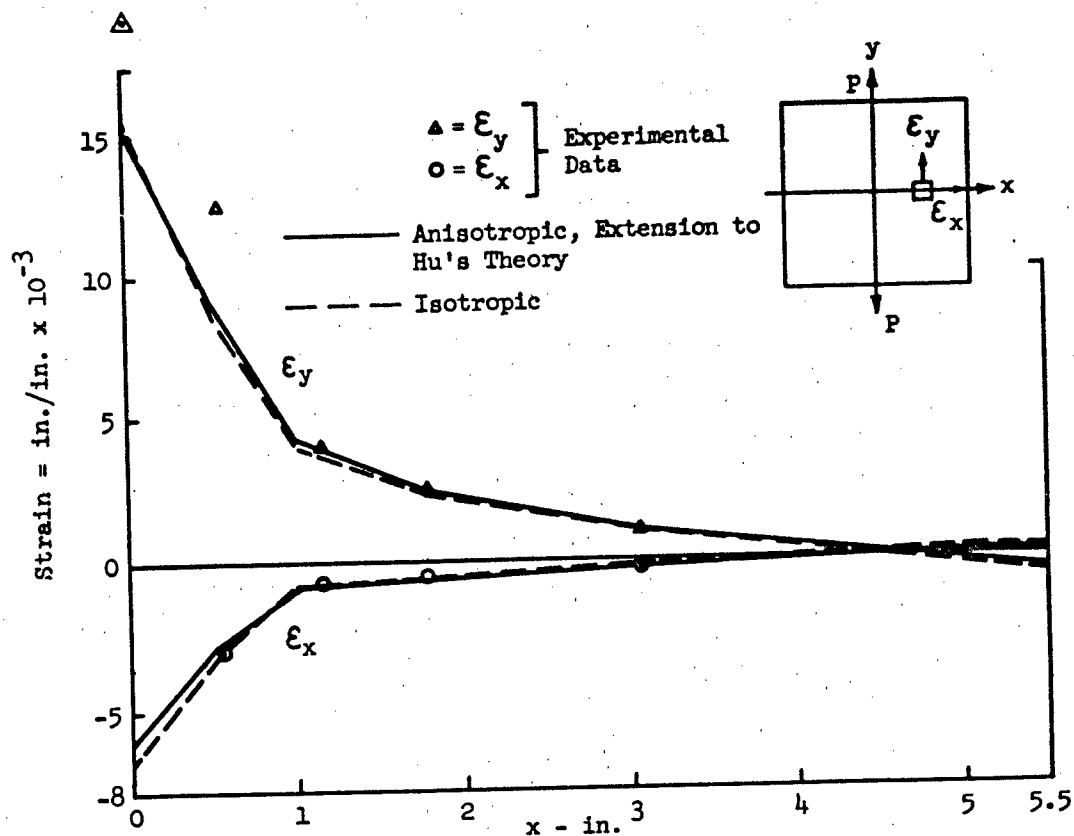


Fig. 39 Strains Along  $x$  - Axis for  $P = 16,760$  lb.  
Isotropic and Anisotropic Analyses

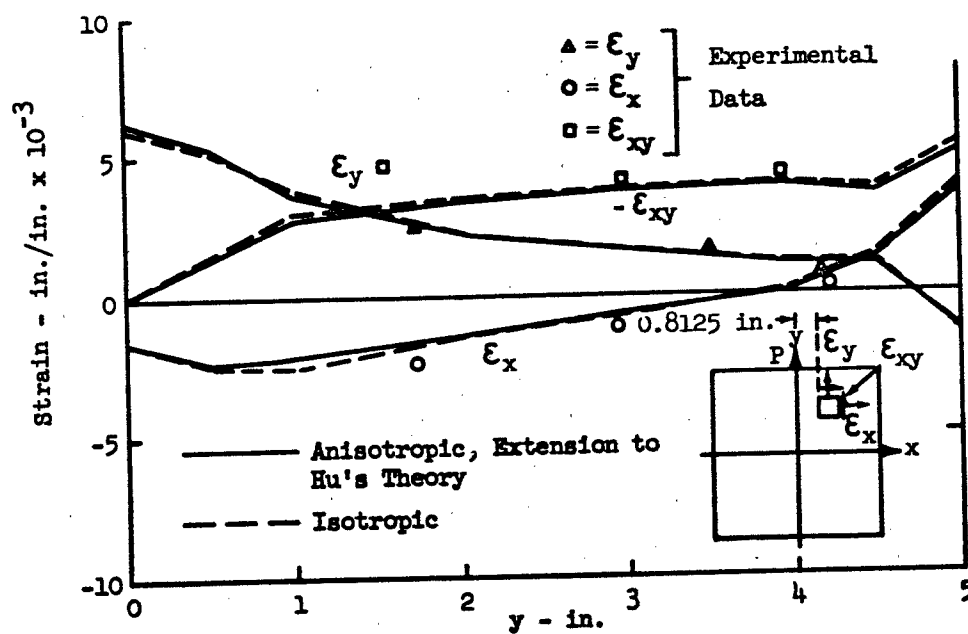


Fig. 40 Strains Along  $x = 0.8125$  in. for  $P = 16,760$  lb.  
Isotropic and Anisotropic Analyses

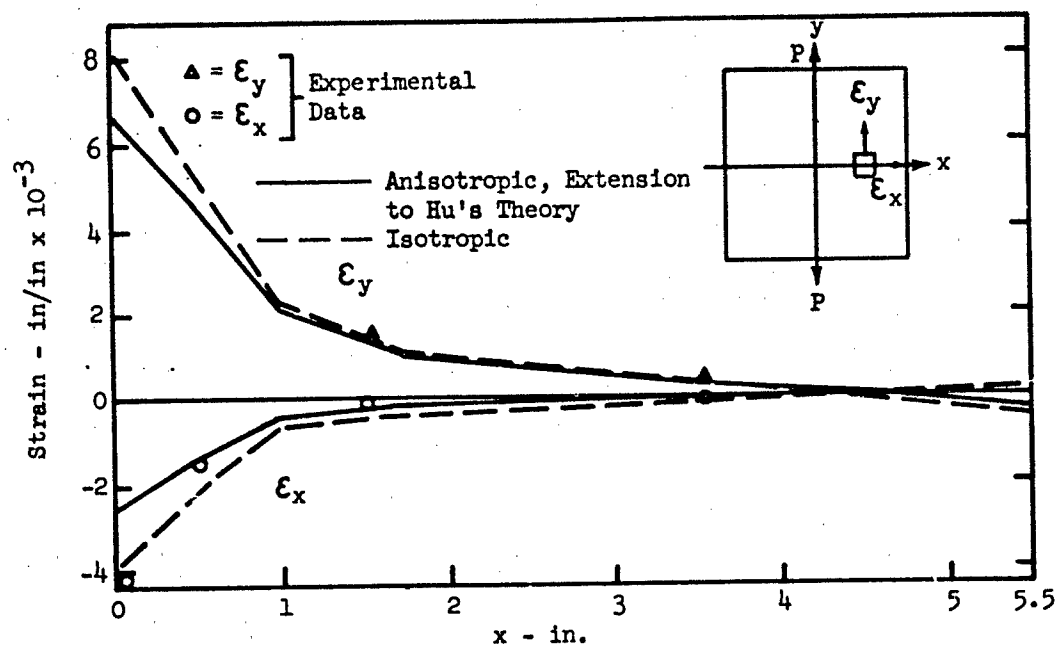


Fig. 41 Strains Along x - Axis for  $P = 2020$  lb and  $t = 3.0$  hr. Isotropic and Anisotropic Analyses

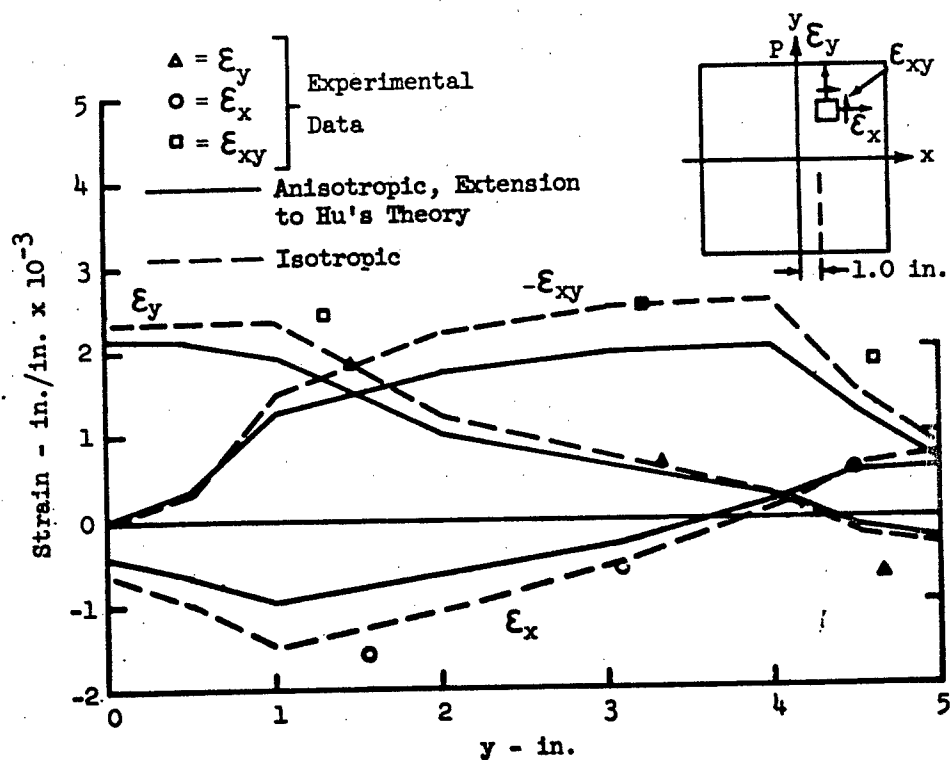


Fig. 42 Strains Along  $x = 1$  in. for  $P = 2020$  lb and  $t = 3.0$  hr. Isotropic and Anisotropic Analyses



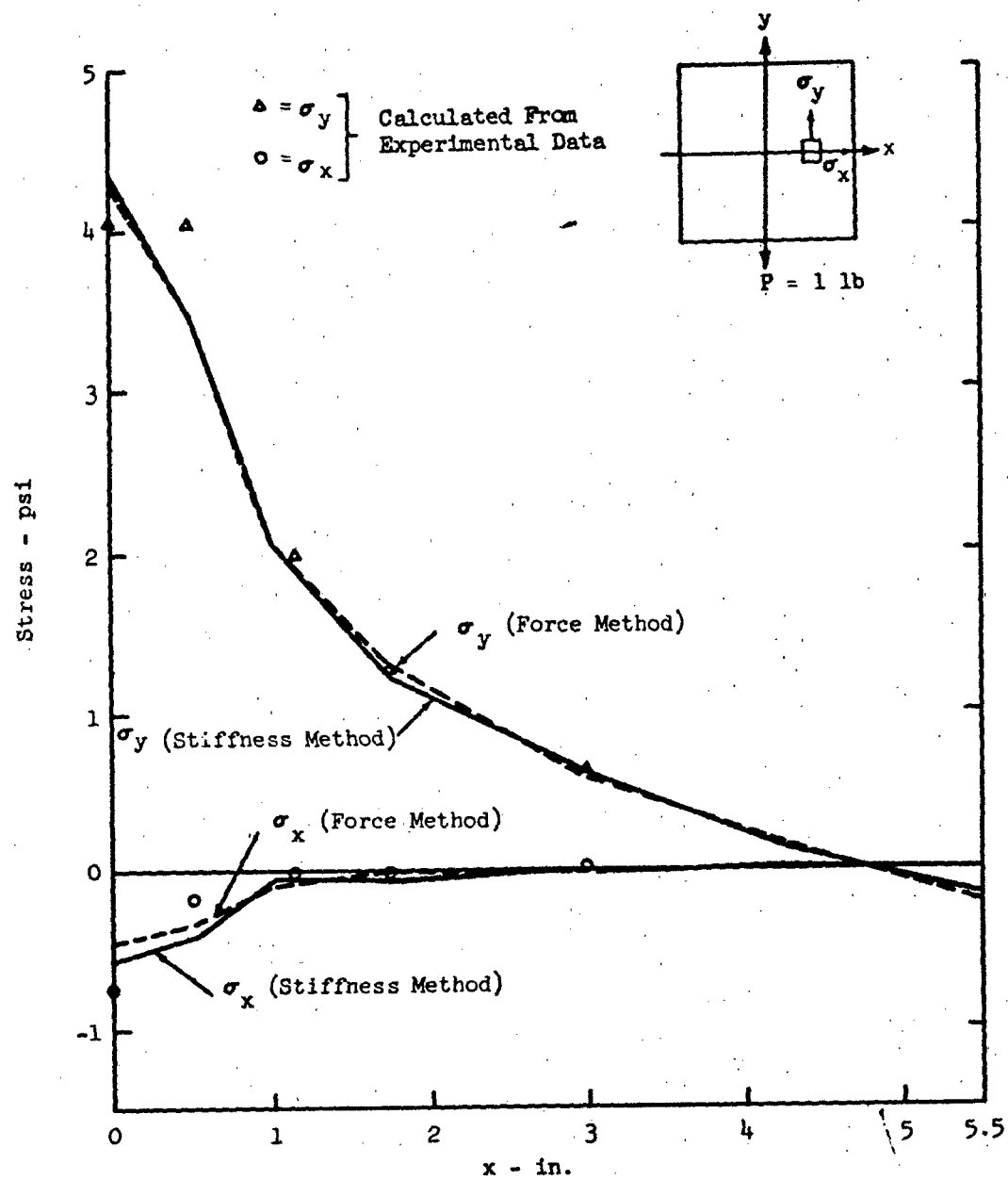


Fig. 43 Elastic Stress Distribution Along x-Axis

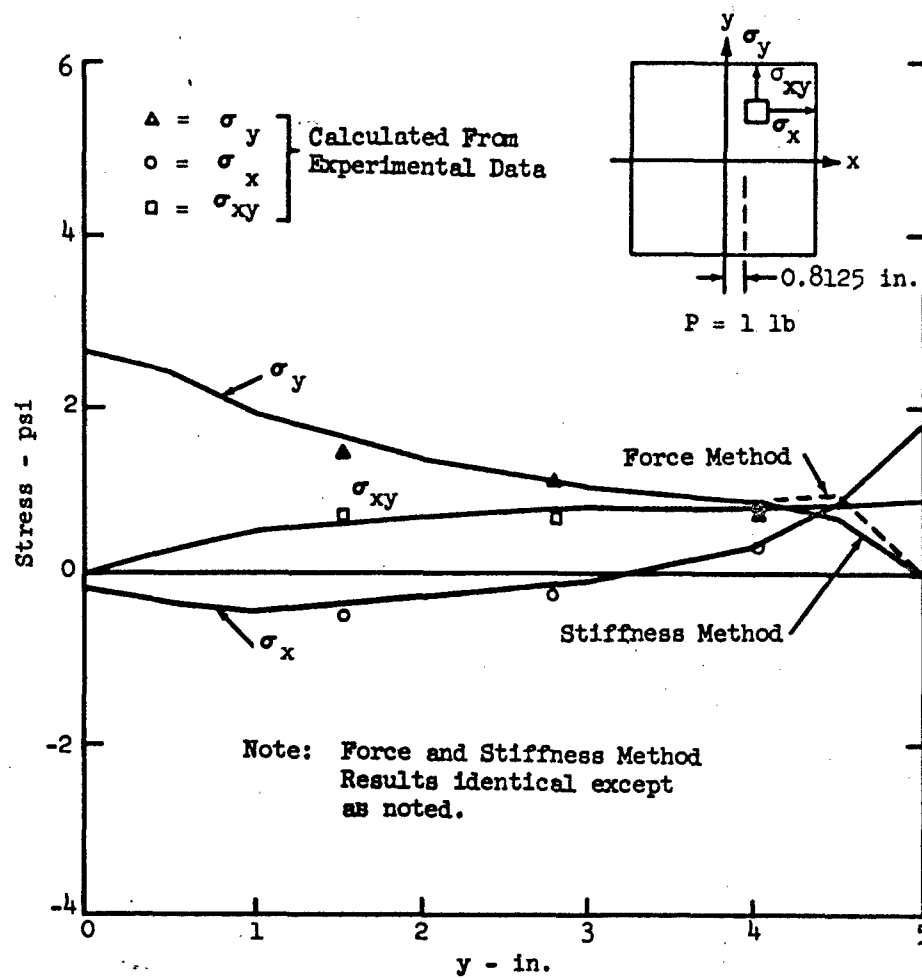


Fig. 44 Elastic Stress Distribution Along  $x = 0.8125$  in.

## APPENDIX I

### ELASTIC ANALYSIS OF SHEAR LAG STRUCTURE

#### A. Idealization of Shear Lag Structure

As stated in the introduction, when a problem is formulated by means of a standard influence coefficient approach, the necessary linear analysis may be carried out using either the force or displacement method. Since published correlations between results of the matrix force and direct stiffness methods of linear elastic analyses for redundant structures have, in the past, left room for doubt as to the equivalence of results, this Appendix presents a comparison of the stresses from two idealizations of the simple shear-lag stiffened-plate structure, Figures (7) and (8). In the past, discrepancies have been due in part to a marked difference in the arrangement of node points for corresponding idealizations, and also to the fact that techniques for obtaining node stresses in finite element analyses are still being improved. An attempt was made to keep the idealizations as comparable as possible with respect to location of nodes and the determination of stresses.

#### B. Force Method

The idealization for the force method may be seen in Figure (8). It comprises conventional bars and shear panels located in the manner shown. The analyses of some previous idealizations of this type have omitted the Poisson's ratio effect. This effect can be incorporated in the manner described in Appendix II.

#### C. Stiffness Method

The idealization for the stiffness method consists of "Turner triangles," which are located as shown in Figure (7). The basic theory of the triangle is to be found in References 8 and 9.

While the conventional procedure was used to obtain node stresses for the force method, comparable stiffness-method stresses can be calculated in several ways. A recent paper, Reference 9, suggests two means of obtaining node stress, one of which was employed in the analysis. This method will be reviewed briefly.

Figure (10) represents a cluster of triangles. It is required to find the stresses at the node common to triangles P to W. The node forces for each triangle at this apex are obtained as described in Turner's former papers. Summing the forces on a vertical section through 1 in both directions gives

$$X_V = X_P + X_Q + X_R + X_S$$

$$Y_V = Y_P + Y_Q + Y_R + Y_S$$

Analogous results  $X_h$  and  $Y_h$  are obtained for the corresponding horizontal cut.

The node stresses at the node are

$$\begin{aligned}\sigma_x &= \frac{X_v}{\frac{1}{2}(ct_p + dt_s)} \\ \sigma_y &= \frac{Y_h}{\frac{1}{2}(at_r + bt_u)} \\ \sigma_{xy} &= \frac{1}{2} \left[ \frac{X_h}{\frac{1}{2}(at_r + bt_u)} + \frac{Y_v}{\frac{1}{2}(ct_p + dt_s)} \right]\end{aligned}$$

where a, b, c, and d are as indicated and t is the thickness.

#### D. Comparison of Elastic Results and Perspective

The results are correlated by means of the curves appearing in Figures (43) and (44) with calculated values from the experimental data of Reference 7.

The correlation between the stresses derived from the force method and from the stiffness method of analysis is excellent and may be regarded as exact for engineering applications. The largest discrepancy is in the direct stresses in the x direction at the middle of the plate as shown in Figure (43). Even in this region the difference is quite small. It is believed that an even closer agreement could be obtained by modifying the idealized structure to provide square shear panels adjacent to the reinforcement and a finer grid at the plate center.

The largest discrepancy between analysis and test results is located in the region of the plate center. Reference 7 indicated that considerable bending was exhibited by the structure as the ends of the stiffener were loaded. The extent to which this affects the gage readings was not determined; however, it may be anticipated that the effect be greatest near the middle of the plate. The curves on Figure (43) reinforce this impression.

On the basis of the excellent agreement noted here, it can be concluded that the incorporation of plastic and creep effects into the present method of structural analysis will not be restricted in any way by the particular linear analysis method employed.

## APPENDIX II

### POISSON'S RATIO EFFECT

The strain energy relationship for an elastic plate in terms of in plane stresses is given by the volume integral:

$$U = \frac{1}{2E} \int_V [\sigma_{xx}^2 + \sigma_{yy}^2 - 2\nu \sigma_{xx}\sigma_{yy} + 2(1 + \nu)\sigma_{xy}^2] dV$$

The idealized structure corresponding to a rectangular plate for a finite element matrix force analysis has orthogonal bars taking only normal stresses and panels in pure shear. Figure (8), the shear-lag specimen, represents a typical idealization of this type. Defining  $\bar{\sigma}_{xx}$  and  $\bar{\sigma}_{yy}$  as the axial stress in the bars and  $\bar{\sigma}_{xy}$  as the shear stress in the panels, the strain energy  $U'$  of the idealized structure is sometimes taken as:

$$U' = \frac{1}{2E} \int_V [\bar{\sigma}_{xx}^2 + \bar{\sigma}_{yy}^2 + 2(1 + \nu)\bar{\sigma}_{xy}^2] dV$$

Comparing the plate strain energy  $U$  with the idealized structure strain energy  $U'$  it is obvious that the finite element expression neglects to account for the interaction term of the plate  $(- 2\nu \sigma_{xx}\sigma_{yy})$  which is due to Poisson's ratio. This uncoupling of the normal stresses has the effect of making the idealized plate less rigid than the actual plate. The finite element idealization is refined by including the term  $(- 2\nu \bar{\sigma}_{xx}\bar{\sigma}_{yy})$  in  $U'$ , making the model more consistent with the elastic plate.

The sketch, Figure (9), shows a shear panel with adjacent axial load carrying bars. Assume the structure represents a portion of a plate structure  $l$  inches long,  $b$  inches wide and  $t$  inches thick. The normal stresses at one corner of the idealized structure are designated  $\sigma_1$  and  $\sigma_2$  in the  $x$  and  $y$  directions respectively. It is sufficiently accurate in accounting for the interaction term to assume that the normal stresses are constant over the plate corresponding to the shaded quadrant and also to assume that these stresses are equal to  $\sigma_1$  and  $\sigma_2$ , the values at the corner. The strain energy term to be included is represented by

$$\frac{1}{2} \sigma_1 \sigma_2^2 \alpha_{12}$$

where  $\alpha_{12}$  represents the interaction flexibility influence coefficient. Carrying out the integration over the quadrant of the plate, the influence coefficient is evaluated.

$$\alpha_{12} = -\frac{1}{E} \nu \int_V dV = -\frac{\nu}{E} \frac{b^2 t}{4}$$

This term together with the reciprocal term  $\alpha_{21}$  and similar terms for other biaxially stressed areas, when included in the flexibility matrix, account for the Poisson's ratio effect.

### APPENDIX III

#### INSTABILITY ANALYSIS OF THE CONSTANT STRESS AND CONSTANT STRAIN METHODS

The stability of the two methods is easily tested by determining whether perturbations introduced into the analysis grow or decay with succeeding steps. It is instructive, however, to take the following approach. In place of the computed quantities, introduce exact quantities, signified by a caret and associated error terms, in the manner

$$\{q_i^{(k)}\} = \{\hat{q}_i^{(k)}\} + \{\epsilon_i^{(k)}\} \quad \text{III-1}$$

The exact relation is taken to be

$$\{\hat{q}_i^{(k)}\} = [\Gamma_{im}]\{P_m^{(k)}\} + [\Gamma_{ij}]\{\hat{e}_j^{(k)}\} \quad \text{III-2}$$

Equation 3 can be written in terms of member loads

$$\{q_i^{(k)}\} = [\Gamma_{im}]\{P_m^{(k)}\} + [\Gamma_{ij}]\{e_j^{(k-1)}\} \quad \text{III-3}$$

Substituting Equation III-1 into Equation III-3 gives

$$\{\hat{q}_i^{(k)}\} + \{\epsilon_i^{(k)}\} = [\Gamma_{im}]\{P_m^{(k)}\} + [\Gamma_{ij}]\{e_j^{(k-1)}\}$$

from which Equation III-2 may be subtracted to yield the following expression for the errors

$$\{\epsilon_i^{(k)}\} = [\Gamma_{ij}]\{e_j^{(k-1)} - \hat{e}_j^{(k)}\} \quad \text{III-4}$$

The constant stress and constant strain methods are now distinguished by the manner in which the  $e_j^{(k-1)}$  are specified. The Ramberg-Osgood stress-strain relation, which we may write in the form

$$e_i^{(k)} = \frac{q_i^{(k)}}{E_i A_i} + \frac{3 \sigma_{oi}}{7 E_i} \left| \frac{q_i^{(k)}}{\sigma_{oi} A_i} \right|^n \frac{q_i^{(k)}}{|q_i^{(k)}|}$$

will be used in examining both methods.

The nonlinear strains, in the constant stress method, are given by

$$\epsilon_j^{(k-1)} = \frac{3\sigma_{oj}}{7E_j} \left| \frac{q_j^{(k-1)}}{\sigma_{oj} A_j} \right|^n \frac{q_j^{(k-1)}}{|q_j^{(k-1)}|}$$

which, on using Equation III-1, may be written in the expanded form

$$\epsilon_j^{(k-1)} = \frac{3\sigma_{oj} \hat{q}_j^{(k-1)}}{7E_j |\hat{q}_j^{(k-1)}|} \left[ \left| \frac{\hat{q}_j^{(k-1)}}{\sigma_{oj} A_j} \right|^n + n \left| \frac{\hat{q}_j^{(k-1)}}{\sigma_{oj} A_j} \right|^{n-1} \frac{\xi_j^{(k-1)}}{\sigma_{oj} A_j} + \dots \right]$$

A similar expansion can be constructed for the  $\hat{\epsilon}_1^{(k)}$  on introducing

$$\{\hat{q}_j^{(k)}\} = \{\hat{q}_j^{(k-1)}\} + \{\Delta \hat{q}_j^{(k)}\}$$

which gives

$$\hat{\epsilon}_j^{(k)} = \frac{3\sigma_{oj}}{7E_j} \frac{\hat{q}_j^{(k)}}{|\hat{q}_j^{(k)}|} \left[ \left| \frac{\hat{q}_j^{(k-1)}}{\sigma_{oj} A_j} \right|^n + n \left| \frac{\hat{q}_j^{(k-1)}}{\sigma_{oj} A_j} \right|^{n-1} \frac{\Delta \hat{q}_j^{(k)}}{\sigma_{oj} A_j} + \dots \right]$$

Substituting the foregoing expression into Equation III-4, and assuming small errors in the sense that  $\xi_1 \ll q_1$  and small steps in the loading such that  $\Delta q_1 \ll q_1$ , so that terms containing the products of these quantities may be dropped, we obtain

$$\{\xi_1^{(k)}\} = [\Gamma_{1j}] \left[ \frac{3n}{7E_j A_j} \frac{\hat{q}_j^{(k-1)}}{|\hat{q}_j^{(k-1)}|} \left| \frac{\hat{q}_j^{(k-1)}}{\sigma_{oj} A_j} \right|^{n-1} \right] \{\xi_j^{(k-1)} - \Delta \hat{q}_j^{(k)}\}$$

which may be re-written

$$\{\xi_1^{(k)}\} = [\Gamma_{1j}] \left[ \frac{1}{\bar{E}_j^{(k-1)}} A_j \right] \left[ 1 - \frac{\Delta \hat{q}_1^{(k)}}{\xi_j^{(k-1)}} \right] \{\xi_j^{(k-1)}\} \quad \text{III-5}$$

where  $\bar{E}_j$  give the slope of the stress versus inelastic-strain curve at the individual element stress levels.



Instability develops when the errors in the  $k^{\text{th}}$  step increase over those in the  $k-1^{\text{st}}$  step. Clearly, the method would be expected to be unstable, if any of the inequalities  $\xi_i^{(k)} > \xi_i^{(k-1)}$  were satisfied directly. A more critical check, however, is to consider the entire set of  $\{\xi_i\}$  as a vector (in  $n$ -dimensional space where  $n$  is equal to the number of elements) and apply the condition that the Euclidean length of this vector does not increase. Mathematically, this means that for stability

$$\{\xi_i^{(k)}\}^T \{\xi_i^{(k)}\} \leq \{\xi_i^{(k-1)}\}^T \{\xi_i^{(k-1)}\}$$

where the critical condition is defined by using the equality sign.

For simplicity, we consider the case of infinitesimally small steps in the loading, so that the  $\Delta q_i$  terms may be neglected, and further, denote

$$\left[ \Gamma_{ij} \right] \left[ 1 / \bar{E}_j^{(k-1)} \right] A_j = \left[ B_{ij}^{(k-1)} \right]$$

The critical condition for instability then becomes

$$\begin{aligned} \{\xi_i^{(k)}\}^T \{\xi_i^{(k)}\} &= \{\xi_i^{(k-1)}\}^T \left[ B_{ij}^{(k-1)} \right]^T \left[ B_{ij}^{(k-1)} \right] \{\xi_i^{(k-1)}\} \\ &= \{\xi_i^{(k-1)}\}^T \{\xi_i^{(k-1)}\} \end{aligned} \quad \text{III-6}$$

It is now observed that the eigenvalues of

$$\left[ B_{ij}^{(k-1)} \right]^T \left[ B_{ij}^{(k-1)} \right]$$

will all be positive, hence the condition that none of these eigenvalues be greater than one (which becomes the stability requirement), can be replaced by the more severe condition that the sum of the eigenvalues not be greater than one. This latter condition can be assured by requiring that the sum of the squares of all elements of  $B_{ij}$  not be greater than one, and in addition, that the absolute sum of any row or

column in  $B_{ij}$  not be greater than one. The critical stress is then found from the largest of these sums.

In the case of the example truss problem, where  $E_1 = E = 10^7$  psi,  $n = 10$ ,  $A_1 = 1.0$  sq. in., and  $\sigma_{oi} = \sigma_o = 10^5$  psi, the sum of the squares approach, viz.,

$$\left\{ \frac{3n}{7E} \left( \frac{\sigma_{cr}}{\sigma_o} \right)^{n-1} \right\}^2 \times \sum_{ij=1}^3 \Gamma_{ij}^2 = 1$$

yields  $\sigma_{cr} = 83,800$  psi., while the rows and columns approach gives  $\sigma_{cr} = 82,900$  psi.

Recall that the foregoing development has determined the minimum value at which instability might occur. It is of interest to compute a critical value of stress at which instability is strongly assured to occur. This can be done by returning to the initial notion that instability will occur if  $\xi_i^{(k)} > \xi_i^{(k-1)}$ . This amounts to restricting attention to the diagonal elements in the  $B_{ij}$  matrix. The corresponding critical stress (lowest value) will be given by the largest (in absolute value) element on the diagonal in the  $B_{ij}$  matrix. This corresponds to the  $-0.414 \times 10^7$  term in the  $\Gamma_{ij}$  matrix, so that the critical stress is given by

$$\frac{3n}{7E} \left( \frac{\sigma_{cr}}{\sigma_o} \right)^{n-1} \times (0.414 \times 10^7) = 1$$

which gives  $\sigma_{cr} = 93,800$  psi. The lowest stress at which instability would develop, in the case of the example truss problem, would therefore be expected to occur between 82,900 psi and 93,800 psi.

Note that if only one structural element were inelastic, then the diagonal term in the  $\Gamma_{ij}$  matrix corresponding to this element would give the correct critical stress by the latter procedure. Both of the foregoing values of critical stress have been indicated in Figure 4, where they are seen to correlate with the experimental (computer) results. The simple approach of considering only the diagonal elements

appears to be advantageous in the present problem. With this approach, it is easy to see that finite values of  $\Delta q_1$ , which make the elements in the second diagonal matrix in Equation III-5 less than one, must raise the stress for instability, which explains the progression of critical stresses (with increasing load step size) appearing in Figure 4.

Finally, it is noted that certain of the foregoing results, viz., the value of  $\sigma_{cr}$  based on one diagonal elements alone, can be obtained simply by introducing  $q_1^{(k)} + \psi_1^{(k)}$  in place of  $q_1^{(k)}$  directly into Equation III-3, and regarding the  $\psi_1^{(k)}$  as perturbations on the  $q_1^{(k)}$ . The additional results, such as the demonstration of the effects of finite  $\Delta q_1$ , however, are not obtained by this procedure.

In the case of the constant strain method, in addition to the error quantities in the member loads

$$\{q_1^{(k)}\} = \{\hat{q}_1^{(k)}\} + \{\xi_1^{(k)}\}$$

we also introduce error quantities for the relaxed loads

$$\{q_{*1}^{(k)}\} = \{\hat{q}_{*1}^{(k)}\} + \{\xi_{*1}^{(k)}\}$$

The equation defining the relaxed loads, written for the generic  $i^{\text{th}}$  member, is

$$\frac{q_1^{(k)}}{E_1 A_1} + \epsilon_1^{(k-1)} = \frac{q_{*1}^{(k)}}{E_1 A_1} + \frac{3q_{*1}^{(k)}}{7E_1 A_1} \left| \frac{q_{*1}^{(k)}}{\sigma_{o1} A_1} \right|^{n-1}$$

which may be written in the following form

$$\begin{aligned} & \left| \frac{\hat{q}_1^{(k)} + \xi_1^{(k)}}{E_1 A_1} \right| \left| \frac{q_1^{(k)}}{q_1^{(k)}} \right| + \frac{3\sigma_{o1}}{7E_1} \left| \frac{\hat{q}_{*1}^{(k-1)} + \xi_{*1}^{(k-1)}}{\sigma_{o1} A_1} \right|^n \frac{q_{*1}^{(k-1)}}{|q_{*1}^{(k-1)}|} \\ & = \left| \frac{q_{*1}^{(k)} + \xi_{*1}^{(k)}}{E_1 A_1} \right| \left| \frac{q_{*1}^{(k)}}{q_{*1}^{(k)}} \right| + \frac{3\sigma_{o1}}{7E_1} \left| \frac{\hat{q}_{*1}^{(k-1)} + \Delta \hat{q}_{*1}^{(k-1)} + \xi_{*1}^{(k)}}{\sigma_{o1} A_1} \right|^n \frac{q_{*1}^{(k)}}{|q_{*1}^{(k)}|} \end{aligned}$$

If we now apply the condition of no load reversals, then the terms  $q_1^{(k)}/|q_1^{(k)}|$  etc., will all produce the same sign (for a given element) and hence may be cancelled out. Applying the condition that all error terms  $\xi_1$  and load increments  $\Delta q_1$  are much smaller than the load magnitude  $|q_1|$ , leads to the result

$$\xi_1^{(k)} = \xi_{*1}^{(k)} - \frac{E_1}{\hat{E}_{*1}^{(k-1)}} \left( \xi_{*1}^{(k-1)} - \xi_{*1}^{(k)} - \Delta q_{*1}^{(k)} \right)$$

where

$$1/\hat{E}_{*1}^{(k-1)} = \frac{3n}{7E_1} \left| \frac{\hat{q}_{*1}^{(k-1)}}{\sigma_{o1} A_1} \right|^{n-1}$$

The corresponding form of Equation III-4 may now be written by introducing the exact load-reduction-increments  $\Delta \hat{q}_{rj}^{(k)}$ , where

$$\Delta \hat{q}_{rj}^{(k)} = \hat{q}_j^{(k)} - \hat{q}_{*j}^{(k)}$$

which leads to

$$\left\{ \xi_1^{(k)} \right\} = \left[ \Gamma_{1j} \right] \left\{ \frac{3\sigma_{o1}}{7E_j} \left| \frac{\hat{q}_{*j}^{(k-1)} + \xi_{*j}^{(k-1)}}{\sigma_{oj} A_j} \right|^n \frac{q_{*j}^{(k-1)}}{|q_{*j}^{(k-1)}|} - \frac{3\sigma_{o1}}{7E_j} \left| \frac{\hat{q}_{*j}^{(k-1)} + \Delta \hat{q}_{rj}^{(k-1)} + \Delta \hat{q}_j^{(k)}}{\sigma_{oj} A_j} \right|^n \frac{\hat{q}_j^{(k)}}{|\hat{q}_j^{(k)}|} \right\}$$

Applying, once again, the smallness requirement on the  $\xi_1$  and  $\Delta q_1$ , yields

$$\left[ 1 + \frac{E_1}{\hat{E}_{*1}^{(k-1)}} \right] \left\{ \xi_{*1}^{(k)} \right\} = \left[ \Gamma_{1j} \right] \left[ 1/(\hat{E}_{*j}^{(k-1)} A_j) \right] \left[ 1 - \frac{\Delta \hat{q}_{rj}^{(k-1)} + \Delta q_j^{(k)}}{\xi_{*1}^{(k-1)}} \right] \quad \text{III-7}$$

$$+ \left[ \frac{E_1}{\bar{E}_{*1}^{(k-1)}} \right] \left[ 1 - \frac{\Delta \sigma_1^{(k)}}{\bar{E}_{*1}^{(k-1)}} \right] \left\{ \bar{\epsilon}_{*1}^{(k-1)} \right\}$$

where the absolute value signs have been omitted for simplicity.

The check for the occurrence of instability may now be carried out in the same manner as for the constant stress method. Thus, considering only the case of infinitesimal load increments, the corresponding form of the  $B_{ij}$  matrix, as defined by Equation III-6, is found to be

$$[B_{ij}] = \left[ \frac{\bar{E}_{(cr)1}}{\bar{E}_{(cr)1} + E_1} \right] \left[ \Gamma_{ij} \right] \left[ 1/(\bar{E}_{(cr)j} A_j) \right] + \left[ E_1/\bar{E}_{(cr)1} \right]$$

A numerical check for the special case of the truss problem shows that the critical condition of the eigenvalues summing to unity calls for physically inadmissible values of  $\bar{E}_{(cr)}$ . A simpler demonstration of this property is provided by the "direct approach" (i.e., setting  $\bar{\epsilon}_1^{(k)} = \bar{\epsilon}_{*1}^{(k-1)}$ ). In this case, the critical stress is given by the lowest value corresponding to the "n" equations obtained by equating the diagonal elements of

$$\left[ 1 + \frac{E_1}{\bar{E}_{(cr)1}} \right]^{-1} \left[ \Gamma_{ij} \right] \left[ 1/(\bar{E}_{(cr)j} A_j) \right] + \left[ E_1/\bar{E}_{(cr)1} \right] = \left[ \pm \quad 1 \right]$$

In the example truss problem, where  $E_1 = E$ ,  $\sigma_{o1} = \sigma_o$ , and  $A_1 = 1.0$ , and where the three diagonal elements in the  $\Gamma_{ij}$  matrix can be denoted by  $-\zeta_i E$ , where in turn  $0 < \zeta_i < 1$ , the foregoing matrix equation reduces to the following simple algebraic equation

$$\frac{-\zeta_i E + E}{\bar{E}_{(cr)1} + E} = \pm 1$$

The indicated critical values are easily seen to be  $-\zeta_i E$  and  $-(2 - \zeta_i)E$ , both of which are physically inadmissible for the Ramberg-Osgood stress-strain relation. Thus, the constant strain method is indicated to be free of instability in this case. The problem of accuracy, of course, is another matter, due to the necessity of working with finite (and preferably large) load steps. These, apparently, are responsible for the slow divergence of the computer results shown in Figure 5.

# APPENDIX IV

## ROTATION OF AXES OF ANISOTROPY

Let the x and y axes be rotated from the axes of anisotropy in a positive sense so that from the strain transformation equations we get:

$$\left. \begin{aligned} d\epsilon_x &= l^2 d\epsilon_{11} + m^2 d\epsilon_{22} + 2lm d\epsilon_{12} \\ d\epsilon_y &= m^2 d\epsilon_{11} + l^2 d\epsilon_{22} - 2lm d\epsilon_{12} \\ d\epsilon_{xy} &= -lm d\epsilon_{11} + lm d\epsilon_{22} + 2(l^2 - m^2) d\epsilon_{12} \end{aligned} \right\} \text{IV-1}$$

when  $l$ , and  $m$  are the usual direction cosines of the x-axis with respect to the orthogonal axes.

Similarly from the stress transformation equations:

$$\left. \begin{aligned} \sigma_{11} &= l^2 \sigma_x + m^2 \sigma_y - 2lm \sigma_{xy} \\ \sigma_{22} &= m^2 \sigma_x + l^2 \sigma_y + 2lm \sigma_{xy} \\ \sigma_{12} &= lm \sigma_x - lm \sigma_y + (l^2 - m^2) \sigma_{xy} \end{aligned} \right\} \text{IV-2}$$

Substituting Equation IV-2 into the appropriate expressions in Equation 12 gives a set of equations as follows:

$$\left. \begin{aligned} d\epsilon_{11} &= \frac{d\bar{\epsilon}}{\bar{\sigma}} \left[ (l^2 \alpha_{11} - m^2 \alpha_{12}) \sigma_x + (m^2 \alpha_{11} - l^2 \alpha_{12}) \sigma_y \right. \\ &\quad \left. - 2lm(\alpha_{11} + \alpha_{12}) \sigma_{xy} \right] \\ d\epsilon_{22} &= \frac{d\bar{\epsilon}}{\bar{\sigma}} \left[ (m^2 \alpha_{22} - l^2 \alpha_{12}) \sigma_x + (l^2 \alpha_{22} - m^2 \alpha_{12}) \sigma_y \right. \\ &\quad \left. + 2lm(\alpha_{22} + \alpha_{12}) \sigma_{xy} \right] \\ d\epsilon_{12} &= \frac{d\bar{\epsilon}}{\bar{\sigma}} 3\alpha_{44} \left[ lm(\sigma_x - \sigma_y) + (l^2 - m^2) \sigma_{xy} \right] \end{aligned} \right\} \text{IV-3}$$

Finally substituting Equation IV-3 into Equation IV-1, simplifying and defining three new coefficients  $\delta$ ,  $\delta_1$  and  $\delta_2$  such that  $\delta = \alpha_{12} - \frac{3}{2}\alpha_{44}$ ,  $\delta_1 = (\alpha_{11} + \delta)$  and  $\delta_2 = (\alpha_{22} + \delta)$  the appropriate incremental flow equations become:

$$\left. \begin{aligned} d\epsilon_x &= \frac{d\bar{\epsilon}}{\bar{\sigma}} \left[ (\ell^4 \delta_1 + m^4 \delta_2 - \delta) \sigma_x - (\alpha_{12} - \ell^2 m^2 \delta_1 - \ell^2 m^2 \delta_2) \sigma_y \right. \\ &\quad \left. - 2\ell m (\ell^2 \delta_1 - m^2 \delta_2) \sigma_{xy} \right] \\ d\epsilon_y &= \frac{d\bar{\epsilon}}{\bar{\sigma}} \left[ (\ell^4 \delta_2 + m^4 \delta_1 - \delta) \sigma_y - (\alpha_{12} - \ell^2 m^2 \delta_2 - \ell^2 m^2 \delta_1) \sigma_x \right. \\ &\quad \left. - 2\ell m (m^2 \delta_1 - \ell^2 \delta_2) \sigma_{xy} \right] \\ d\epsilon_{xy} &= \frac{d\bar{\epsilon}}{\bar{\sigma}} \left[ (3\alpha_{44} + 4\ell^2 m^2 \delta_1 + 4\ell^2 m^2 \delta_2) \sigma_{xy} \right. \\ &\quad \left. - 2\ell m (\ell^2 \delta_1 - m^2 \delta_2) \sigma_x - 2\ell m (m^2 \delta_1 - \ell^2 \delta_2) \sigma_y \right] \end{aligned} \right\} \text{IV-4}$$

Insertion of Equation IV-2 into 11 gives the expression for effective stress:

$$\left. \begin{aligned} \bar{\sigma}^2 &= \left[ (\ell^4 \delta_1 + m^4 \delta_2 - \delta) \sigma_x^2 - 2(\alpha_{12} - \ell^2 m^2 \delta_1 - \ell^2 m^2 \delta_2) \sigma_x \sigma_y \right. \\ &\quad \left. + (\ell^4 \delta_2 + m^4 \delta_1 - \delta) \sigma_y^2 + (3\alpha_{44} + 4\ell^2 m^2 \delta_1 + 4\ell^2 m^2 \delta_2) \sigma_{xy}^2 \right. \\ &\quad \left. - 4\ell m (\ell^2 \delta_1 - m^2 \delta_2) \sigma_x \sigma_{xy} - 4\ell m (m^2 \delta_1 - \ell^2 \delta_2) \sigma_y \sigma_{xy} \right] \end{aligned} \right\} \text{IV-5}$$

Now suppose we make an uniaxial stress-strain test for the x-direction. The valid expressions become:

$$\begin{aligned} d\epsilon_x &= \frac{d\bar{\epsilon}}{\bar{\sigma}} (\ell^4 \delta_1 + m^4 \delta_2 - \delta) \sigma_x \\ \bar{\sigma}^2 &= (\ell^4 \delta_1 + m^4 \delta_2 - \delta) \sigma_x^2 \end{aligned}$$

From the three Equations IV-4, we obtain equations similar to Equation 15. This equation is augmented under restrictions of equal plastic work thus:

$$a \sqrt{\alpha_{11}} = b \sqrt{\alpha_{22}} \quad c \sqrt{\alpha_{33}} = d \sqrt{\ell^4 \delta_1 + m^4 \delta_2 - \delta} \quad \text{IV-6}$$

Assigning the value of unity to one " $\alpha$ " as before we obtain the relative values of the others. In particular we now obtain a value for  $(\ell^4 \delta_1 + m^4 \delta_2 - \delta)$  which is a function of  $\alpha_{11}$ ,  $\alpha_{22}$ ,  $\alpha_{33}$  all known and  $\alpha_{44}$  unknown. Therefore  $\alpha_{44}$  may be determined.



## APPENDIX V

### INELASTIC MATRIX COMPUTER PROGRAM

#### A. Program Description

This is a brief description of the Grumman inelastic matrix program for carrying out elastic-plastic-creep analysis - deck No. 45128 - Elastic Unloading (follows Hooke's Law when unloading), including anisotropy.

This program for elastic-plastic analysis has proved to be quite adaptable for analytic investigations. It has been modified to include an option for anisotropic analysis. Previously, the program was modified to use time-hardening theory, deformation theory, inelastic unloading, and constant stress theory (none of which have been retained in the final program). It was not necessary to do major program revisions to accommodate these variations. The program housekeeping is arranged so that modifications to the manipulation of data will not affect the housekeeping. Thus the program makes a convenient framework to explore various calculation procedures.

The program is written in Fortran II to run on the Grumman IBM 7094s. These are 2 channel (A and B) machines with 6 drives per channel; 32,768 words of core storage; on-line card reader; on-line printer; and printer clock. The program is set to run under Fortran Monitor control which uses a \$JOB card for identification. Input is on logical tape 7 (A-2), print output on logical tape 6 (A-2) and punched output on logical tape 5 (B-4) (not used by this program). Logical tape 8 (B-1) is used for storage of binary output which is converted to BCD print output in link 6 (at the end of job). The program will accept an input data tape on logical tape 9 (A-5) and will write a binary save tape for restart on logical tape 11 (A-6). These 2 auxiliary tapes are optional for each run (see description of the control cards). The Grumman IOU subroutine, as well as the subroutines for rewinding and unloading a tape (RUN) and for moving to the start of a designated file (FILTAP) are included, as required in the program, in column binary form.

The program tape furnished to Wright Patterson Air Force Base contains all the information needed to duplicate our analysis. It is in the following sequence:

File 1 - a 1-card BCD label tested by the program to distinguish BCD data tape from binary save tape.

File 2 - BCD card images for matrices SIM AND SIJ. See pages 79 and 80 for a description of the matrices and their format.

File 3 - BCD card images of Fortran program (6 links), each link including binary subroutines previously mentioned.

Multiple ( 6 ) end of file marks.

We recommend that all 3 files of this tape be copied for use, then that file 3 be punched onto Fortran cards. The punching program must be able to handle mixed-mode cards to accommodate the short binary subroutines. This deck of cards, with the proper \*I.D. or \$JOB card, will then be in proper form for a Fortran compile and execute, using the copied tape on drive A-5 (logical 9). The program uses only the data from files 1 and 2; it will not move into file 3. This 2-file format for the data tape is generated by the GISMO matrix system in use at Grumman and elsewhere.

Each link of the program contains the non-IBM subroutines needed for operation. Standard input-output subroutines etc. will be taken from the library tape. As a point of information, the program contains six links numbered consecutively from 1 to 6.

- 1) Link 1 reads the first control card, and reads all other decimal input supplied.
- 2) Link 2 is used only on a restart job. It reads the modified step table, if provided, and part of the binary input tape.
- 3) Link 3 is used only on a restart job, and reads the balance of the binary input tape.
- 4) Link 4 is the processing link. It does all the calculation, print control, and writing of binary output on tape B-1 to be converted to BCD print output by Link 6.
- 5) Link 5 writes a binary tape for restart, then transfers to Link 6. If no binary tape is to be written, exit is from Link 6.
- 6) Link 6 reads the binary output stored on tape B-1 and converts it to BCD output on tape A-3 for printing. When tape B-1 has been completely processed, a message to the operator indicates that it need not be saved. If, due to machine error or operator intervention, tape B-1 is not processed into prints on A-3, but is saved, then Link 6 can be used as a separate program using B-1 as a data tape and will process B-1 into prints on A-3. Link 6 does not use any data from COMMON. All necessary clues are stored on B-1.

Sequencing and details of the data cards follow. The symbols used in the program for various items of input data are listed on page 77 and are shown on the sample key-punching sheet page 78.

The data cards are used in the following sequence, immediately after the \*DATA card required by the Monitor:

1. General clue card (FORMAT 1) containing KLU<sup>4</sup>, NINCLD, NA, KLU<sup>7</sup>, KLUIISO, ALPHA, BETA, GAMMA, GNU, and a title or caption.
2. Table of load or time steps desired. Up to ten cards defining ten steps may be used. Load steps and time steps may be used in any sequence. The maximum level for each load or time step may be above or below the previous maximum level of load or time. The program verifies the algebraic sign of the increment, and corrects it if necessary. Each card contains four variables TEMP1, TEMP2, TEMP3, TEMP<sup>4</sup> in FORMAT 2.
3. Data matrices. These may be provided in any sequence. Each matrix has a header card in FORMAT 3, one or more data cards in FORMAT 4, and a blank card to end it. The last input matrix on the Monitor input tape must be followed by one added blank card (two total) to trip the program into operation.

In the event that a job is running overtime, and it is desired to stop the program in a restartable form, mount a blank tape on logical tape 11 (drive A-6) and set Sense Switch 6 on. This will write the contents of memory on A-6 in proper form to continue the run later. The program distinguishes between the saved binary tape and a decimal input tape at starting time. Either is mounted on logical tape 9 (Drive A-5).

Built-in pauses in the program are as follows:

1. Pause 11111 to mount the data input tape at the start of the program, if all matrices are not on the Monitor input tape A-2. For this KLU<sup>4</sup>, in the first data card, should be a "1" to "4" indicating the count of decimal matrices on A-5. If A-5 is a binary saved tape from a preceding run, any digit (except zero) acceptable for KLU<sup>4</sup>.
2. Pause 1 to mount a blank tape on A-6 to receive memory. This is reached either with Sense Switch 6, or with a card in the table of steps punched TAPE in columns 7-10.

#### B. Symbols and Format of the Data Cards

##### 1. General Clue Card - FORMAT 1

Cols. Field Symbol

1	11	KLU <sup>4</sup>	This gives the number of input matrices on the auxiliary input tape (A-5). If all matrices are on the monitor tape, leave this blank. If using binary restart tape, use a digit. Maximum number of decimal input matrices on the auxiliary input tape is 4.
---	----	------------------	---

Cols. Field Symbol

2-4	I3	NINCLD	This gives the number of non-increment re-cycles at each load or time level. The total cycles at each level is NINCLD + 1. When printing, the first, tenth, twentieth, etc., and last cycle of each printable level will be printed.
5-7	I3	NA	This sets the frame size for the problem to be handled. NA is three times the number of nodes. Maximum value is 165 (55 nodes).
8	I1	KLU7	0, or blank, prints 5 preselected matrices on cycles indicated by the step table; 1 prints all matrices on cycles indicated by the step table. 2 prints 5 preselected matrices on all cycles; 3-9 print all matrices on all cycles.
9	I1	KLUISO	0 indicates an isotropic run 1 indicates an anisotropic run
10	1X		Not used
11-20	E10.3	ALPHA	A variable defined by the creep-strain equation.
21-30	E10.3	BETA	A variable defined by the creep-strain equation.
31-35	F5.2	GAMMA	A variable defined by the creep-strain equation.
36-40	F5.2	GNU	Poisson's ratio "nu"
41-50	10X		Not used
51-80	5A6	TA-TE	Any 30 characters of alpha-numeric text to be printed as a heading for identification purposes.

2. Table of Steps (limited to ten entries) - FORMAT 2

Cols. Field

1-6	6X	Not used
7-10	A4	LOAD indicates a load step, TIME indicates a time step, TAPE indicates write memory on a save-tape on drive A-6 (logical #11) then exit.

Cols.	Field
-------	-------

FINS or blank indicates end of table (this may be the 11th card in the table).

11-20	E10.6	Upper limit of step in pounds or hours
21-30	E10.1	Interval or increment for calculation
31-40	E10.1	Interval or increment for print output. Prints are generated on tape A-3 for the current cycle when the current load or time level is an integral multiple of the print interval. If the print interval is left blank, no prints are generated for cycles in this step. If print interval is very small compared to the current level, then numeric problems sometimes occur in the print control subroutine (OUTPUT), and it may be necessary to re-run with the every-cycle print control "2" or "3" for KLU7 punched in the first control card.
41-80		Ignored

### 3. Data Matrices - Header Card - FORMAT 3

Cols.	Field
-------	-------

1-6	6X	Not used
7-10	4X	Not used. We use the letters MTRX for compatibility with the GISMO Matrix System, which reads and writes matrices in this format.
11	1X	Not used
12-17	A6	This is the identification name for the input matrices and must correspond exactly with one of the following names: <div style="margin-left: 20px;">             bbbSIM Matrix of stresses for applied loads                        maximum size 165x1              bbbSLJ Matrix of stresses for member strains                        maximum size 165x165              bTSMGN Table of stress values 11x1              bTSPSN Table of strain values 11x1           </div>

These two matrices define the stress-strain curve as a series of chords. The data is entered in this format

merely to conform to the format of the SIM-SIJ matrices which were generated using the GISMO Matrix System. Note that the first value in both TSIGN and TEPSN must be zero to avoid upsetting the interpolation procedure.

TALF 12	$\alpha_{12}$	} Basic anisotropic parameters 11x1
TALF 23	$\alpha_{23}$	
TALF 31	$\alpha_{31}$	
TALF 44	$\alpha_{44}$	

18	1X	Not used
19-21	I3	Number of rows in this matrix
22-24	I3	Number of columns in this matrix
25-32	8X	Not used
33	I1	The digit 3
34-80		Not used

#### 4. Data Matrices - Data Cards - FORMAT 4

Cols.	Field	
1	1X	Not used
2-4	I3	Row index for the first element
5-7	I3	Column index for the first element
8-23	E16.8	The first element on this card
24	1X	Not used
25-27	I3	Row index for the second element
28-30	I3	Column index for the second element
31-46	E16.8	The second element on this card
47	1X	Not used
48-50	I3	Row index for the third element
51-53	I3	Column index for the third element

Cols.	Field	
54-69	E16.8	The third element on this card
70-80		Not used

The last card of a matrix must be completely blank (tested in Col. 2-4). The last matrix on the Monitor input tape 7 (drive A-2) must be followed by one added blank card (two total) to trip the program into operation.

The input matrices on the Monitor tape may be in any sequence as long as each matrix starts with a header card, has all its data cards next, and ends with a blank card.

#### C. Anisotropic Parameter Matrices

If a run is indicated as isotropic in the first control card (KLUI50 in Col. 9 is zero or blank) the program will read in the anisotropic parameters, if provided; then it will replace them with the built-in parameters for the isotropic condition. If a run is indicated as anisotropic in the first control card (KLUI50 is 1 to 9), then one each of the anisotropic parameter matrices must be provided or the program will terminate on an error.

#### D. Restart Procedure

If the run being set up is a restart, the input deck can be in several forms. The first control card must have a digit in KLUI<sup>4</sup> so that the program will read tape A-5; NINCLD and KLU7 are read from this card. The other factors are carried from the previous run. The continuation of an isotropic run will always be isotropic, and conversely, regardless of the clue provided (KLUI50).

The table of steps may be read in again (modified) if the previous run is stopped with sense switch 6, or it may be retained and continued from the previous run. However, if the previous run is stored on tape A-6 by using a TAPE card in the step table, then a new step table must be read in.

In either case, the last data card on a restart job must be FINS or blank in columns 7-10. This means a restart data deck will have a minimum of two cards (clue card and a blank), or a maximum of 12 cards (clue card, 10 step cards and a FINS or blank).

#### E. Time Estimates

For time estimates, allow 3.5 minutes to compile the Fortran, 1.5 minutes to read the input tape, 2.0 seconds per cycle printed, and 100 to 110 cycles of calculation per minute. Each printed cycle writes approximately 3 feet of print tape (55 node problems).

## Matrix Analysis of an Inelastic Plate - E

01	02	03	04	05	06	07	08	09	10	11	12	13	14	15	16	17	18	19	20	21	22	23	24	25	26	27	28	29	30	31	32	33	34	35	36	37	38	39	40	41							
GENERAL CONTROL CARD - ONE REQUIRED.																															FORMAT 1																
I1	I3		I3	I1	I1	IX																																									
4	NINCE		NA	7	ISO																																										
STEP TABLE (ONE TO TEN CARDS PLUS A FINS OR BLANK CARD)																																															
6X			A4			E10.6			E10.1			E10.1																																			
			TEMP1			TEMP2			TEMP3			TEMP4																																			
			LOAD			UPPER LIMIT OF STEP			INCREMENT FOR CALCULATION			INCREMENT FOR PRINT																																			
			TIME			UPPER LIMIT OF STEP			INCREMENT FOR CALCULATION			INCREMENT FOR PRINT																																			
			TAPE																																												
			FINS																																												
MATRIX HEADER CARDS (DEFINE THE NAME, SIZE AND START OF A MATRIX)																																															
6X			4X			IX			A6			IX			I3			I3			8X			I1																							
									NAME			NROWS			NCOLS									NFORM																							
			MTRX						\$IM			SIZE			I									3																							
			MTRX						\$IJ			SIZE			SIZE									3																							
			MTRX						T\$IGN			I I			I									3																							
			MTRX						TEP\$N			I I			I									3																							
			MTRX						TALF12			I I			I									3			(TALF23, TAL																				
MATRIX DATA CARDS (THREE ELEMENTS PER CARD - ROW SORT - LAS																																															
IX			I3			I3						E16.8						IX			I3			I3						E16.8																	
			NR(1)			ND(1)						EL(1)						NR(2)			ND(2)						EL(2)																				
			ROW			COL.						ELEMENT						ROW			COL.						ELEMENT																				
EACH MATRIX IS TERMINATED BY ONE COMPLETELY BLANK CARD																																															

## CODING INSTRUCTIONS:

1. Alphabetical characters are written as follows  
A B C D E F G H I J K L M N O P Q R S T U V W X Y Z
2. Numerical characters are written as follows  
1 2 3 4 5 6 7 8 9 0



otropic - Anisotropic

e - Elastic Unloading (Follows Hooke's Law)

40	41	42	43	44	45	46	47	48	49	50	51	52	53	54	55	56	57	58	59	60	61	62	63	64	65	66	67	68	69	70	71	72	73	74	75	76	77	78	79	80
----	----	----	----	----	----	----	----	----	----	----	----	----	----	----	----	----	----	----	----	----	----	----	----	----	----	----	----	----	----	----	----	----	----	----	----	----	----	----	----	----

JOX

SA6

TA-TE (TITLE OR HEADING)

FORMAT 2

VARY LOAD LEVEL AT CONSTANT TIME

VARY TIME, HOLD LOAD LEVEL CONSTANT

STORE MEMORY ON TAPE A-6 (LOGICAL NO. 11) FOR RESTART, THEN EXIT

END OF TABLE ENTRIES (BLANK CARD IS ALSO ACCEPTED)

ATRIX) FORMAT 3

3, TALF31 AND TALF44 ARE SIMILAR)

LAST CARD MAY HAVE 1 OR 2 ELEMENTS) FORMAT 4

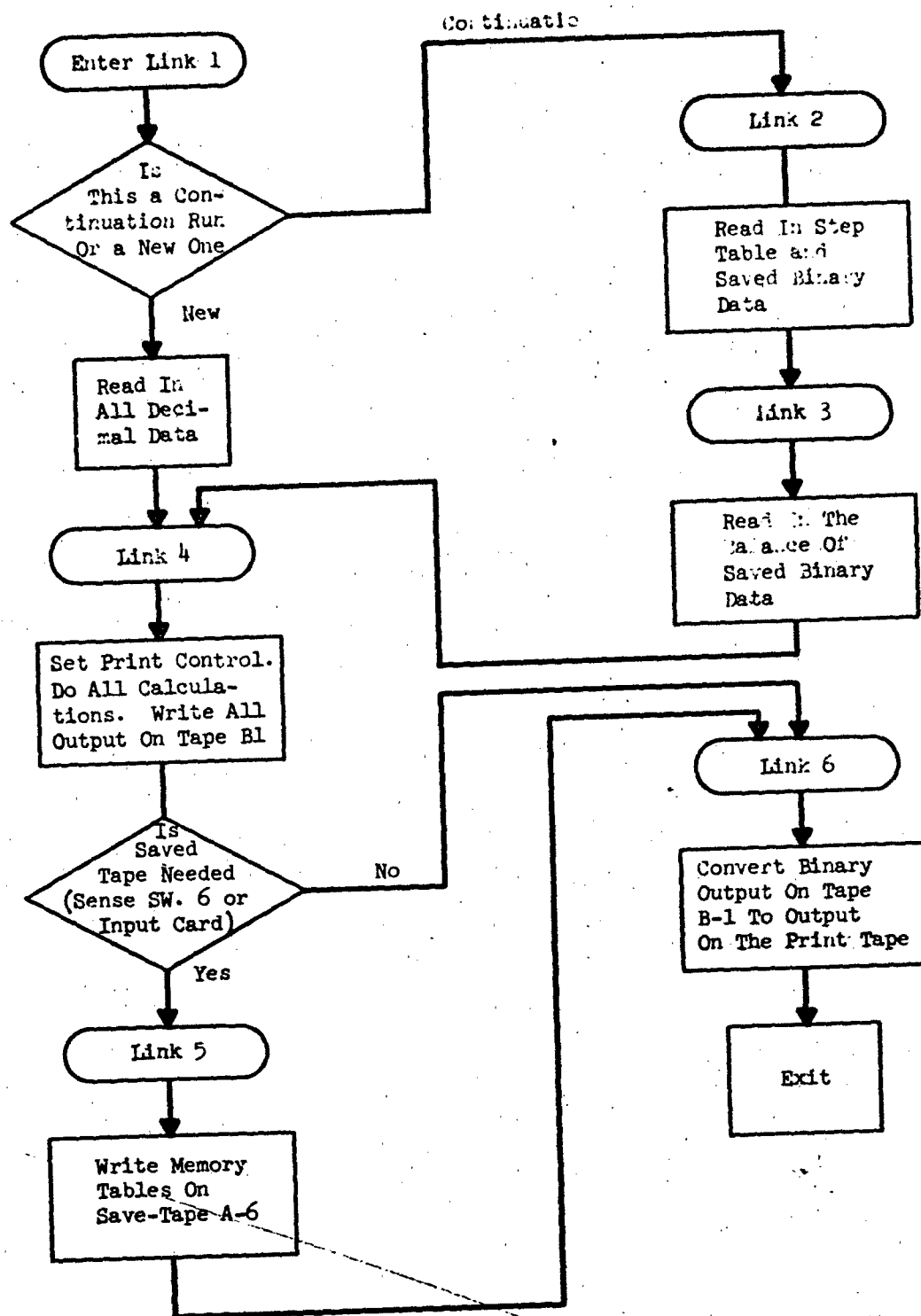
IX	I3	I3	E16.8
NR(3)	ND(3)		EL(3)
ROW	COL		ELEMENT

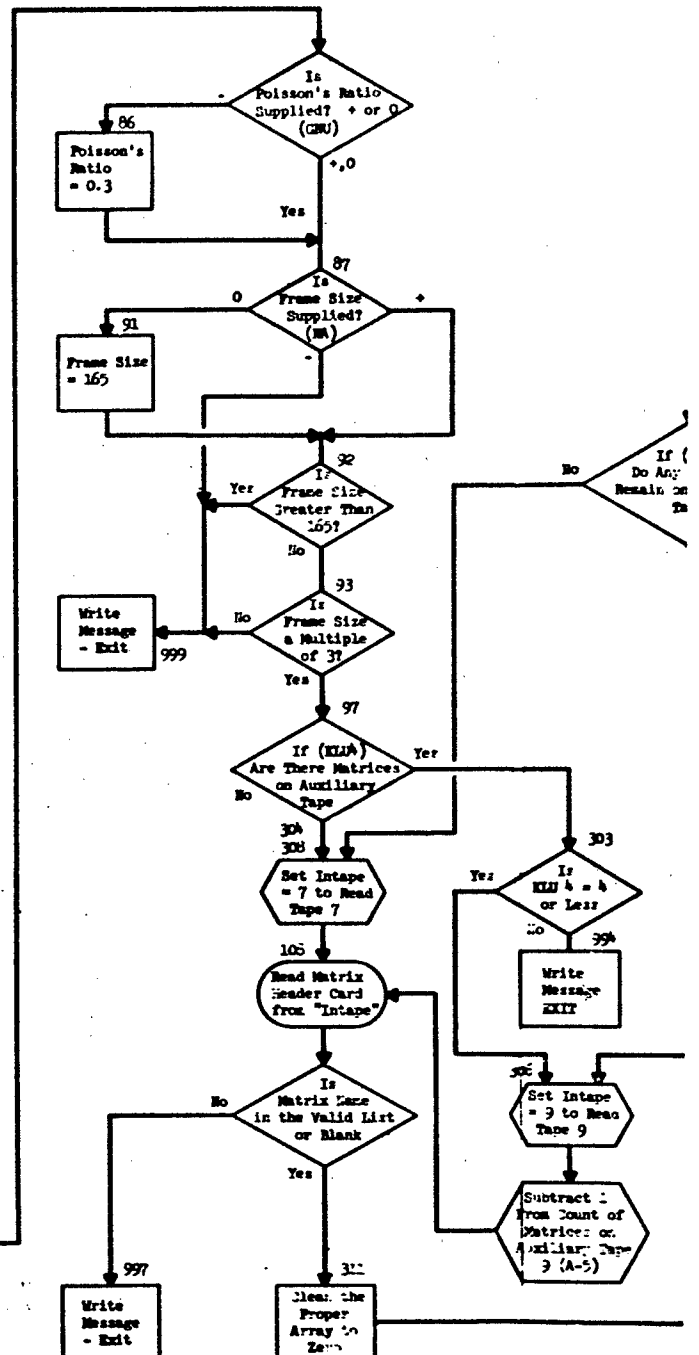
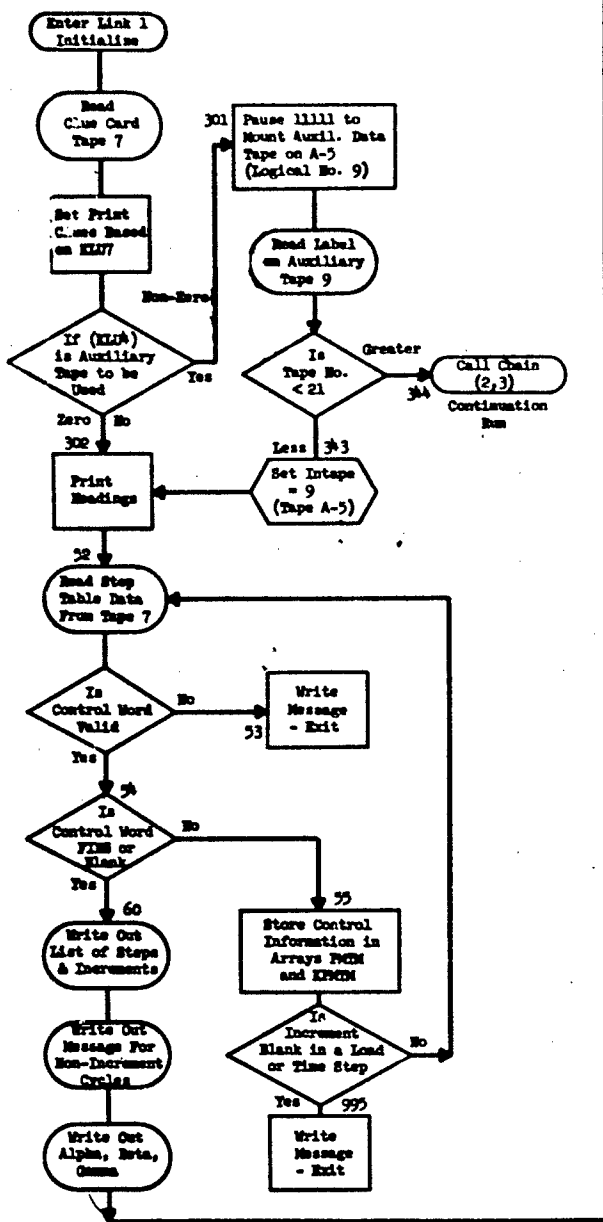
RD

39	40	41	42	43	44	45	46	47	48	49	50	51	52	53	54	55	56	57	58	59	60	61	62	63	64	65	66	67	68	69	70	71	72	73	74	75	76	77	78	79	80
----	----	----	----	----	----	----	----	----	----	----	----	----	----	----	----	----	----	----	----	----	----	----	----	----	----	----	----	----	----	----	----	----	----	----	----	----	----	----	----	----	----

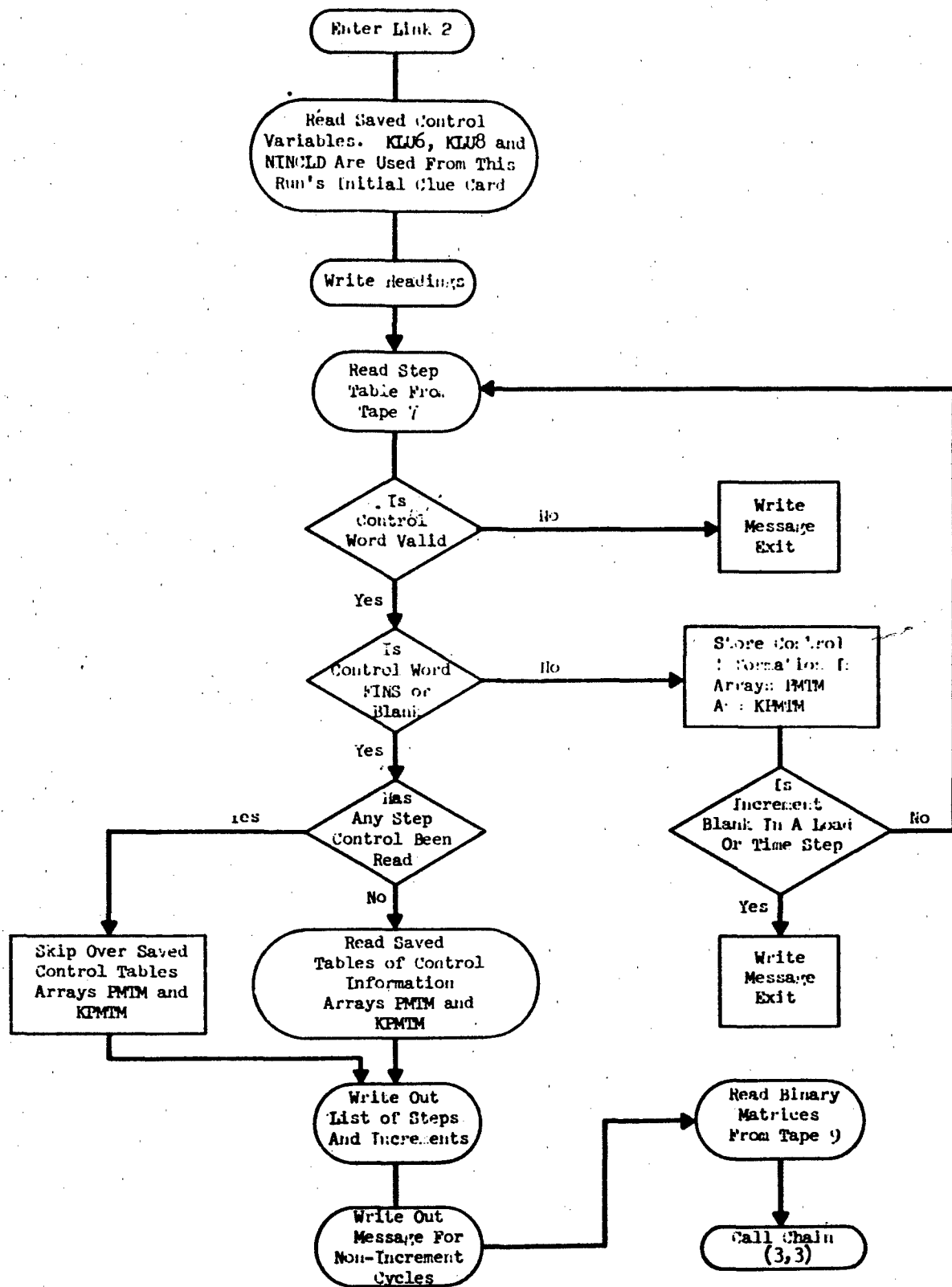
December, 1965

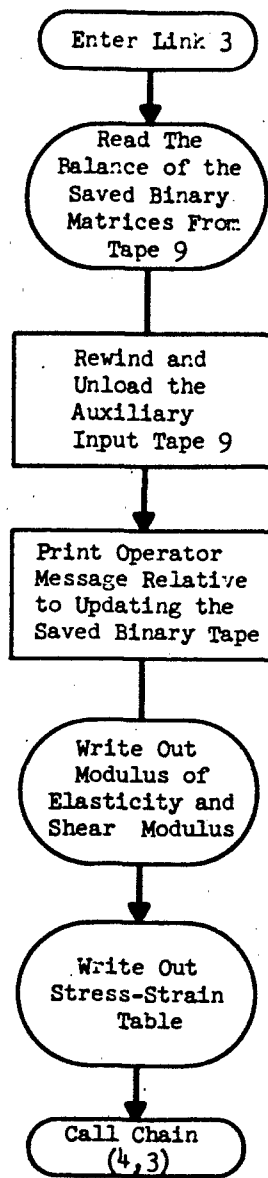
FLOW CHART FOR  
INELASTIC PLATE  
ANALYSIS

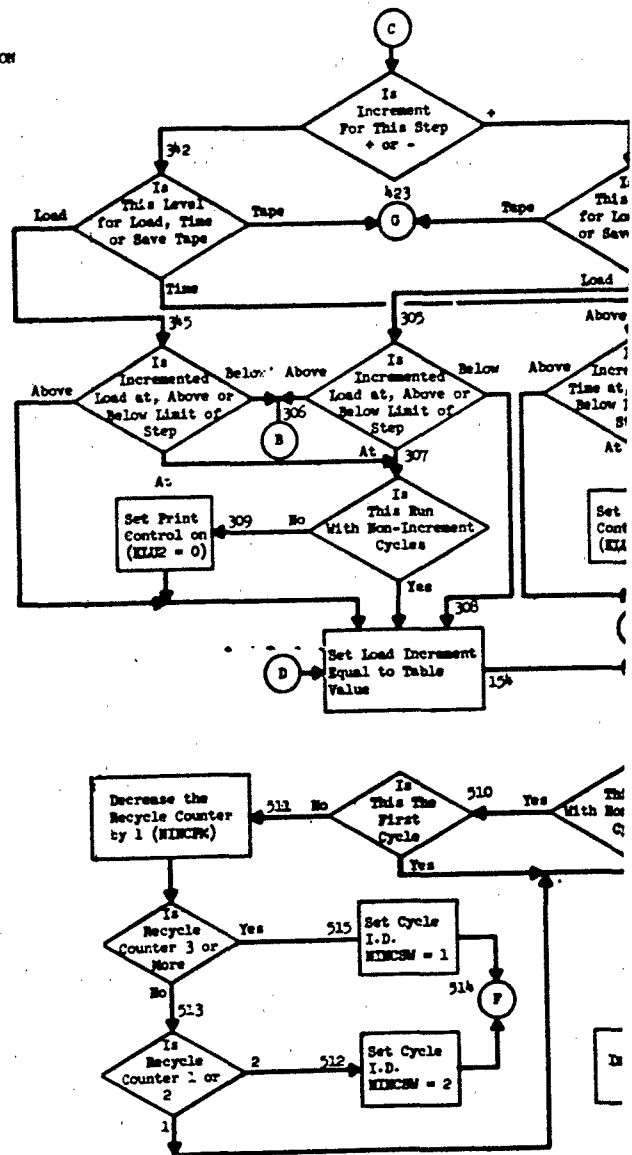
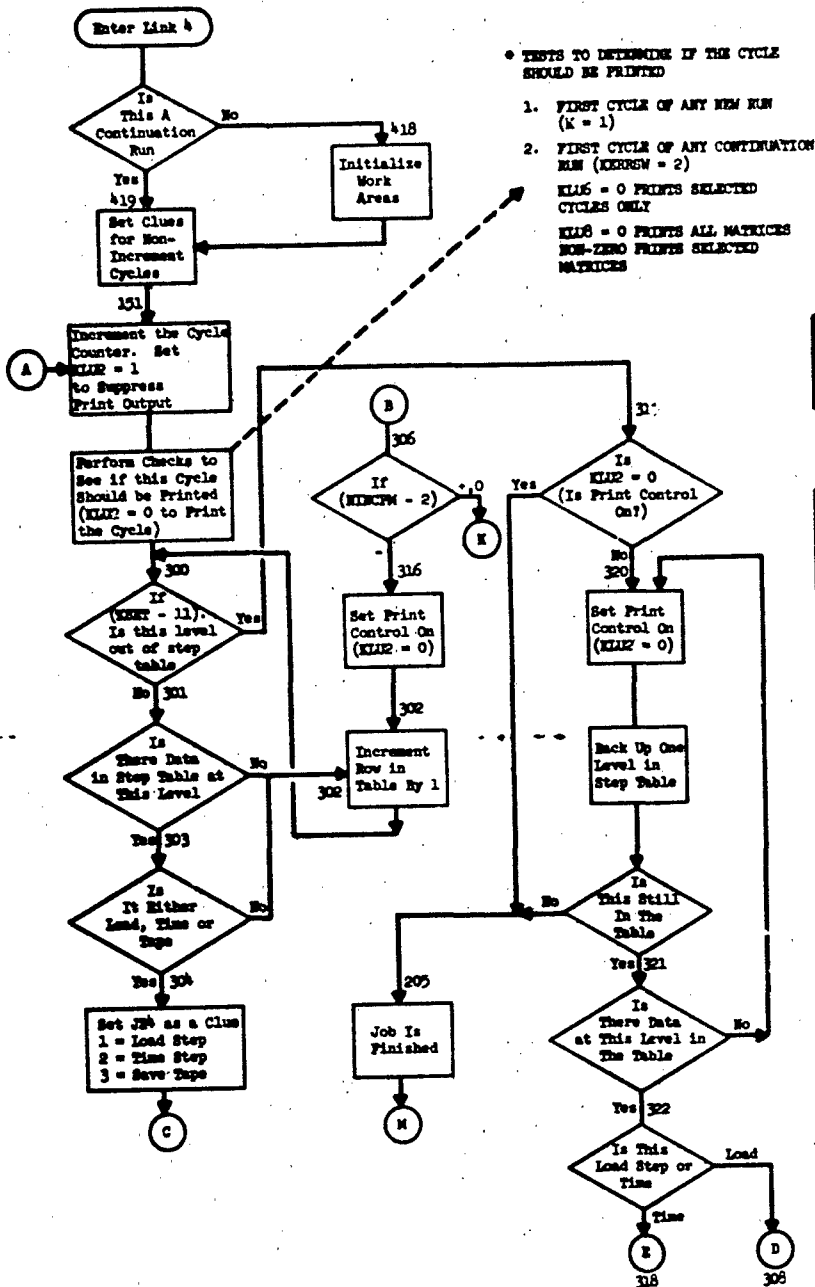




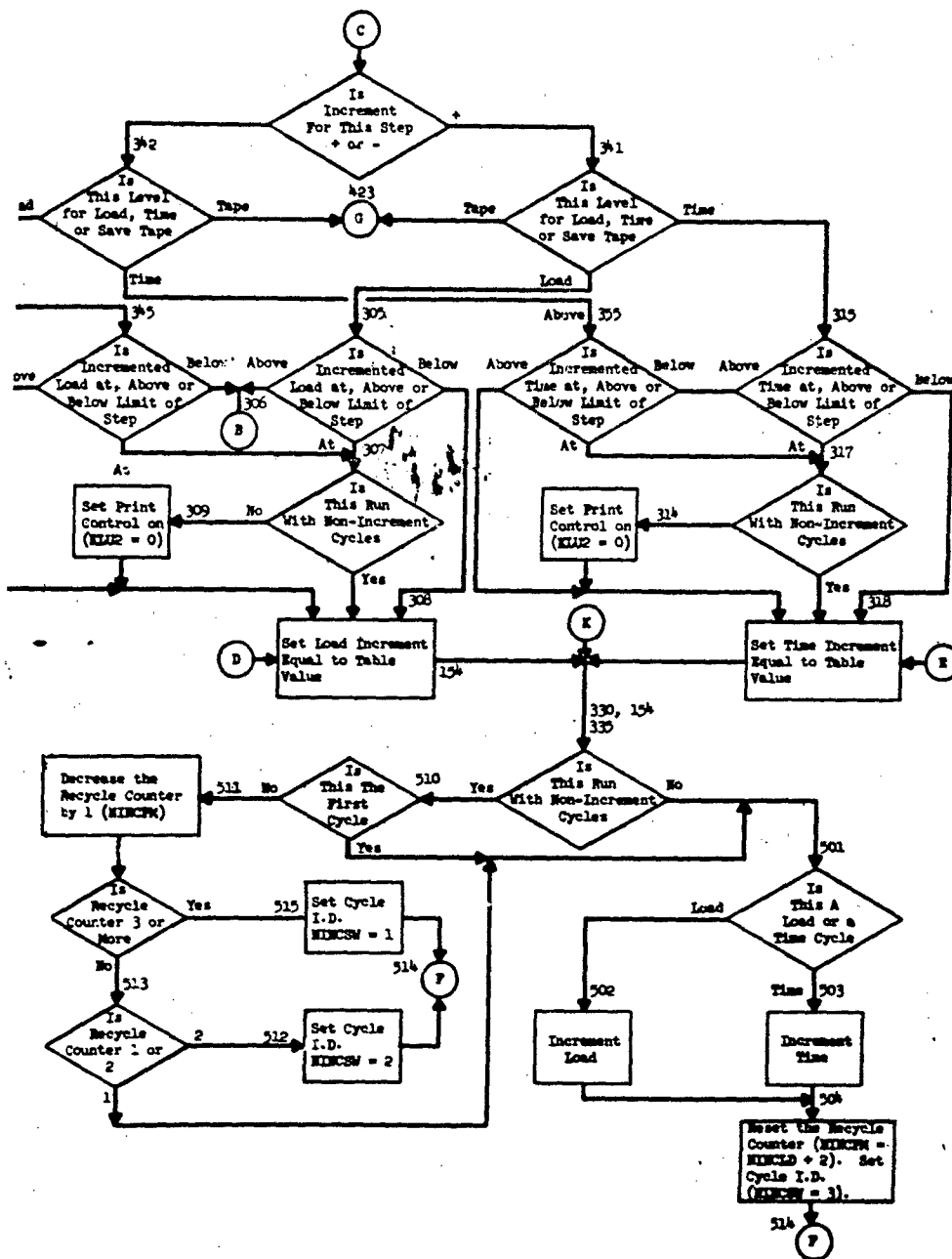


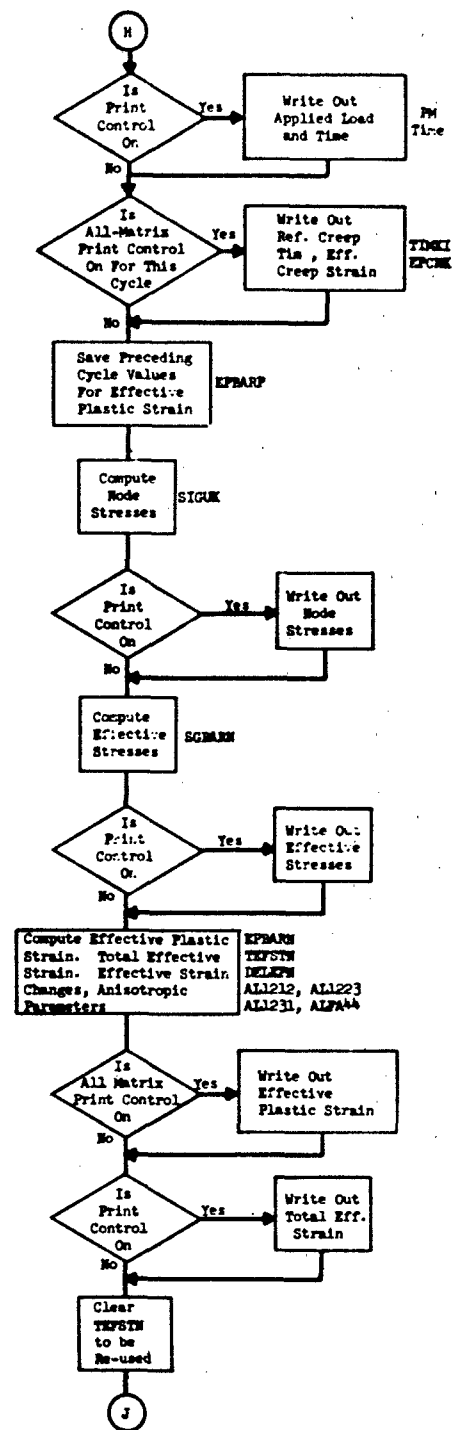
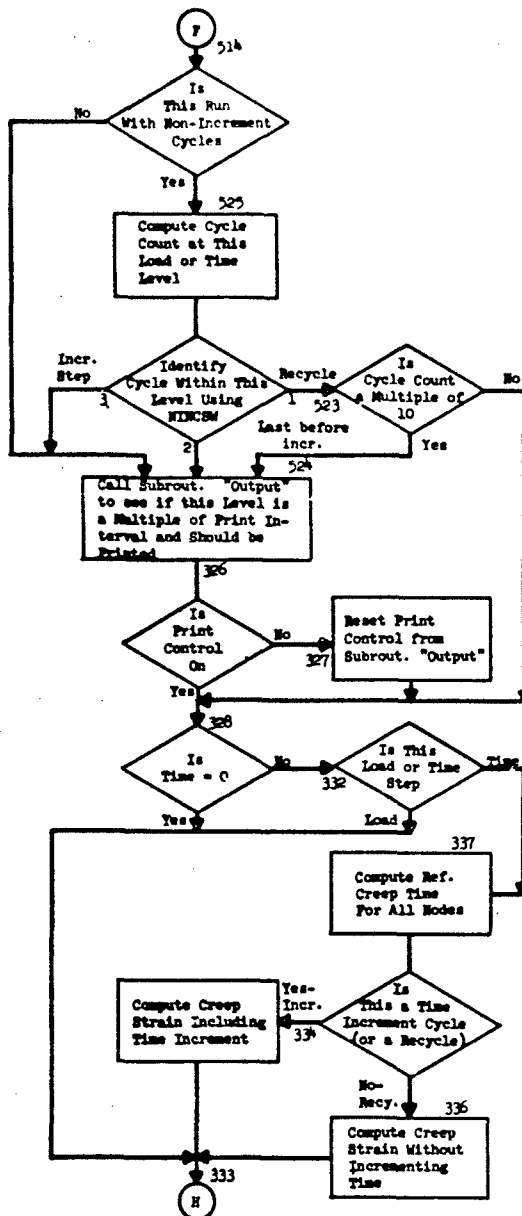












Com Stri Node Stri  
 AL Pri  
 Co Te St  
 2  
 Wit  
 37  
 42  
 423,  
 Wr Te Id of  
 My Dr Re

Write Out  
Applied Load  
and Time

PM  
Time

Write Out  
Eff. Creep  
Time, Eff.  
Creep Strain

TIMCK  
EPCNK

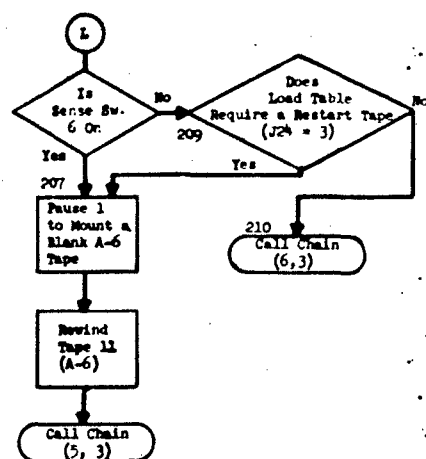
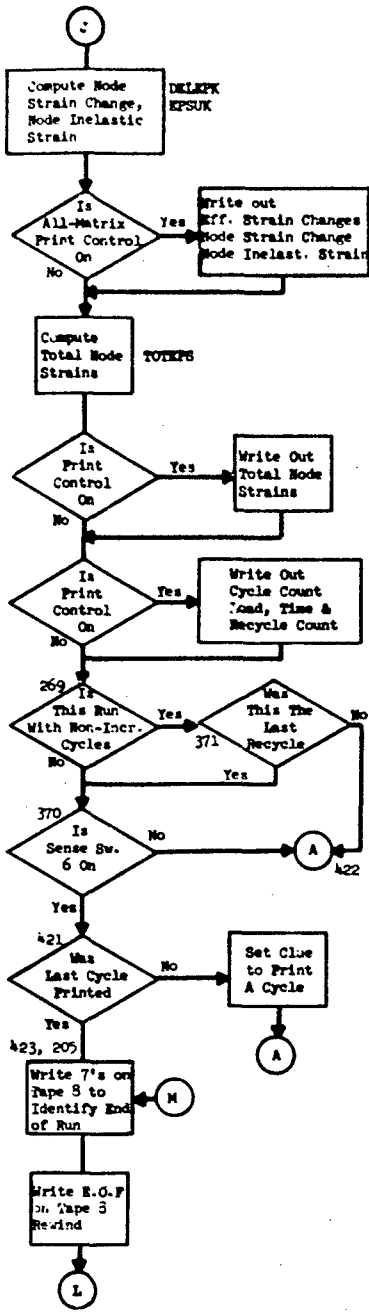
Write Out  
Node  
Stresses

Write Out  
Effective  
Stresses

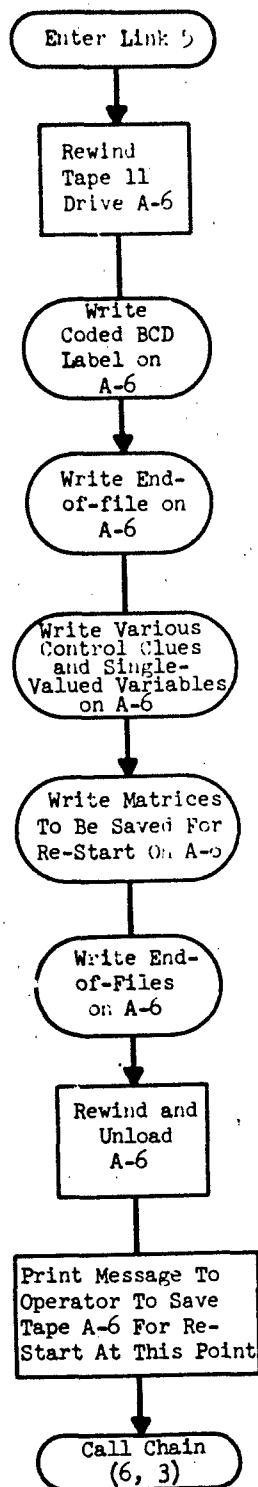
NEW  
NEW  
NEW  
212, ALL223  
231, ALP444

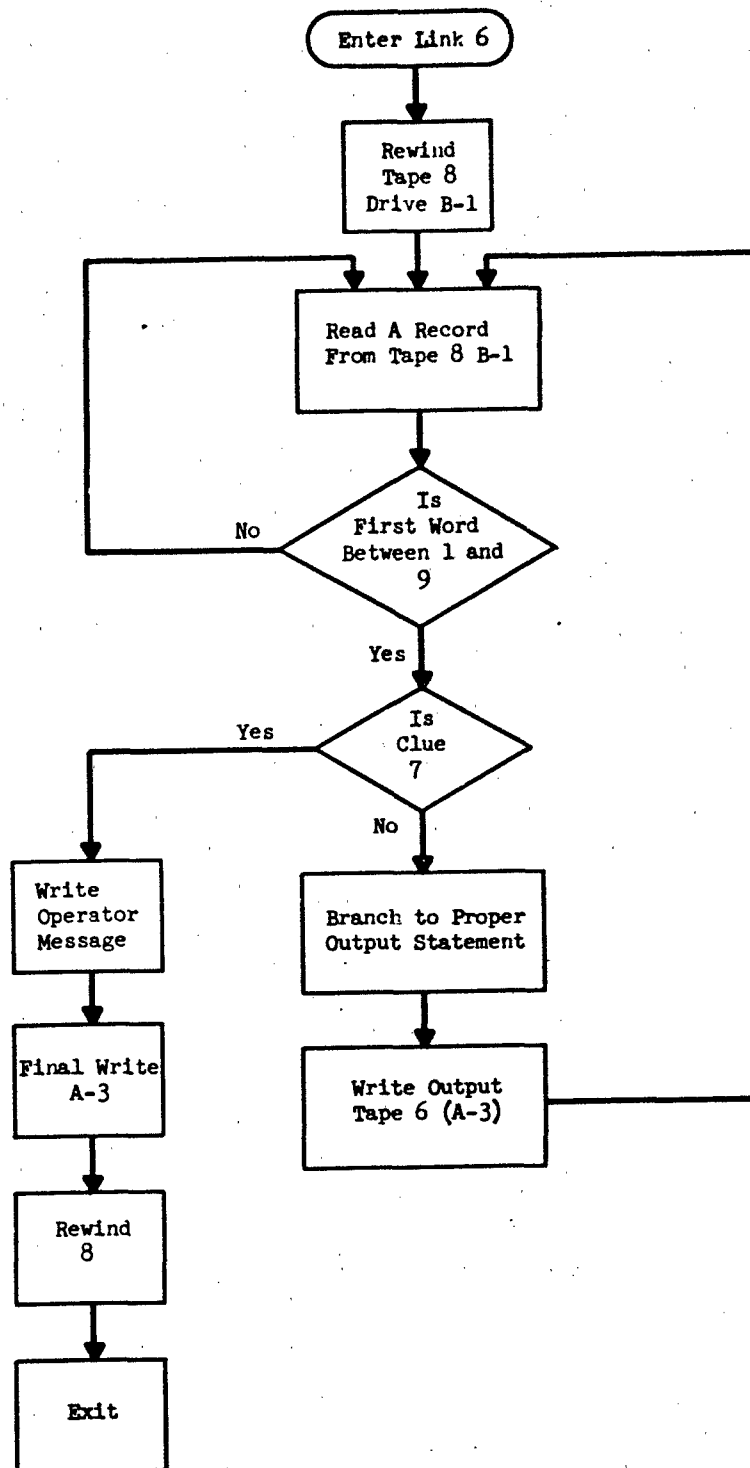
Write Out  
Effective  
Elastic Strain

Write Out  
Total Eff.  
Strain



2





FORTRAN II LISTING  
FOR INELASTIC PLATE  
ANALYSIS

*	XEQ	0001
*	CHAIN(1,3)	0002
*	LIST8	0003
451281 GRUMMAN AIRCRAFT ENGINEERING CORP. DECK NO. 45128 LINK 1		
C	MATRIX ANALYSIS FOR ISOTROPIC OR ANISOTROPIC INELASTIC STRUCTURES	0005
C	IN THE PLASTIC AND CREEP REGIME	0006
C		0007
C		0008
C	THIS PROGRAM WRITTEN FOR AIR FORCE CONTRACT AF 33(615)-2260	0009
C		0010
C	*** TABLE OF SYMBOLS USED ***	0011
C		0012
C	*** ARRAYS ***	0013
C	AL1212 - MATRIX OF ANISOTROPIC PARAMETERS FOR EACH NODE	0014
C	AL1223 - MATRIX OF ANISOTROPIC PARAMETERS FOR EACH NODE	0015
C	AL1231 - MATRIX OF ANISOTROPIC PARAMETERS FOR EACH NODE	0016
C	ALFA44 - MATRIX OF ANISOTROPIC PARAMETERS FOR EACH NODE	0017
C	DELEPK - MATRIX OF NODE STRAIN CHANGES (DELTA EPSILON)	0018
C	FOR THE X AND Y DIRECTIONS, AND THE SHEAR STRAIN CHANGE	0019
C	DELEPN - MATRIX OF EFFECTIVE INELASTIC STRAIN CHANGES	0020
C	EPBARN - MATRIX OF EFFECTIVE INELASTIC STRAINS (EPSILON BAR SUB N)	0021
C	FOR K-TH CYCLE	0022
C	EPBARP - MATRIX OF EFFECTIVE INELASTIC STRAINS (EPSILON BAR SUB N)	0023
C	FOR K-1 CYCLE (THE PRECEDING CYCLE)	0024
C	EPCNK - MATRIX OF EFFECTIVE CREEP STRAINS FOR THIS CYCLE	0025
C	EPCNP - MATRIX OF EFFECTIVE CREEP STRAINS FOR PREVIOUS CYCLE	0026
C	EPSUK - MATRIX OF NODE PLASTIC STRAINS (EPSILON SUB U) FOR THE	0027
C	X, Y AND SHEAR STRAINS, FOR THE K-TH CYCLE	0028
C	KPMTM - TABLE OF CONTROL CLUES (LOAD STEP, TIME STEP, WRITE SAVE	0029
C	TAPE) READ-IN CONTROL INFORMATION USED WITH PMTM	0030
C	PMTM - TABLE OF LOAD INCREMENTS, PRINT CONTROL INCREMENTS AND	0031
C	UPPER LOAD LEVEL PER STEP (CONTROL INFORMATION)	0032
C	SGBARM - MATRIX OF EFFECTIVE NODE STRESSES FOR LAST CYCLE THAT	0033
C	SHOWED AN INCREASE AT A PARTICULAR NODE	0034
C	SGBARN - MATRIX OF EFFECTIVE NODE STRESSES FOR CURRENT CYCLE	0035
C	SGBARP - MATRIX OF EFFECTIVE NODE STRESSES FOR PREVIOUS CYCLE	0036
C	SIGUK - MATRIX OF NODE STRESSES (SIGMA SUB U) FOR K-TH CYCLE	0037
C	SIJ - MATRIX OF STRESSES FOR MEMBER STRAINS	0038
C	SIM - MATRIX OF STRESSES FOR APPLIED LOADS	0039
C	TALF12 - MATRIX OF ANISOTROPIC PARAMETERS (INPUT DATA)	0040
C	TALF23 - MATRIX OF ANISOTROPIC PARAMETERS (INPUT DATA)	0041
C	TALF31 - MATRIX OF ANISOTROPIC PARAMETERS (INPUT DATA)	0042
C	TALF44 - MATRIX OF ANISOTROPIC PARAMETERS (INPUT DATA)	0043
C	TEFSTN - MATRIX OF TOTAL EFFECTIVE STRAINS	0044
C	TEPSN - TABLE OF STRAIN VALUES DEFINING THE STRESS-STRAIN CURVE	0045
C	TIMK1 - MATRIX OF REFERENCE CREEP TIMES FOR ALL NODES	0046
C	TOTEPS - MATRIX OF TOTAL NODE STRAINS	0047
C	TSIGN - TABLE OF STRESS LEVELS DEFINING THE STRESS-STRAIN CURVE	0048
C		0049
C	*** VARIABLES AND CLUES ***	0050
C	ALPHA - PARAMETER USED IN THE CREEP EQUATIONS	0051
C	BETA - PARAMETER USED IN THE CREEP EQUATIONS	0052
C	E - MODULUS OF ELASTICITY	0053
C	GAMMA - PARAMETER USED IN THE CREEP EQUATIONS	0054
C	GNU - POISSONS RATIO	0055
C	K - THE CYCLE COUNTER	0056
C	KERRSW - CLUE USED FOR TEMPORARY INDICATOR BETWEEN LINKS	0057
C	KLU4 - CLUE INDICATING TOTAL COUNT OF MATRICES ON AUXILIARY TAPE	0058
C	KLU5 - CLUE INDICATING MATRICES STILL NOT READ FROM AUXIL. TAPE	0059

C	KLU6	- CLUE FOR PRINT CONTROL (WHICH CYCLES)	0060
C	KLU8	- CLUE FOR PRINT CONTROL (WHICH MATRICES)	0061
C	KLUISO	- CLUE FOR ISOTROPIC OR ANISOTROPIC RUN (INPUT)	0062
C	KSET	- CLUE FOR THE LOAD OR TIME LEVEL CURRENTLY IN USE	0063
C	NA	- 3 TIMES THE NODE COUNT (INPUT)	0064
C	NC	- NUMBER OF NODES	0065
C	NINCLD	- NUMBER OF NON-INCREMENT CYCLES AT EACH LOAD LEVEL (INPUT)	0066
C	PM	- CURRENT LOAD LEVEL	0067
C	SHRMOD	- SHEAR MODULUS	0068
C	TIME	- CURRENT TIME LEVEL	0069
C			0070
C	OUTPUT	- SUBROUTINE TO CONTROL PRINTING AT VARYING LOAD LEVELS	0071
C			0072
C			0073
C	ELASTIC UNLOADING (FOLLOWS HOOKE'S LAW WHEN UNLOADING)		0074
C	COMMON TEFSTN, TOTEPS		0075
C	COMMON KLU4, KLU5, KLU6, KLU8, NA, NC, K		0076
C	COMMON KERRSW, NINCLD, KSET, PM, E, GNU, SHRMOD		0077
C	COMMON ALPHA, BETA, GAMMA, TIME, KLUISO		0078
C	COMMON PMTM, KPMTM, SIM, SIJ, TSIGN, TEPSN		0079
C	COMMON TALF12, TALF23, TALF31, TALF44		0080
C	COMMON AL1212, AL1223, AL1231, ALFA44		0081
C	DIMENSION TALF12(11), TALF23(11), TALF31(11), TALF44(11)		0082
C	DIMENSION AL1212(55), AL1223(55), AL1231(55), ALFA44(55)		0083
C	EQUIVALENCE (TIMK1, TEFSTN), (TOTEPS, DELEPK)		0084
C	THESE FOUR ARRAYS ARE EQUIVALENCED TO SAVE CORE SPACE.		0085
C	DIMENSION TIMK1(55), TEFSTN(55), TOTEPS(165), DELEPK(165)		0086
C	DIMENSION PMTM(10,3), KPMTM(10), SIM(165), SIJ(165,165), TSIGN(11)		0087
C	DIMENSION TEPSN(11)		0088
C	DIMENSION BL(5), ID(9), NR(3), NU(3), EL(3)		0089
C	DIMENSION PSTEP(3)		0090
C	EQUIVALENCE (ID(1), AD1), (ID(2), AD2), (ID(3), AD3), (ID(4), AD4), (ID(5), AD5), (ID(6), AD6), (ID(7), AD7), (ID(8), AD8), (ID(9), AD9)		0091
B	AD1 = 606060623144		0093
B	AD2 = 606060623141		0094
B	AD3 = 606362312745		0095
B	AD4 = 606325476245		0096
B	AD5 = 632143260102		0097
B	AD6 = 632143260203		0098
B	AD7 = 632143260301		0099
B	AD8 = 632143260404		0100
B	AD9 = 606060606060		0101
B	BL(1) = 434621246060		0102
B	BL(2) = 633144256060		0103
B	BL(3) = 632147256060		0104
B	BL(4) = 263145626060		0105
B	BL(5) = 606060606060		0106
	KERRSW = 1		0107
	INTAPE = 7		0108
	KLU5 = 0		0109
	KLU6 = 0		0110
	KLU8 = 10000		0111
	KLUALF = 0		0112
	PSTEP(1) = 0.0		0113
	PSTEP(2) = 0.0		0114
	PSTEP(3) = 0.0		0115



	DO 51 J22=1,10	0116
51	KPMTH(J22) = 0	0117
	LROW = 0	0118
	READ INPUT TAPE 7,1,KLU4,NINCLD,NA,KLU7,KLUISO,ALPHA,BETA,GAMMA,	0119
	IGNU,TA,TB,TC,TD,TE	0120
	WRITE OUTPUT TAPE 6,21,TA,TB,TC,TD,TE	0121
C	KLU7 (INPUT) = 0 TO PRINT PRE-SELECTED MATRICES ON SELECTED CYCLES	0122
C	KLU7 (INPUT) = 1 TO PRINT ALL MATRICES ON SELECTED CYCLES	0123
C	KLU7 (INPUT) = 2 TO PRINT PRE-SELECTED MATRICES ON ALL CYCLES	0124
C	KLU7 (INPUT) = 3-9 TO PRINT ALL MATRICES ON ALL CYCLES	0125
	IF(KLU7)384,384,381	0126
381	IF(KLU7-1)383,383,382	0127
382	KLU6 = 1	0128
C	KLU6 (OUTPUT) = 1 TO PRINT EACH CYCLE, 0 TO PRINT SELECTED CYCLES	0129
	IF(KLU7-2)384,384,383	0130
383	KLU8 = 0	0131
C	KLU8 (OUTPUT) = 0 TO PRINT ALL MATRICES	0132
C	KLU8 (OUTPUT) = 10000 TO PRINT SELECTED MATRICES	0133
384	CONTINUE	0134
	IF(KLU4)302,302,301	0135
301	PRINT 17	0136
	PAUSE 11111	0137
C	TEST INPUT TAPE TO DISTINGUISH GISMO BCD FROM INELASTIC PROG. SAVE	0138
	READ INPUT TAPE 9,31,LTAPE	0139
	REWIND 9	0140
C	SUBROUTINE FILTAP POSITIONS A TAPE AT THE FIRST RECORD OF ANY FILE	0141
	CALL FILTAP(9,2)	0142
	IF(LTAPE-21)343,343,344	0143
344	CONTINUE	0144
C	SAVED TAPE FROM PREVIOUS RUN OF INELASTIC PLATE	0145
C	THIS RUN IS A CONTINUATION	0146
	CALL CHAIN (2,3)	0147
343	CONTINUE	0148
C	GISMO FORMAT BCD TAPE	0149
C	THIS RUN IS A NEW ONE	0150
	KLU5 = KLU4	0151
	INTAPE = 9	0152
302	CONTINUE	0153
C	KLUISO = 0 FOR ISOTROPIC RUN	0154
C	KLUISO = 1 FOR ANISOTROPIC RUN	0155
	WRITE OUTPUT TAPE 6,9	0156
	IF(KLUISO)380,380,379	0157
379	CONTINUE	0158
	WRITE OUTPUT TAPE 6,10	0159
380	CONTINUE	0160
52	READ INPUT TAPE 7,2,TEMP1,TEMP2,TEMP3,TEMP4	0161
	LROW = LROW + 1	0162
	DO 53 J22=1,5	0163
B	IF(TEMP1*(-BL(J22)))53,54,53	0164
53	CONTINUE	0165
C	BAD CONTROL CARD	0166
	WRITE OUTPUT TAPE 6,12,LROW	0167
	WRITE OUTPUT TAPE 6,2,TEMP1,TEMP2,TEMP3,TEMP4	0168
	CALL EXIT	0169
54	GO TO(55,55,55,60,60),J22	0170
55	IF(LROW-10)56,56,53	0171

C	KPMTM( N ) = 1 FOR A LOAD STEP	0172
C	KPMTM( N ) = 2 FOR A TIME STEP	0173
C	KPMTM( N ) = 3 TO DUMP MEMORY INTO A SAVE TAPE	0174
C	PMTM( N,1 ) = UPPER LIMIT OF STEP	0175
C	PMTM( N,2 ) = INTERVAL (INCREMENT) FOR CALCULATION	0176
C	PMTM( N,3 ) = INTERVAL (INCREMENT) FOR PRINT OUTPUT	0177
	56 KPMTM(LROW) = J22	0178
	PMTM(LROW,1) = TEMP2	0179
	TEMP5 = TEMP2 - PSTEP(J22)	0180
	PMTM(LROW,2) = SIGNF(TEMP5,TEMP5)	0181
	PSTEP(J22) = TEMP2	0182
	IF(PMTM(LROW,2)) 57,63,57	0183
	63 GO TO(995,995,57),J22	0184
	57 CONTINUE	0185
	PMTM(LROW,3) = TEMP4	0186
	GO TO 52	0187
	60 CONTINUE	0188
	DO 361 J23 = 1,10	0189
	IF(KPMTM(J23)) 361,361,362	0190
	362 IF(KPMTM(J23)-4) 363,361,361	0191
	363 J24 = KPMTM(J23)	0192
	GO TO (364,366,368),J24	0193
	364 WRITE OUTPUT TAPE 6,22,PMTM(J23,2),PMTM(J23,1)	0194
	IF(PMTM(J23,3)) 361,361,365	0195
	365 WRITE OUTPUT TAPE 6,23,PMTM(J23,2)	0196
	GO TO 361	0197
	366 WRITE OUTPUT TAPE 6,24,PMTM(J23,2),PMTM(J23,1)	0198
	IF(PMTM(J23,3)) 361,361,367	0199
	367 WRITE OUTPUT TAPE 6,26,PMTM(J23,2)	0200
	GO TO 361	0201
	368 WRITE OUTPUT TAPE 6,27	0202
	361 CONTINUE	0203
	WRITE OUTPUT TAPE 6,28,NINCLD	0204
	WRITE OUTPUT TAPE 6,25,ALPHA,BETA,GAMMA	0205
	IF(GNU) 86,87,87	0206
	86 GNU = .3	0207
	87 CONTINUE	0208
	IF(NA) 999,91,92	0209
	91 NA = 165	0210
	92 IF(NA-165) 93,93,999	0211
	93 CONTINUE	0212
	96 IF(NA-3*(NA/3)) 999,97,999	0213
	97 NC = NA/3	0214
	IF(KLU4) 304,304,303	0215
	303 IF(KLU4-4) 306,306,994	0216
	306 CONTINUE	0217
	INTAPE = 9	0218
	KLU5 = KLU5 - 1	0219
	108 READ INPUT TAPE INTAPE, 3,NAME,NROWS,NCOLS,NFORM	0220
	DO 110 I21=1,	0221
	IF(NAME-ID(I21)) 110,311,110	0222
	110 CONTINUE	0223
C	BAD INPUT - MATRIX NAME NOT ACCEPTABLE	0224
	GO TO 997	0225
	311 GO TO (321,322,323,324,325,326,327,328,111),I21	0226
	321 DO 331 I1 = 1,165	0227

331	SIM(I1) = 0.0	0228
	WRITE OUTPUT TAPE 6,20,NAME,NROWS,NCOLS,INTAPE	0229
	GO TO 111	0230
322	DO 332 I1 = 1,165	0231
	DO 332 I2 = 1,165	0232
332	SIJ(I1,I2) = 0.0	0233
	GO TO 111	0234
323	DO 333 I1 = 1,11	0235
333	TSIGN(I1) = 0.0	0236
	GO TO 111	0237
324	DO 334 I1 = 1,11	0238
334	TEPSN(I1) = 0.0	0239
	GO TO 111	0240
325	DO 335 I1 = 1,11	0241
335	TALF12(I1) = 0.0	0242
	KLUALF = KLUALF + 1	0243
	GO TO 111	0244
326	DO 336 I1 = 1,11	0245
336	TALF23(I1) = 0.0	0246
	KLUALF = KLUALF + 2	0247
	GO TO 111	0248
327	DO 337 I1 = 1,11	0249
337	TALF31(I1) = 0.0	0250
	KLUALF = KLUALF + 4	0251
	GO TO 111	0252
328	DO 338 I1 = 1,11	0253
338	TALF44(I1) = 0.0	0254
	KLUALF = KLUALF + 8	0255
	GO TO 111	0256
111	GO TO (112,112,112,112,112,112,112,112,150),121	0257
112	READ INPUT TAPE INTAPE,4,(NR(I22),ND(I22),EL(I22),I22=1,3)	0258
	IF(NR(1))996,109,113	0259
109	IF(KLU5)308,308,306	0260
308	INTAPE = 7	0261
	GO TO 108	0262
304	GO TO 308	0263
113	GO TO (121,122,125,126,201,202,203,204,150),121	0264
C	READ IN ARRAY SIGMA-IM	0265
121	MROW = NR(1)	0266
	WRITE OUTPUT TAPE 6,4,(NR(I22),ND(I22),EL(I22),I22=1,3)	0267
	SIM (MROW) = EL(1)	0268
	IF(EL(2))127,128,127	0269
127	MROW = NR(2)	0270
	SIM (MROW) = EL(2)	0271
128	IF(EL(3))129,112,129	0272
129	MROW = NR(3)	0273
	SIM (MROW) = EL(3)	0274
	GO TO 112	0275
C	READ IN ARRAY SIGMA-IJ	0276
122	MROW = NR(1)	0277
	MCOL = ND(1)	0278
	SIJ (MROW,MCOL) = EL(1)	0279
	IF(EL(2))130,131,130	0280
130	MROW = NR(2)	0281
	MCOL = ND(2)	0282
	SIJ (MROW,MCOL) = EL(2)	0283

131	IF(EL(3))132,112,132	0284
132	MROW = NR(3)	0285
	MCOL = ND(3)	0286
	SIJ (MROW,MCOL) = EL(3)	0287
	GO TO 112	0288
C	READ IN ARRAY TSIGN (TABLE OF SIGMA BAR N)	0289
125	MROW = NR(1)	0290
	TSIGN(MROW) = EL(1)	0291
	IF(EL(2))139,140,139	0292
139	MROW = NR(2)	0293
	TSIGN(MROW) = EL(2)	0294
140	IF(EL(3))141,112,141	0295
141	MROW = NR(3)	0296
	TSIGN(MROW) = EL(3)	0297
	GO TO 112	0298
C	READ IN ARRAY TEPN (TABLE OF EPSILON BAR N)	0299
126	MROW = NR(1)	0300
	TEPN(MROW) = EL(1)	0301
	IF(EL(2))142,143,142	0302
142	MROW = NR(2)	0303
	TEPN(MROW) = EL(2)	0304
143	IF(EL(3))144,112,144	0305
144	MROW = NR(3)	0306
	TEPN(MROW) = EL(3)	0307
	GO TO 112	0308
C	READ IN ALPHA TABLES	0309
201	MROW = NR(1)	0310
	TALF12(MROW) = EL(1)	0311
	IF(EL(2))221,222,221	0312
221	MROW = NR(2)	0313
	TALF12(MROW) = EL(2)	0314
222	IF(EL(3))223,112,223	0315
223	MROW = NR(3)	0316
	TALF12(MROW) = EL(3)	0317
	GO TO 112	0318
202	MROW = NR(1)	0319
	TALF23(MROW) = EL(1)	0320
	IF(EL(2))224,225,224	0321
224	MROW = NR(2)	0322
	TALF23(MROW) = EL(2)	0323
225	IF(EL(3))226,112,226	0324
226	MROW = NR(3)	0325
	TALF23(MROW) = EL(3)	0326
	GO TO 112	0327
203	MROW = NR(1)	0328
	TALF31(MROW) = EL(1)	0329
	IF(EL(2))227,228,227	0330
227	MROW = NR(2)	0331
	TALF31(MROW) = EL(2)	0332
228	IF(EL(3))229,112,229	0333
229	MROW = NR(3)	0334
	TALF31(MROW) = EL(3)	0335
	GO TO 112	0336
204	MROW = NR(1)	0337
	TALF44(MROW) = EL(1)	0338
	IF(EL(2))230,231,230	0339

230	MROW = NR(2)	0340
	TALF44(MROW) = EL(2)	0341
231	IF(EL(3))232,112,232	0342
232	MROW = NR(3)	0343
	TALF44(MROW) = EL(3)	0344
	GO TO 112	0345
150	CONTINUE	0346
	IF(KLUISO)165,165,161	0347
161	IF(KLUALF-15)167,167,162	0348
162	WRITE OUTPUT TAPE 6,32,KLUALF	0349
	IF(KLU4)164,164,163	0350
C	SUBROUTINE RUN REWINDS AND UNLOADS THE DESIGNATED TAPE	0351
163	CALL RUN(9)	0352
164	CALL EXIT	0353
165	DO 166 I = 1,11	0354
	TALF12(I) = 0.5	0355
	TALF23(I) = 0.5	0356
	TALF31(I) = 0.5	0357
166	TALF44(I) = 1.0	0358
167	CONTINUE	0359
	E = TSIGN(2)/TEPSN(2)	0360
81	SHRMOD = E/(2.*(1.+GNU))	0361
	WRITE OUTPUT TAPE 6,5,E,SHRMOD,GNU	0362
	WRITE OUTPUT TAPE 6,6	0363
	DO 149 I1=1,11	0364
149	WRITE OUTPUT TAPE 6,7,I1,TSIGN(I1),TEPSN(I1),TALF12(I1),TALF23(I1)	0365
	1,TALF31(I1),TALF44(I1)	0366
	K = 0	0367
	PM = 0.0	0368
	IF(KLU4)152,152,209	0369
C	SUBROUTINE RUN REWINDS AND UNLOADS THE DESIGNATED TAPE	0370
209	CALL RUN(9)	0371
151	PRINT 19	0372
152	CALL CHAIN(4,3)	0373
994	WRITE OUTPUT TAPE 6,18,KLU4	0374
	CALL EXIT	0375
995	WRITE OUTPUT TAPE 6,16,LROW	0376
	CALL EXIT	0377
996	CONTINUE	0378
	WRITE OUTPUT TAPE 6,14,NAME	0379
	WRITE OUTPUT TAPE 6,4,(NR(I22),ND(I22),EL(I22),I22=1,3)	0380
	CALL EXIT	0381
997	CONTINUE	0382
	WRITE OUTPUT TAPE 6,13,NAME	0383
	CALL EXIT	0384
999	WRITE OUTPUT TAPE 6,11,NA	0385
	CALL EXIT	0386
	1 FORMAT(11,2I3,2I1,1X,2E10.3,2F5.2,10X,5A6)	0387
	2 FORMAT(6X,A4,E10.6,E10.1,E10.1)	0388
	3 FORMAT(11X,A6,1X,2I3,8X,I1)	0389
	4 FORMAT(3(1X,2I3,E16.8) )	0390
	5 FORMAT(26H1 MODULUS OF ELASTICITY = ,F11.0,4H PSI,6X,16HSHEAR MODU	0391
	ILUS = ,F11.0,4H PSI,6X,5HNU = ,F6.3)	0392
	6 FORMAT(41H0 TABLE OF VALUES FOR STRESS-STRAIN CURVE //	0393
	15X,29HPPOINT STRESS LEVEL STRAIN,7X,8HALPHA 12,7X,8HALPHA 23,7X	0394
	1,8HALPHA 31,7X,8HALPHA 44/16X,3HPSI,9X,7HIN./IN.//)	0395

7	FORMAT(6X,13,2X,F11.2,5(3X,F12.6))	0396
9	FORMAT(//79H THIS ISOTROPIC RUN USES ELASTIC UNLOADING (HOOKE'S L	0397
	AW) WITH STRAIN HARDENING)	0398
10	FORMAT(1H+,5X,2HAN)	0399
11	FORMAT(10H ERROR NA=14)	0400
12	FORMAT(26H ERROR- INCREMENT CARD NO.,13,5H N.G.)	0401
13	FORMAT(14H ERROR-MATRIX ,A6)	0402
14	FORMAT(17H ERROR-NEG. INDEX A6)	0403
16	FORMAT(33H ERROR-NO INTERVAL-INCREMENT CARD,13)	0404
17	FORMAT(51H0 PAUSE 11111 TO MOUNT INPUT DATA TAPE ON DRIVE A-5/////)	0405
18	FORMAT(7H ERROR-15,18H INPUT MATRICES NG)	0406
19	FORMAT(89H DEMOUNT AND SAVE TAPE A-5. DATA HAS BEEN READ INTO MEMO	0407
	RY. THE PROGRAM CONTINUES TO RUN.//)	0408
20	FORMAT(//5X,7HMATRIX ,A6,1X,13,6H ROWS X ,13,19H COLUMNS FROM TAPE	0409
	1 ,12)	0410
21	FORMAT(1H1,29X,5A6)	0411
22	FORMAT(5X,16HLOAD INCREMENTS ,F9.2,11H POUNDS TO ,F10.2,7H POUNDS)	0412
23	FORMAT(1H+,61X,19HPRINT OUTPUT EVERY ,F9.2,7H POUNDS)	0413
24	FORMAT(5X,16HTIME INCREMENTS ,F9.4,11H HOURS TO ,F10.4,6H HOURS)	0414
25	FORMAT(// 9H ALPHA = ,E10.3,5X,7HDELTA = ,E10.3,5X,8H GAMMA = ,E10.3)	0415
26	FORMAT(1H+,61X,19HPRINT OUTPUT EVERY ,F9.4,6H HOURS)	0416
27	FORMAT(5X,35HSTORE MEMORY ON TAPE A-6, THEN EXIT)	0417
28	FORMAT(//5X,13,48H NON-INCREMENT CYCLES AT EACH LOAD OR TIME LEVEL	0418
	1)	0419
31	FORMAT(10X,12)	0420
32	FORMAT(5X,12,65H ALPHA TABLES WERE READ IN UP 4 REQUIRED. CHECK YOU	0421
	R INPUT CARDS.)	0422
	END(1,1,0,0,0,0,1,1,0,1,0,0,0,0,0)	
*	CHAIN(2,3)	0424
*	LIST8	0425

C451282	MATRIX ANALYSIS OF INELASTIC PLATE - LINK 2 - WITH CREEP	0427
C	THIS LINK READS IN A SAVED BINARY TAPE - FIRST PART	0428
	COMMON TEFSTN, TOTEPS	0429
	COMMON KLU4, KLU5, KLU6, KLU8, NA, NC, K	0430
	COMMON KERRSW, NINCLD, KSET, PM, E, GNU, SHRMOD	0431
	COMMON ALPHA, BETA, GAMMA, TIME, KLUISO	0432
	COMMON PMTM, KPMTM, SIM, SIJ, TSIGN, TEPSTN	0433
	COMMON TALF12, TALF23, TALF31, TALF44	0434
	COMMON AL1212, AL1223, AL1231, ALFA44	0435
	DIMENSION TALF12(11),TALF23(11),TALF31(11),TALF44(11)	0436
	DIMENSION AL1212(55),AL1223(55),AL1231(55),ALFA44(55)	0437
	COMMON SIGUK, EPSUK	0438
	EQUIVALENCE (TIMK1,TEFSTN),(TOTEPS,DELEPK)	0439
C	THESE FOUR ARRAYS ARE EQUIVALENCED TO SAVE CORE SPACE.	0440
	DIMENSION TIMK1(55),TEFSTN(55),TOTEPS(165),DELEPK(165)	0441
	DIMENSION PMTM(10,3),KPMTM(10),SIM(165),SIJ(165,165),TSIGN(11)	0442
	DIMENSION TEPSTN(11),SIGUK(165),EPSUK(165)	0443
	DIMENSION BL(5)	0444
	DIMENSION PSTEP(3)	0445
	READ TAPE 9,KLU4,KLU5, LA, LB,NA,NC,K,KERRSW, LC,KSET,PM,E,	0446
	IGNU,SHRMOD,ALPHA,BETA,GAMMA,TIME,KLUISO	0447
C	KLU6 = 1 WILL PRINT EVERY CYCLE, 0 WILL PRINT ONLY SELECTED CYCLES	0448
C	KLU8 = 0 WILL PRINT ALL MATRICES, NON-ZERO PRINTS SELECTED MATRICES	0449
C	NINCLD (NON-INCREMENT CYCLES AT EACH LOAD LEVEL) ACCEPTED FROM	0450
C	INPUT CONTROL CARD	0451
	WRITE OUTPUT TAPE 6,9	0452
	IF(KLUISO)380,380,379	0453
379	CONTINUE	0454
	WRITE OUTPUT TAPE 6,10	0455
380	CONTINUE	0456
	NCLU = 1	0457
	KERRSW = 2	0458
B	BL(1) = 434621246060	0459
B	BL(2) = 633144256060	0460
B	BL(3) = 632147256060	0461
B	BL(4) = 263145626060	0462
B	BL(5) = 606060606060	0463
	DO 51 I42 = 1,10	0464
51	KPMTM(I42) = 0	0465
	PSTEP(1) = 0.0	0466
	PSTEP(2) = 0.0	0467
	PSTEP(3) = 0.0	0468
	LROW = 0	0469
52	READ INPUT TAPE 7,2,TEMP1,TEMP2,TEMP3,TEMP4	0470
	LROW = LROW + 1	0471
	DO 53 J22=1,5	0472
B	IF(TEMP1*(-BL(J22)))53,54,53	0473
53	CONTINUE	0474
C	BAD CONTROL CARD	0475
	WRITE OUTPUT TAPE 6,12,LROW	0476
	WRITE OUTPUT TAPE 6,2,TEMP1,TEMP2,TEMP3,TEMP4	0477
	CALL EXIT	0478
54	GO TO(55,55,55,60,60),J22	0479
55	IF(LROW-10)56,56,53	0480
C	KPMTM( N ) = 1 FOR A LOAD STEP	0481

C	KPMTM( N ) = 2 FOR A TIME STEP	0482
C	KPMTM( N ) = 3 TO DUMP MEMORY INTO A SAVE TAPE	0483
C	PMTM( N,1 ) = UPPER LIMIT OF STEP	0484
C	PMTM( N,2 ) = INTERVAL (INCREMENT) FOR CALCULATION	0485
C	PMTM( N,3 ) = INTERVAL (INCREMENT) FOR PRINT OUTPUT	0486
56	KPMTM(LKOW) = J22	0487
	NCLU = 2	0488
	KSET = 1	0489
	PMTM(LROW,1) = TEMP2	0490
	TEMP5 = TEMP2- PSTEP(J22)	0491
	PMTM(LROW,2) = SIGNF(TEMP5,TEMP5)	0492
	PSTEP(J22) = TEMP2	0493
	IF(PMTM(LROW,2))57,63,57	0494
63	GO TO (995,995,57),J22	0495
57	CONTINUE	0496
	PMTM(LROW,3) = TEMP4	0497
	GO TO 52	0498
60	CONTINUE	0499
	GO TO (61,62),NCLU	0500
62	CONTINUE	0501
	READ TAPE 9,JUNK	0502
	READ TAPE 9,JUNK	0503
	GO TO 64	0504
61	CONTINUE	0505
	READ TAPE 9,PMTM	0506
	READ TAPE 9,KPMTM	0507
64	CONTINUE	0508
	WRITE OUTPUT TAPE 6,1	0509
	DO 361 J23 = 1,10	0510
	IF(KPMTM(J23))361,361,362	0511
362	IF(KPMTM(J23)-4)363,361,361	0512
363	J24 = KPMTM(J23)	0513
	GO TO (364,366,368),J24	0514
364	WRITE OUTPUT TAPE 6,22,PMTM(J23,2),PMTM(J23,1)	0515
	IF(PMTM(J23,3))361,361,365	0516
365	WRITE OUTPUT TAPE 6,23,PMTM(J23,3)	0517
	GO TO 361	0518
366	WRITE OUTPUT TAPE 6,24,PMTM(J23,2),PMTM(J23,1)	0519
	IF(PMTM(J23,3))361,361,367	0520
367	WRITE OUTPUT TAPE 6,25,PMTM(J23,3)	0521
	GO TO 361	0522
368	WRITE OUTPUT TAPE 6,27	0523
361	CONTINUE	0524
	WRITE OUTPUT TAPE 6,26,NINCLD	0525
	READ TAPE 9,SIM	0526
	READ TAPE 9,SIJ	0527
	READ TAPE 9,TSIGN	0528
	READ TAPE 9,TEPSN	0529
	READ TAPE 9,TALF12	0530
	READ TAPE 9,TALF23	0531
	READ TAPE 9,TALF31	0532
	READ TAPE 9,TALF44	0533
	READ TAPE 9,AL1212	0534
	READ TAPE 9,AL1223	0535
	READ TAPE 9,AL1231	0536
	READ TAPE 9,ALFA44	0537



READ TAPE 9,SIGUK	0538
READ TAPE 9,EPSUK	0539
CALL CHAIN (3,3)	0540
995 WRITE OUTPUT TAPE 6,16,LROM	0541
CALL EXIT	0542
1 FORMAT(1H0,29X,37HCONTINUATION RUN - INELASTIC ANALYSIS)	0543
2 FORMAT(6X,A4,E10.6,E10.1,E10.1)	0544
9 FORMAT(/79H THIS ISOTROPIC RUN USES ELASTIC UNLOADING (HOOKE'S L	0545
AW) WITH STRAIN HARDENING)	0546
10 FORMAT(1H+,5X,2HAN)	0547
12 FORMAT(26H ERROR- INCREMENT CARD NO.,13,5H N.G.)	0548
16 FORMAT(33H ERROR-NU INTERVAL-INCREMENT CARD,13)	0549
22 FORMAT(5X,16HLOAD INCREMENTS ,F9.2,11H POUNDS TO ,F10.2,7H POUNDS)	0550
23 FORMAT(1H+,61X,19HPRINT OUTPUT EVERY ,F9.2,7H POUNDS)	0551
24 FORMAT(5X,16HTIME INCREMENTS ,F9.4,11H HOURS TO ,F10.4,6H HOURS)	0552
25 FORMAT(1H+,61X,19HPRINT OUTPUT EVERY ,F9.4,6H HOURS)	0553
26 FORMAT(/5X,13,48H NON-INCREMENT CYCLES AT EACH LOAD OR TIME LEVEL	0554
1)	0555
27 FORMAT(5X,35HSTORE MEMORY ON TAPE A-6, THEN EXIT)	0556
END(1,1,0,0,0,0,1,1,0,1,0,0,0,0)	
* CHAIN(3,3)	0558
* LIST8	0559

```

C451283 MATRIX ANALYSIS OF INELASTIC PLATE LINK 3 - WITH CREEP 0561
C THIS IS THE SECOND HALF OF OLD LINK 2 0562
C THIS LINK READS IN A SAVED BINARY TAPE - SECOND PART 0563
COMMON TEFSTN, TOTEPS 0564
COMMON KLU4, KLU5, KLU6, KLU8, NA, NC, K 0565
COMMON KERRSW, NINCLO, KSET, PM, E, GNU, SHRMUD 0566
COMMON ALPHA, BETA, GAMMA, TIME, KLUSO 0567
COMMON PMTM, KPMTM, SIM, SIJ, TSIGN, TEPSEN 0568
COMMON TALF12, TALF23, TALF31, TALF44 0569
COMMON AL1212, AL1223, AL1231, ALFA44 0570
DIMENSION TALF12(11), TALF23(11), TALF31(11), TALF44(11) 0571
DIMENSION AL1212(55), AL1223(55), AL1231(55), ALFA44(55) 0572
COMMON SIGUK, EPSUK 0573
COMMON SGBARN, SGBARP, SGBARM, EPBARN, EPBARP, DELEPN 0574
COMMON EPCNK, EPCNP 0575
EQUIVALENCE (TIMK1, TEFSTN), (TOTEPS, DELEPK) 0576
C THESE FOUR ARRAYS ARE EQUIVALENCED TO SAVE CORE SPACE. 0577
DIMENSION TIMK1(55), TEFSTN(55), TOTEPS(165), DELEPK(165) 0578
DIMENSION PMTM(10,3), KPMTM(10), SIM(165), SIJ(165,165), TSIGN(11) 0579
DIMENSION TEPSEN(11), SIGUK(165), EPSUK(165), SGBARN(55), SGBARP(55) 0580
DIMENSION SGBARM(55), EPBARN(55), EPBARP(55), DELEPN(55), EPCNK(55) 0581
DIMENSION EPCNP(55) 0582
READ TAPE 9, SGBARN 0583
READ TAPE 9, SGBARP 0584
READ TAPE 9, SGBARM 0585
READ TAPE 9, EPBARN 0586
READ TAPE 9, EPBARP 0587
READ TAPE 9, DELEPN 0588
READ TAPE 9, EPCNK 0589
READ TAPE 9, EPCNP 0590
C SUBROUTINE RUN REWINDS AND UNLOADS THE DESIGNATED TAPE 0591
CALL RUN(9) 0592
PRINT 31 0593
WRITE OUTPUT TAPE 6,5,E,SHRMUD,GNU 0594
WRITE OUTPUT TAPE 6,6 0595
DO 149 I1=1,11 0596
149 WRITE OUTPUT TAPE 6,7,I1,TSIGN(I1),TEPSN(I1),TALF12(I1),TALF23(I1) 0597
1,TALF31(I1),TALF44(I1) 0598
CALL CHAIN(4,3) 0599
5 FORMAT(26H0 MODULUS OF ELASTICITY = ,F11.0,4H PSI,6X,16HSHFEAR MODU 0600
ILUS = ,F11.0,4H PSI,6X,5HNU = ,F6.3) 0601
6 FORMAT(41H0 TABLE OF VALUES FOR STRESS-STRAIN CURVE // 0602
15X,29HPOINT STRESS LEVEL STRAIN,7X,8HALPHA 12,7X,8HALPHA 23,7X 0603
1,8HALPHA 31,7X,8HALPHA 44/10X,3HPSI,9X,7HIN./IN.//) 0604
7 FORMAT(6X,13,2X,F11.2,5(3X,F12.8)) 0605
31 FORMAT(118H0IF NECESSARY TO STOP THIS RUN BECAUSE IT EXCEEDS THE T 0606
IME ESTIMATE, PUT A RING IN THE SAVE TAPE ON A-5 AND CHANGE IT / 0607
256H TO DRIVE A-6 TO UPDATE IT, THEN PUT SENSE SWITCH 6 ON. //) 0608
END(1,1,0,0,0,0,1,1,0,1,0,0,0,0,0)

*
* SAVE TAPE 8-1 UNLESS ON-LINE PRINT SAYS IT HAS BEEN PROCESSED 0610
* 0611
* PUT SENSE SWITCH 6 ON TO END THE RUN IF IT EXCEEDS THE TIME ESTIM. 0612
* 0613
* IF PAUSE 1 OCCURS (SENSE SWITCH 6 OR INTERNAL CONTROL), MOUNT A 0614
* BLANK TAPE ON A-6. THIS TAPE WILL HAVE RESTART DATA WRITTEN ON IT, 0615
* AND MUST BE SAVED. 0616
* CHAIN(4,3) 0617
* LIST8 0618
* 0619

```

```

C451284 MATRIX ANALYSIS OF INELASTIC PLATE - LINK 4 - WITH CREEP 0621
C THIS LINK DOES THE CALCULATION AND WRITES PRINT OUTPUT 0622
COMMON TEFSTN, TOTEPS 0623
COMMON KLU4, KLU5, KLU6, KLU8, NA, NC, K 0624
COMMON KERRSW, NINCLD, KSET, PM, E, GNU, SHRMUD 0625
COMMON ALPHA, BETA, GAMMA, TIME, KLUI50 0626
COMMON PMTM, KPMTM, SIM, SIJ, TSIGN, TEPSTN 0627
COMMON TALF12, TALF23, TALF31, TALF44 0628
COMMON AL1212, AL1223, AL1231, ALFA44 0629
COMMON TALF12(11), TALF23(11), TALF31(11), TALF44(11) 0630
COMMON AL1212(55), AL1223(55), AL1231(55), ALFA44(55) 0631
COMMON SIGUK, EPSUK 0632
COMMON SGBARN, SGBARP, SGBARM, EPBARN, EPBARP, DELEPN 0633
COMMON EPCNK, EPCNP 0634
EQUIVALENCE (TIMK1, TEFSTN), (TOTEPS, DELEPK) 0635
C THESE FOUR ARRAYS ARE EQUIVALENCED TO SAVE CORE SPACE. 0636
C THEY ARE NOT THE SAME, BUT ARE NOT NEEDED AT THE SAME TIME 0637
C AND DO NOT CARRY FROM CYCLE TO CYCLE. 0638
DIMENSION TIMK1(55), TEFSTN(55), TOTEPS(165), DELEPK(165) 0639
DIMENSION PMTM(10,3), KPMTM(10), SIM(165), SIJ(165,165), TSIGN(11) 0640
DIMENSION TEPSTN(11), SIGUK(165), EPSUK(165), SGBARN(55), SGBARP(55) 0641
DIMENSION SGBARM(55), EPBARN(55), EPBARP(55), DELEPN(55), EPCNK(55) 0642
DIMENSION EPCNP(55) 0643
KSET = KSET 0644
KERRSW = KERRSW 0645
GO TO (418,419), KERRSW 0646
C INITIALIZE WORK AREAS 0647
418 DO 102 I1 = 1,165 0648
EPSUK(I1) = 0.0 0649
102 SIGUK(I1) = 0.0 0650
DO 103 I1 = 1,55 0651
DELEPN(I1) = 0.0 0652
SGBARN(I1) = 0.0 0653
SGBARP(I1) = 0.0 0654
SGBARM(I1) = 0.0 0655
EPBARP(I1) = 0.0 0656
EPCNK(I1) = 0.0 0657
EPCNP(I1) = 0.0 0658
AL1212(I1) = 2.*TALF12(2) 0659
AL1223(I1) = TALF12(2) + TALF23(2) 0660
AL1231(I1) = TALF12(2) + TALF31(2) 0661
ALFA44(I1) = TALF44(2) 0662
103 EPBARN(I1) = 0.0 0663
KSET = 1 0664
TIME = 0.0 0665
419 CONTINUE 0666
REWIND 8 0667
KSET = KSET 0668
KERRSW = KERRSW 0669
NINCPM = NINCLD + 2 0670
NINTOT = NINCLD + 1 0671
151 K = K + 1 0672
KLU2 = 1 0673
C IF KLU2 = 0, THE CYCLE OF OPERATIONS WILL BE PRINTED 0674
C KLU6 = 1 WILL PRINT EVERY CYCLE, 0 WILL PRINT ONLY SELECTED CYCLES 0675

```

C	KLUB = 0 WILL PRINT ALL MATRICES, NON-ZERO PRINTS SELECTED UNES	0676
	IF(KLU6)248,248,249	0677
249	KLUB = 0	0678
248	CONTINUE	0679
	IF(K-1)270,270,271	0680
270	KLUB = 0	0681
271	CONTINUE	0682
	GO TO (416,417),KERRSW	0683
417	KLUB = 0	0684
	KERRSW = 1	0685
416	CONTINUE	0686
C	KSET IS THE ROW OF KPMTM OR PMTM BEING USED (CURRENT LOAD OR	0687
C	TIME LEVEL)	0688
300	IF(KSET-1)301,319,319	0689
301	IF(KPMTM(KSET))302,302,303	0690
302	KSET = KSET + 1	0691
	GO TO 300	0692
303	IF(KPMTM(KSET))-4)304,302,302	0693
C	VARIABLE (J24) INDICATES A LOAD CYCLE (1), A TIME CYCLE (2),	0694
C	OR WRITE MEMORY ON A SAVE TAPE (3)	0695
304	J24 = KPMTM(KSET)	0696
	KSET = KSET	0697
	KERRSW = KERRSW	0698
	IF(PMTM(KSET,2))342,342,341	0699
341	GO TO (305,315,423),J24	0700
342	GO TO (345,355,423),J24	0701
305	IF(PMTM(KSET,1)-(PM+PMTM(KSET,2)))306,307,308	0702
345	IF(PMTM(KSET,1)-(PM+PMTM(KSET,2)))308,307,306	0703
307	IF(NINCLD)309,309,308	0704
309	KLUB = 0	0705
308	DELP = PMTM(KSET,2)	0706
	GO TO 154	0707
306	IF(NINCPM-2)316,316,154	0708
316	KLUB = 0	0709
	GO TO 302	0710
315	IF(PMTM(KSET,1)-(TIME+PMTM(KSET,2)))306,317,318	0711
355	IF(PMTM(KSET,1)-(TIME+PMTM(KSET,2)))318,317,306	0712
317	IF(NINCLD)314,314,318	0713
314	KLUB = 0	0714
318	DELTIM = PMTM(KSET,2)	0715
	GO TO 330	0716
319	IF(KLU2)205,205,320	0717
320	KLUB = 0	0718
	KSET = KSET - 1	0719
	IF(KSET)205,205,321	0720
321	IF(KPMTM(KSET))320,320,322	0721
322	J24 = KPMTM(KSET)	0722
	GO TO (308,318),J24	0723
329	CONTINUE	0724
328	CONTINUE	0725
327	CONTINUE	0726
	IF(NINCLD)501,501,510	0727
510	IF(K-1)501,501,511	0728
511	NINCPM = NINCPM - 1	0729
	IF(NINCPM-3)513,515,515	0730
513	CONTINUE	0731

	GO TO (501,512),NINCPM	0732
C	NINCSW = 1 MEANS THIS IS A RE-CYCLE STEP (NO LOAD OR TIME INCREASE)	0733
C	NINCSW = 2 MEANS THIS IS LAST RE-CYCLE AT THIS LOAD OR TIME LEVEL	0734
C	NINCSW = 3 MEANS THIS IS A LOAD OR TIME INCREMENT STEP	0735
512	NINCSW = 2	0736
	GO TO 514	0737
515	NINCSW = 1	0738
	GO TO 514	0739
501	GO TO (502,503),J24	0740
502	PM = PM + DELPM	0741
	GO TO 504	0742
503	TIME = TIME + DELTIM	0743
504	NINCPM = NINCLD + 2	0744
	NINCSW = 3	0745
514	CONTINUE	0746
	IF(NINCLD)524,524,525	0747
525	NINKCY = NINCLD + 3 - NINCPM	0748
	GO TO (523,524,524),NINCSW	0749
523	NINKLU = NINKCY - (NINKCY/10)*10	0750
	IF(NINKLU)328,524,328	0751
C	NINKCY IS COUNT OF TOTAL CYCLES AT THIS LOAD OR TIME LEVEL	0752
C	NINKLU = 0 WILL PRINT EACH TENTH CYCLE, IF THIS LOAD OR	0753
C	TIME LEVEL IS TO BE PRINTED	0754
524	GO TO (324,325),J24	0755
324	CALL OUTPUT(PM,PMTM(KSET,3),KLU1)	0756
	GO TO 326	0757
325	CALL OUTPUT(TIME,PMTM(KSET,3),KLU1)	0758
326	IF(KLU2)327,328,327	0759
327	KLU2 = KLU1	0760
328	CONTINUE	0761
	IF(TIME)333,333,332	0762
332	GO TO(333,337),J24	0763
C	COMPUTE REFERENCE CREEP TIME FOR ALL NODES	0764
337	DO 331 I3 = 1,NC	0765
	EPCNP(I3) = EPCNK(I3)	0766
	FACNUM = ABSF(EPCNP(I3))	0767
	EXPON = BETA*ABSF(SGBARN(I3))	0768
	FACDN1 = ( 2.71828183**EXPON)-1.	0769
	TIMK1(I3) = (FACNUM/(ALPHA*FACDN1))**(1./GAMMA)	0770
	GO TO (336,336,334),NINCSW	0771
336	CONTINUE	0772
	EPCNK(I3) = (ALPHA*(TIMK1(I3))**GAMMA)*FACDN1	0773
	GO TO 331	0774
334	CONTINUE	0775
	EPCNK(I3) = (ALPHA*(TIMK1(I3)+DELTIM)**GAMMA)*FACDN1	0776
331	CONTINUE	0777
333	CONTINUE	0778
B 156	FA = 214747433125	0779
	KLU9 = 1	0780
	IF(KLU2)250,250,251	0781
250	CONTINUE	0782
C	LABEL = APPLIED LOAD	0783
B	FB = 246043462124	0784
B	FC = 606060606060	0785
	KLUSIZ = 2	0786
	WRITE TAPE 8,KLU9,KLUSIZ,FA,FB,FC,PM,TIME	0787

251	CONTINUE	0788
	KLU9 = 2	0789
	IF(KLU2+KLU8)252,252,253	0790
252	CONTINUE	0791
C	LABEL = REF. CREEP TIME	0792
B	FA = 512526336023	0793
B	FB = 512525476063	0794
B	FC = 314425606060	0795
	WRITE TAPE 8,KLU9, NC,FA,FB,FC,(TIMK1(J1),J1=1,NC)	0796
B	FA = 252626336023	0798
B	FB = 512525476062	0799
B	FC = 635121314560	0800
	WRITE TAPE 8,KLU9, NC,FA,FB,FC,(EPCNK(J1),J1=1,NC)	0801
253	CONTINUE	0802
C	SAVE PRECEDING CYCLE VALUES OF EPBARN	0803
	DO 152 I1 = 1,55	0804
152	EPBARN(I1) = EPBARN(I1)	0805
C	CALCULATE NODE STRESSES - MATRIX SIGUK - FRAME SIZE 165 X 1	0806
	DO 861 I5 = 1,NA	0807
	SIGUK(I5) = SIM(I5)*PM	0808
	DO 861 I6 = 1,NA	0809
	SIGUK(I5) = SIGUK(I5) + SIJ(I5,I6)*EPSUK(I6)	0810
861	CONTINUE	0811
	IF(KLU2)254,254,255	0812
254	CONTINUE	0813
C	LABEL = NODE STRESSES	0814
B	FA = 454624256062	0815
B	FB = 635125626225	0816
B	FC = 626060606060	0817
	WRITE TAPE 8,KLU9, NA,FA,FB,FC,(SIGUK(J1),J1=1,NA)	0818
255	CONTINUE	0819
C	CALCULATE MAGNITUDE AND SIGN OF EFFECTIVE STRESS AT EACH NODE	0820
C	CALCULATE EFFECTIVE STRESSES - MATRIX SGBARN - FRAME SIZE 55 X 1	0821
	DO 166 I7 = 1,NC	0822
	SGBARN(I7) = SGBARN(I7)	0823
	M3 = 3*I7	0824
	M32 = M3-2	0825
	M31 = M3-1	0826
	SGBARN(I7)=SQRTF(AL1231(I7)*SIGUK(M32)**2-AL1212(I7)*SIGUK(M32)*	0827
	1SIGUK(M31)+AL1223(I7)*SIGUK(M31)**2+3.*ALFA44(I7)*SIGUK(M3)**2)	0828
166	CONTINUE	0829
	IF(KLU2)256,256,257	0830
256	CONTINUE	0831
C	LABEL = EFF. STRESSES	0832
B	FA = 252626336062	0833
B	FB = 635125626225	0834
B	FC = 626060606060	0835
	WRITE TAPE 8,KLU9, NC,FA,FB,FC,(SGBARN(J1),J1=1,NC)	0836
257	CONTINUE	0837
C	CALCULATE EFFECTIVE INELASTIC STRAIN FOR EACH NODE - INTERPOLATE	0838
C	IN TABLE (TSIGN VS. TEPSTN)	0839
	DO 181 I8 = 1,NC	0840
C	SGBARN IS EFFECTIVE STRESS OF PREVIOUS CYCLE	0841
	IF(SGBARN(I8)-SGBARN(I8))411,401,401	0842
C	EFFECTIVE STRESS IS ABOVE PREVIOUS LEVEL	0843
C	SGBARN IS EFFECTIVE STRESS OF LAST CYCLE TO SHOW AN INCREASE	0844

401	IF(SGBARN(18)-SGBARM(18))411,402,402	0845
C	EFFECTIVE STRESS IS ABOVE KNEE OF PREVIOUS DROP-OFF, IF ANY	0846
402	IF(SGBARP(18)-SGBARM(18))403,403,403	0847
403	SGBARM(18) = SGBARN(18)	0848
	DU 171 19 = 1,11	0849
	ESUPRK =(SGBARN(18)/E) + EPBARP(18)	0850
	IF(ESUPRK-TEPSN(19))173,172,171	0851
171	CONTINUE	0852
	GO TO 998	0853
172	BARSGN = TSIGN(19)	0854
	IF(SGBARN(18)-TSIGN(2))176,177,177	0855
177	AL1212(18)= 2.*TALF12(19)	0856
	AL1223(18)= TALF12(19)+ TALF23(19)	0857
	AL1231(18)= TALF12(19)+ TALF31(19)	0858
	ALFA44(18)= TALF44(19)	0859
178	CONTINUE	0860
	GO TO 174	0861
173	KKK2 = 19	0862
	KKK1 = 19 - 1	0863
	STNRAT = (ESUPRK-TEPSN(KKK1))/(TEPSN(KKK2)-TEPSN(KKK1))	0864
	BARSGN = TSIGN(KKK1)+(TSIGN(KKK2)-TSIGN(KKK1))*STNRAT	0865
	IF(SGBARN(18)-TSIGN(2))176,175,175	0866
175	CONTINUE	0867
	ALFA12 = TALF12(KKK1)+(TALF12(KKK2)-TALF12(KKK1))*STNRAT	0868
	ALFA23 = TALF23(KKK1)+(TALF23(KKK2)-TALF23(KKK1))*STNRAT	0869
	ALFA31 = TALF31(KKK1)+(TALF31(KKK2)-TALF31(KKK1))*STNRAT	0870
	ALFA44(18)=TALF44(KKK1)+(TALF44(KKK2)-TALF44(KKK1))*STNRAT	0871
	AL1212(18)= 2.*ALFA12	0872
	AL1223(18)= ALFA12 + ALFA23	0873
	AL1231(18)= ALFA12 + ALFA31	0874
176	CONTINUE	0875
	GO TO 174	0876
174	EPBARN(18) = ESUPRK - BARSGN / E	0877
C	CALCULATE TOTAL EFFECTIVE STRAIN - MATRIX TEFSTN - FRAME SIZE 55X1	0878
	TEFSTN(18) = ESUPRK	0879
415	TEFSTN(18) = TEFSTN(18) + EPCNK(18)	0880
C	CALCULATE EFFECTIVE STRAIN CHANGES - MATRIX DELEPN - FRAME 55 X 1	0881
C	CALCULATE INCREMENTAL EFFECTIVE INELASTIC STRAIN	0882
	DELEPN(18) = EPBARN(18) - EPBARP(18)	0883
	GO TO (420,425),J24	0884
425	DELEPN(18) = DELEPN(18) + EPCNK(18) - EPCNP(18)	0885
420	CONTINUE	0886
	GO TO 181	0887
C	DROP-OFF OF EFFECTIVE STRESS	0888
C	OR STILL BELOW THE KNEE OF PREVIOUS DROP-OFF	0889
411	EPBARN(18) = EPBARP(18)	0890
	TEFSTN(18) = EPBARP(18)+(SGBARN(18)/E)	0891
	TEFSTN(18) = TEFSTN(18) + EPCNK(18)	0892
	DELEPN(18) = 0.0	0893
	GO TO (424,426),J24	0894
426	DELEPN(18) = EPCNK(18) - EPCNP(18)	0895
424	CONTINUE	0896
	GO TO 181	0897
181	CONTINUE	0898
	IF(KLU2+KLU8)266,266,267	0899
266	CONTINUE	0900

C	LABEL = EFF. PLASTIC STRAIN	0901
B	FA = 252626334743	0902
B	FB = 216263312360	0903
B	FC = 626351213145	0904
	WRITE TAPE 8, KLU9, NC, FA, FB, FC, (EPBARN(J1), J1=1, NC)	0905
267	CONTINUE	0906
	IF (KLU2) 258, 258, 259	0907
258	CONTINUE	0908
C	LABEL = TOTAL EFF. STRAIN	0909
B	FA = 634663214360	0910
B	FB = 252626336062	0911
B	FC = 635121314560	0912
	WRITE TAPE 8, KLU9, NC, FA, FB, FC, (TEFSTN(J1), J1=1, NC)	0913
259	CONTINUE	0914
	DO 862 I25=1, NC	0915
862	TEFSTN(I25) = 0.0	0916
C	CALCULATE NODE STRAIN CHANGE - MATRIX DELEPK - FRAME SIZE 165 X 1	0917
	DO 191 I11 = 1, NC	0918
	TEMPA = DELEPN(I11) / SGBARN(I11)	0919
	M3 = 3 * I11	0920
	M32 = M3 - 2	0921
	M31 = M3 - 1	0922
	DELEPK(M32) = TEMPA * (AL1231(I11) * SIGUK(M32) - .5 * AL1212(I11) * SIGUK(M31	0923
	1))	0924
	DELEPK(M31) = TEMPA * (AL1223(I11) * SIGUK(M31) - .5 * AL1212(I11) * SIGUK(M32	0925
	1))	0926
	DELEPK(M3) = TEMPA * (3. * AL1444(I11) * SIGUK(M3))	0927
191	CONTINUE	0928
C	CALCULATE NODE PLASTIC STRAIN - MATRIX EPSUK - FRAME SIZE 165 X 1	0929
C	CALCULATE NODE POINT STRAINS	0930
	DO 192 I23=1, NA	0931
192	EPSUK(I23) = EPSUK(I23) + DELEPK(I23)	0932
	IF (KLU2 + KLU8) 260, 260, 261	0933
260	CONTINUE	0934
C	LABEL = EFF. STRAIN CHANGES	0935
B	FA = 252626336263	0936
B	FB = 512131456023	0937
B	FC = 302145272562	0938
	WRITE TAPE 8, KLU9, NC, FA, FB, FC, (DELEPN(J1), J1=1, NC)	0939
C	LABEL = NUDE STRAIN CHANGE	0940
B	FA = 454624256062	0941
B	FB = 635121314560	0942
B	FC = 233021452725	0943
	WRITE TAPE 8, KLU9, NA, FA, FB, FC, (DELEPK(J1), J1=1, NA)	0944
C	LABEL = NUDE INELAS. STRAIN	0945
B	FA = 454624256031	0946
B	FB = 452543216233	0947
B	FC = 626351213145	0948
	WRITE TAPE 8, KLU9, NA, FA, FB, FC, (EPSUK(J1), J1=1, NA)	0949
261	CONTINUE	0950
C	CALCULATE TOTAL NODE STRAINS - MATRIX TOTEPS - FRAME SIZE 165 X 1	0951
	DO 201 I14=1, NC	0952
	M32 = 3 * I14 - 2	0953
	M31 = 3 * I14 - 1	0954
	M3 = 3 * I14	0955
	TOTEPS(M32) = EPSUK(M32) + SIGUK(M32) / E - GNU * SIGUK(M31) / E	0956



	TOTEPS(M31)=EPSUK (M31)+SIGUK(M31)/E -GNU*SIGUK(M32)/E	0957
201	TOTEPS(M3 )=EPSUK (M3 )+SIGUK(M3 )/SHRMOD	0958
	IF(KLU2)262,262,263	0959
262	CONTINUE	0960
C	LABEL = TOT. NODE STRAINS	0961
B	FA = 634663336045	0962
B	FB = 462425606263	0963
B	FC = 512131456260	0964
	WRITE TAPE 8,KLU9, NA,FA,FB,FC,(TOTEPS(J1),J1=1,NA)	0965
263	CONTINUE	0966
	IF(KLU2)268,268,269	0967
268	CONTINUE	0968
	KLU9 = 3	0969
	KLUSIZ = 2	0970
	WRITE TAPE 8,KLU9,KLUSIZ, K,PM,PM,PM,TIME	0971
	IF(NINCLD)269,269,273	0972
273	CONTINUE	0973
	KLU9 = 4	0974
	KLUSIZ = 2	0975
	WRITE TAPE 8,KLU9,KLUSIZ,PM,PM,PM,NINCKY,NINTOT	0976
269	CONTINUE	0977
	IF(NINCLD)370,370,371	0978
371	IF(NINCSW-2)422,370,422	0979
370	CONTINUE	0980
	IF(SENSE SWITCH 6)421,422	0981
422	CONTINUE	0982
	GO TO 151	0983
421	IF(KLU2)423,423,208	0984
423	CONTINUE	0985
205	KLU9 = 7	0986
B	FA = 777777777777	0987
	DO 206 125 = 1,10	0988
206	WRITE TAPE 8,KLU9,KLU9,FA,FA,FA,FA,FA,FA,FA,FA,FA,FA	0989
	END FILE 8	0990
	END FILE 8	0991
	END FILE 8	0992
	END FILE 8	0993
	END FILE 8	0994
	END FILE 8	0995
	REWIND 8	0996
	IF(SENSE SWITCH 6)207,209	0997
209	IF(J24-3)210,207,210	0998
207	CONTINUE	0999
	PAUSE 1	1000
	REWIND 11	1001
	CALL CHAIN(5,3)	1002
210	CONTINUE	1003
	CALL CHAIN(6,3)	1004
208	KERRSW = 2	1005
C	KERRSW SET TO 2 TO MAKE KLU2 = 0 AND PRINT A CYCLE	1006
	GO TO 151	1007
998	KLU9 = 6	1008
	KLUSIZ = 3	1009
	WRITE TAPE 8,KLU9,KLUSIZ, K,18,PM,ESUPRK,SGBARN(18),TIME	1010
	GO TO 205	1011
	END(1,1,0,0,0,0,1,1,0,1,0,0,0,0,0)	
*	LIST8	1013

	SUBROUTINE OUTPUT(VALUE1,STEP1,KLUI)	1014
C	THIS SUBROUTINE SETS KLUI = 0 IF THE CURRENT CYCLE IS TO BE PRINTED	1015
	VALUE = ABSF(VALUE1)	1016
	STEP = ABSF(STEP1)	1017
102	IF(VALUE-STEP)131,100,100	1018
100	NTEST1 = (VALUE/STEP)*1.00001	1019
	NTEST2 = (VALUE/STEP)+.998	1020
	IF(NTEST1-NTEST2)131,130,131	1021
130	KLUI = 0	1022
	GO TO 135	1023
131	KLUI = 1	1024
135	RETURN	1025
	END(1,1,0,0,0,0,1,1,0,1,0,0,0,0,0)	
* *	CHAIN(5,3)	1027
	LISTB	1028

C	451285 MATRIX ANALYSIS OF INELASTIC PLATE - LINK 5 - WITH CREEP	1030
	THIS LINK WRITES A SAVE TAPE FOR RESTART	1031
	COMMON TEFSTN, TOTEPS	1032
	COMMON KLU4, KLU5, KLU6, KLU8, NA, NC, K	1033
	COMMON KERRSW, NINCLD, KSET, PM, E, GNU, SHRMOO	1034
	COMMON ALPHA, BETA, GAMMA, TIME, KLUI50	1035
	COMMON PMTH, KPMTM, SIM, SIJ, TSIGN, TEP5N	1036
	COMMON TALF12, TALF23, TALF31, TALF44	1037
	COMMON AL1212, AL1223, AL1231, ALFA44	1038
	DIMENSION TALF12(11), TALF23(11), TALF31(11), TALF44(11)	1039
	DIMENSION AL1212(55), AL1223(55), AL1231(55), ALFA44(55)	1040
	COMMON SIGUK, EPSUK	1041
	COMMON SGBARN, SGBARP, SGBARM, EPBARN, EPBARP, DELEPN	1042
	COMMON EPCNK, EPCNP	1043
	EQUIVALENCE (TIMK1, TEFSTN), (TOTEPS, DELEPK)	1044
C	THESE FOUR ARRAYS ARE EQUIVALENCED TO SAVE CORE SPACE.	1045
	DIMENSION TIMK1(55), TEFSTN(55), TOTEPS(165), DELEPK(165)	1046
	DIMENSION PMTH(10,3), KPMTM(10), SIM(165), SIJ(165,165), TSIGN(11)	1047
	DIMENSION TEP5N(11), SIGUK(165), EPSUK(165), SGBARN(55), SGBARP(55)	1048
	DIMENSION SGBARM(55), EPBARN(55), EPBARP(55), DELEPN(55), EPCNK(55)	1049
	DIMENSION EPCNP(55)	1050
	REWIND 11	1051
	WRITE OUTPUT TAPE 11,33	1052
	END FILE 11	1053
	WRITE TAPE 11, KLU4, KLU5, KLU6, KLU8, NA, NC, K, KERRSW, NINCLD, KSET, PM, E,	1054
	IGNU, SHRMOO, ALPHA, BETA, GAMMA, TIME, KLUI50	1055
	WRITE TAPE 11, PMTH	1056
	WRITE TAPE 11, KPMTM	1057
	WRITE TAPE 11, SIM	1058
	WRITE TAPE 11, SIJ	1059
	WRITE TAPE 11, TSIGN	1060
	WRITE TAPE 11, TEP5N	1061
	WRITE TAPE 11, TALF12	1062
	WRITE TAPE 11, TALF23	1063
	WRITE TAPE 11, TALF31	1064
	WRITE TAPE 11, TALF44	1065
	WRITE TAPE 11, AL1212	1066
	WRITE TAPE 11, AL1223	1067
	WRITE TAPE 11, AL1231	1068
	WRITE TAPE 11, ALFA44	1069
	WRITE TAPE 11, SIGUK	1070
	WRITE TAPE 11, EPSUK	1071
	WRITE TAPE 11, SGBARN	1072
	WRITE TAPE 11, SGBARP	1073
	WRITE TAPE 11, SGBARM	1074
	WRITE TAPE 11, EPBARN	1075
	WRITE TAPE 11, EPBARP	1076
	WRITE TAPE 11, DELEPN	1077
	WRITE TAPE 11, EPCNK	1078
	WRITE TAPE 11, EPCNP	1079
	END FILE 11	1080
	END FILE 11	1081
	END FILE 11	1082
C	SUBROUTINE RUN REWINDS AND UNLOADS THE DESIGNATED TAPE	1083
	CALL RUN (11)	1084
	PRINT 32	1085
	KERRSW = 5	1086
	CALL CHAIN(6,3)	1087
	32 FORMAT(17/52H * * * SAVE TAPE A-6 FOR RESTART AT THIS POINT * * *)	1088
	33 FORMAT(167HCONTIN 99 SAVE THIS TAPE FOR RERUN DECK 45128 INELAST	1089
	11C ANALYSIS )	1090
	END(1,1,0,0,0,0,0,1,1,0,1,0,0,0,0,0)	
	* CHAIN(6,3)	1092
	* LIST8	1093

```

C451286 MATRIX ANALYSIS OF INELASTIC PLATE - LINK 6 - WITH CREEP      1095
C THIS LINK CONVERTS BINARY OUTPUT ON TAPE 8 TO MCD                     1096
C ON THE MONITOR PRINT TAPE                                           1097
COMMON TEFSTN, TOTEPS                                                1098
COMMON KLU4, KLU5, KLU6, KLU8, NA, NC, K                             1099
COMMON KEKRSW, NINCLO, KSEI, PH, E, GNU, SHRMUJ                      1100
COMMON ALPHA, BETA, GAMMA, TIME, KLUISO                              1101
DIMENSION TEFSTN(55),TOTEPS(105)                                    1102
DIMENSION ARRAY(165),LIST(105)                                       1103
EQUIVALENCE (FA,IFA),(FB,IFB),(FC,IFC),(ARRAY,LIST)                1104
REWIND 8                                                              1105
101 READ TAPE 8,KLU9,KLUSIZ,FA,FB,FC,(ARRAY(J1),J1=1,KLUSIZ)        1106
IF(KLU9)101,101,106                                                  1107
106 IF(KLU9-9)111,111,101                                             1108
111 GO TO(121,122,123,124,125,126,127,128,129),KLU9               1109
121 CONTINUE                                                         1110
WRITE OUTPUT TAPE 6,22,FA,FB,FC,ARRAY(1),ARRAY(2)                  1111
GO TO 101                                                             1112
122 CONTINUE                                                         1113
WRITE OUTPUT TAPE 6,21,FA,FB,FC,(ARRAY(J1),J1=1,KLUSIZ)            1114
GO TO 101                                                             1115
123 CONTINUE                                                         1116
WRITE OUTPUT TAPE 6,31,IFA,ARRAY(1),ARRAY(2)                        1117
GO TO 101                                                             1118
124 CONTINUE                                                         1119
WRITE OUTPUT TAPE 6,32,LIST(1),LIST(2)                               1120
GO TO 101                                                             1121
126 CONTINUE                                                         1122
WRITE OUTPUT TAPE 6,12,ARRAY(1),ARRAY(2)                             1123
WRITE OUTPUT TAPE 6,13,IFA,IFB,FC,ARRAY(3)                          1124
GO TO 101                                                             1125
127 CONTINUE                                                         1126
PRINT 14                                                              1127
WRITE OUTPUT TAPE 6,14                                               1128
REWIND 8                                                              1129
IF(KEKRSW-5)132,131,132                                             1130
131 PRINT 33                                                         1131
132 CALL EXIT                                                         1132
125 CONTINUE                                                         1133
128 CONTINUE                                                         1134
129 CONTINUE                                                         1135
GO TO 101                                                             1136
12 FORMAT(46H VALUE NOT FOUND IN TABLE FOR EPSILON BAR N = ,F15.8, 1137
119H ( SIGMA BAR N = ,E15.8,2H ) )                                     1138
13 FORMAT(16H CYCLE NUMBER = ,I5,20H ELEMENT INDEX = ,I4,17H LO     1139
1AD LEVEL = ,F9.2,11H TIME = ,F8.4)                                  1140
14 FORMAT(76H DO NOT SAVE TAPE B-1 - IT HAS BEEN COMPLETELY PROCESSED 1141
1 ONTO THE PRINT TAPE)                                              1142
21 FORMAT(// 1X,3A6,5(1PE16.7)/(19X,5E16.7))                        1143
22 FORMAT(//1X,3A6,2X,F12.2,5X,6HTIME = ,F12.6)                     1144
31 FORMAT(2H0 ,16,27H CYCLES COMPLETED - LOAD = ,F 9.2,           1145
1 12H TIME = ,F 8.4)                                                 1146
32 FORMAT(1H+,68X,6HCYCLE ,I3,4H OF ,I3,27H AT THIS LOAD OR TIME LEVE 1147
1L)                                                                    1148
33 FORMAT(//52H * * * SAVE TAPE A-o FOR RESTART AT THIS POINT * * *) 1149

END(1,1,0,0,0,0,1,1,0,1,0,0,0,0)

```

\* DATA

1151

## APPENDIX VI

### STRESS DISTRIBUTIONS DUE TO UNIT INITIAL STRAINS

The basic matrix utilized in the nonlinear and inelastic analysis described in this report is the initial strain influence coefficient matrix  $[\Gamma_{uv}]$ . Elements of this matrix provide the  $u^{\text{th}}$  stress component caused by a unit initial strain at the  $v^{\text{th}}$  stress location. The first description and derivation of this useful matrix was made by Denke in 1954, Reference 20. The matrix is generated by a structural analysis which may be of the force or stiffness type.

#### A. Force Method Application

The method utilized here is a simple extension of redundant structure analysis. Essentially, the additional work involved is the calculation of displacements at the applied loads and redundants in the statically determinant structure caused by initial strains. These displacements are combined with those caused by the applied loads and redundants. The final step is to adjust the magnitude of the redundants to eliminate the total displacements at the redundants. From this point the determination of stress distributions for the redundant structure is carried out as before.

The displacement in the statically determinate structure at the  $t^{\text{th}}$  applied load or redundant due to initial strain can be expressed by use of the principle of virtual work as follows:

$$\alpha_{tv} = \sum_a \int (\sigma_{xt} \cdot \epsilon_{xv}) dV \quad (\text{A-1})$$

Volume of  
 $a^{\text{th}}$  member

In the above expression,  $\alpha_{tv}$  is the displacement at the  $t^{\text{th}}$  unit applied load or redundant due to the  $v^{\text{th}}$  initial strain,  $\sigma_{xt}$  is the direct stress in the  $a^{\text{th}}$  member due to the unit load, and  $\epsilon_{xv}$  is the initial strain in the  $a^{\text{th}}$  member at the corresponding stress point. The summation  $\sum_a$  indicates that the virtual work in all members affected by the induced strain,  $\epsilon_{xv}$ , must be considered.

Equation A-1 is written for the uniaxial direct stress condition that is commonly assumed to exist in bar members as pictured in Figure (1). The effect of a shear panel has been omitted in the derivation for simplicity. Terms necessary for inclusion of shear may be derived in a similar manner.

Suppose that the  $a^{\text{th}}$  member of a structure is a bar, with cross sectional area  $A$ , linearly varying axial load  $\sigma_{xt} \cdot A$ , and linearly varying initial strain  $\epsilon_{xv}$ .

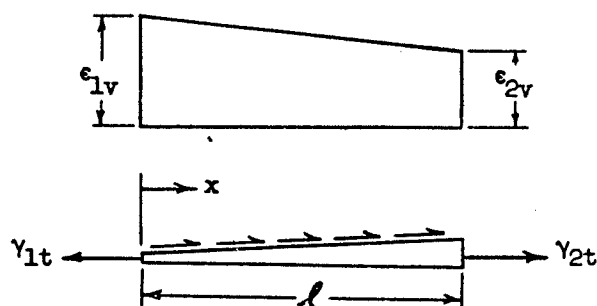


Figure 1

Then

$$\sigma_{xt} = \frac{1}{A} \left\{ \gamma_{1t} \left(1 - \frac{x}{l}\right) + \gamma_{2t} \frac{x}{l} \right\}$$

$$\epsilon_{xv} = \epsilon_{1v} \left(1 - \frac{x}{l}\right) + \epsilon_{2v} \frac{x}{l}$$

and after evaluation

$$\int_{\text{Volume of } a^{\text{th}} \text{ member}} \sigma_{xt} \cdot \epsilon_{xv} dV = [\gamma_{1t} \quad \gamma_{2t}] \begin{bmatrix} L_{a11} & L_{a12} \\ L_{a21} & L_{a22} \end{bmatrix} \begin{Bmatrix} \epsilon_{1v} \\ \epsilon_{2v} \end{Bmatrix}$$

where

$$\begin{aligned} L_{a11} &= L_{a22} = \frac{l}{3} \\ L_{a12} &= L_{a21} = \frac{l}{6} \end{aligned}$$

The  $L_{a1j}$  matrix can be similarly determined for other types of structural elements. For rectangular shear panels, of dimensions  $b$  and  $h$ , it can be shown that the  $L_{a1j}$  factor for shear strain  $\gamma_{xy}$ , is  $bh$ , the panel flat plate area. For nonorthogonal structure (swept panels) other  $L_{a1j}$  factors may be developed. The sum of such matrices for the entire structure is designated  $[L_{1j}]$ .

The matrix expression for the displacements at all of the applied loads and redundants due to unit initial strain is

$$\begin{bmatrix} \alpha_{mv} \\ \alpha_{rv} \end{bmatrix} = \begin{bmatrix} \gamma_{im} & \gamma_{ir} \end{bmatrix}^T \begin{bmatrix} L_{iv} \end{bmatrix} \quad A-2$$

The  $\epsilon_v$ 's are the initial strains corresponding to each of the member loads  $q_v$ .

Utilizing Equation A-2, the redundants are evaluated by

$$\begin{bmatrix} \alpha_{rm} & \alpha_{rv} & \alpha_{rs} \end{bmatrix} \begin{Bmatrix} P_m \\ \epsilon_v \\ q_s \end{Bmatrix} = 0$$

the solution of which is

$$\{q_s\} = \begin{bmatrix} \Gamma_{sm} & \Gamma_{sv} \end{bmatrix} \begin{Bmatrix} P_m \\ \epsilon_v \end{Bmatrix}$$

where

$$\begin{bmatrix} \Gamma_{sm} & \Gamma_{sv} \end{bmatrix} = - \begin{bmatrix} \alpha_{rs} \end{bmatrix}^{-1} \begin{bmatrix} \alpha_{rm} & \alpha_{rv} \end{bmatrix}$$

The member loads in the redundant structure become

$$\{q_i\} = \begin{bmatrix} \Gamma_{im} & \Gamma_{iv} \end{bmatrix} \begin{Bmatrix} P_m \\ \epsilon_v \end{Bmatrix} \quad A-3$$

where

$$\begin{bmatrix} \Gamma_{im} & \Gamma_{iv} \end{bmatrix} = \begin{bmatrix} \gamma_{im} & \gamma_{ir} \end{bmatrix} \begin{bmatrix} \frac{I}{\Gamma_{rm}} & \frac{0}{\Gamma_{rv}} \end{bmatrix}$$

Member stresses are obtained by pre-multiplying member loads by  $[\beta_{ui}]$ , the reciprocal values of appropriate bar areas and skin gages.

$$\begin{bmatrix} \Gamma_{um} & \Gamma_{uv} \end{bmatrix} = [\beta_{ui}] \begin{bmatrix} \Gamma_{im} & \Gamma_{iv} \end{bmatrix}$$

then

$$\{\sigma_u\} = \begin{bmatrix} \Gamma_{um} & \Gamma_{uv} \end{bmatrix} \begin{Bmatrix} P_m \\ \epsilon_v \end{Bmatrix} \quad A-4$$

Digital computer programs which are available for conventional force method analyses may be used to determine the  $\Gamma_{um}$ ,  $\Gamma_{uv}$  matrices. This is readily accomplished by redefining several input matrices.

- (1) replace  $[\gamma_{im}]$ , the usual unit load distribution in the statically determinate structure due to applied loads by

$$\begin{bmatrix} \gamma_{im} & 0 \\ 0 & I \end{bmatrix} \quad (2i) \times (m + 1)$$

the unit diagonal matrix  $I$  has as many elements as there are member loads in the structure.

- (2) replace  $[\gamma_{ir}]$ , the usual unit load distribution in the statically determinate structure due to redundants by

$$\begin{bmatrix} \gamma_{ir} \\ 0 \end{bmatrix} \quad 2i \times r$$

- (3) replace  $[\alpha_{ij}]$ , the member flexibility matrix by

$$\begin{bmatrix} \alpha_{ij} & L_{iy} \\ L_{iv} & 0 \end{bmatrix} \quad 2i \times 2i$$

The  $L_{iv}$  values are the geometrical factors of Equation A-2. Straightforward matrix operation will now yield a load distribution matrix for the redundant structure which may be identified as follows:

$$\begin{bmatrix} \Gamma_{im} & \Gamma_{iv} \\ 0 & I \end{bmatrix}$$

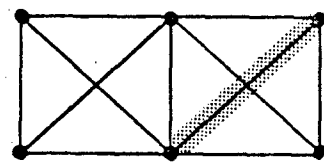
The upper portion  $[\Gamma_{im} \mid \Gamma_{iv}]$  are the values defined by Equation A-3, and stresses may be obtained by using Equation A-4.



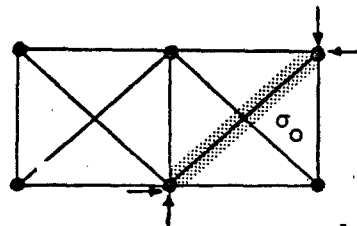
## B. Direct Stiffness Method

Consider a truss shown in Figure (2a) where all the nodes are "locked" (prevented from displacing). If a strain  $\epsilon_0$  is induced in a

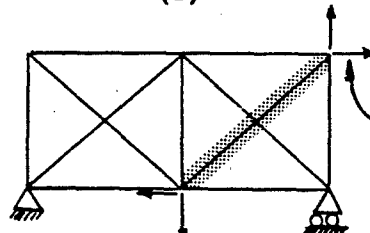
particular member it will produce a stress in only that member equal to  $\sigma_0 = -E\epsilon_0$  since all the nodes are locked. This stress requires node forces as shown in Figure (2b). The negatives of these node forces are applied to the "unlocked" structure and the stresses in all the members, (Figure 2c) are computed. The final stress will be the superposition of the "locked in" stresses and the stresses produced by the node forces acting on the unlocked structure. That is



(a)



(b)



(c)

$\epsilon_0$  produces  $\sigma_0$

$$\sigma_T = \sigma + \sigma_0$$

Applied loads produce  $\sigma$

Figure 2

Derivation of  $[\Gamma_{um}]$  and  $[\Gamma_{uv}]$

Consider an element of the total structure, let this element be supported in a statically determinate fashion. The total strain  $\epsilon$  is then written as the sum of two strains namely  $\epsilon_\sigma$  - the strains due to stresses, and  $\epsilon_0$  - a set of induced strains. Thus

$$\{\epsilon\} = \{\epsilon_\sigma\} + \{\epsilon_0\} \quad \text{B-1}$$

Rewriting this,

$$\{\epsilon_\sigma\} = \{\epsilon\} - \{\epsilon_0\} \quad \text{B-2}$$

The stresses may be expressed in terms of the strains by using Hooke's law,

$$\{\sigma\} = [b]\{\epsilon_o\} \quad B-3$$

Thus

$$\{\sigma\} = [b]\{\epsilon\} - [b]\{\epsilon_o\} \quad B-4$$

$\{\epsilon\}$  (the total strains) may be expressed in terms of the displacements of the nodes that affect the particular member in question. That is

$$\{\epsilon\} = [a]\{\delta\} \quad B-5$$

It should be noted that the expression contains the basic assumption governing the behavior of the element. For example, for a triangle or bar element it will contain the assumption that the strains are constant throughout the element. Substituting this into Equation B-4

$$\{\sigma\} = [b][a]\{\delta\} - [b]\{\epsilon_o\} \quad B-6a$$

$$= [s_d]\{\delta\} - [b]\{\epsilon_o\} \quad B-6b$$

From virtual work it can be shown that the nodal forces  $\{f\}$ , associated with  $\{\delta\}$ , may be expressed in terms of the stresses by:

$$\{f\} = \int_{Vol} [a]^T \{\sigma\} dV \quad B-7$$

Substituting B-6a into B-7 yields:

$$\{f\} = \int_{Vol} [a]^T [b][a]\{\delta\} dV - \int_{Vol} [a]^T [b]\{\epsilon_o\} dV \quad B-8$$

For simple elements such as bars or triangles where the strains are assumed to be constant over the element none of the matrices within the integrals will be functions of the coordinates  $x$ ,  $y$  or  $z$  and hence they are independent of the integration. The first portion of (B-8) yields the standard stiffness matrix  $[k]$  while the second portion yields the nodal forces due to induced strains  $\{\epsilon_o\}$ .

$$\{f\} = [k]\{\delta\} - V[a]^T [b]\{\epsilon_o\} \quad B-9$$

In this expression,  $V$  is the volume of the element. Noting that  $[a]^T[b] = [b][a]^T = [s_d]^T$  yields

$$\{f\} = [k]\{\delta\} - V[s_d]^T\{\epsilon_o\} \quad B-10$$

The total stiffness matrix for the entire structure is obtained by superposing the stiffnesses for the individual elements to yield:

$$\{F\} = [K]\{\Delta\} - [S_d]^T[V]\{\epsilon_{oT}\} \quad B-11$$

Where  $\{F\}$  represents all of the external nodal forces,  $\{\Delta\}$  represents all of the nodal displacements,  $\{\epsilon_{oT}\}$  represents a column of all the induced strain components and  $[V]$  is a diagonal matrix containing the values of the volumes of the various elements. (Note that for a triangle, where three strain components may be induced, the volume will appear three times).  $[S_d]$  is the total stress matrix array which is obtained by proper arrangement of the individual stress matrices  $[s_d]$ .

Applying boundary conditions (via matrix  $[BC]$ ) to equation (B-11) and introducing the applied external loads  $\{P\}$ , with nodal distribution  $[L]$ , yields:

$$[L]\{P\} = [BC]^T[K][BC]\{\Delta'\} - [BC]^T[S_d]^T[V]\{\epsilon_{oT}\} \quad B-12$$

which may be solved to give the allowed nodal displacements under the boundary conditions:

$$\{\Delta'\} = [K_{11}]^{-1}[L]\{P\} + [K_{11}]^{-1}[BC]^T[S_d]^T[V]\{\epsilon_{oT}\} \quad B-13$$

where

$$[K_{11}] = [BC]^T[K][BC]$$

For the total structure, B-6b may be written as:

$$\{\sigma_T\} = [S_d]\{\Delta\} - [B]\{\epsilon_{oT}\} \quad B-14$$

where  $[B]$  is a diagonal block of the elastic relations  $[b]$  for each member. Substituting (B-13) into (B-14) and using the relation  $\{\Delta\} = [BC]\{\Delta'\}$  yields:

$$\begin{aligned} \{\sigma_T\} &= [S_d][BC][K_{11}]^{-1}[L]\{P\} \\ &+ \left[ [S_d][BC][K_{11}]^{-1}[BC]^T[S_d]^T[V] - [B] \right] \{e_{OT}\} \end{aligned} \quad B-15$$

which, to use the previous notation, may be written as:

$$\{\sigma_u\} = [\Gamma_{um}]\{P_m\} + [\Gamma_{uv}]\{e_v\} \quad B-16$$

The first matrix,  $[\Gamma_{um}]$ , of this expression, is the conventional distribution obtained for unit applied loads as indicated in Section A of this appendix.

# REFERENCES

1. Denke, P. H., Digital Analysis of Plasticity in Plates, Appendix C of "Effects of Compressive Loads on Structural Fatigue at Elevated Temperatures," Technical Document Report ASD-TDR-62-448, October 1962.
2. Kobayashi, A. S. and Weikel, R. C., "A Method of Estimating Creep Deformations and Stress Relaxations in Plane Structures" - The Trend in Engineering, October 1961.
3. Gallagher, R. H., Padlog, J., and Bijlaard, P. P., "Stress Analysis of Heated Complex Shapes," ARS Journal, Volume 32, No. 5, pages 700-707, May 1962.
4. Padlog, J., Huff, R. D., and Holloway, F. G., Unelastic Behavior of Structures Subjected to Cyclic Thermal and Mechanical Stressing Conditions, WADD Technical Report 60-271, December 1960.
5. Manson, S. S., "Thermal Stresses in Design," Machine Design, Parts 11, 12, and 13, July 9, July 23, August 6, 1959.
6. Mentel, T. J., Comparison of Matrix Methods for Inelastic Structural Analysis, Grumman Advanced Development Report No. ADR 02-11-64.1, February 1964.
7. Percy, J. H., Loden, W. A., and Navaratna, D., A Study of Matrix Analysis Methods for Inelastic Structures, Air Force Systems Command, Technical Document Report No. RDT-TDR-63-4032, October 1963.
8. Turner, M. J., The Direct Stiffness Method of Structural Analysis, Paper presented at the AGARD Structures and Material Panel Meeting, Aachen, Germany, September 1959.
9. Turner, M. J., Martin, N. C., and Weikel, R. C., "Further Development and Applications of the Stiffness Method," from Text, Matrix Methods of Structural Analysis - edited by F. de Veubeke, Macmillan Company, New York, 1964.
10. Hill, R., The Mathematical Theory of Plasticity, Clarendon Press, Oxford, 1950.
11. Hu, L. W., "Studies on Plastic Flow of Anisotropic Metals," Journal of Applied Mechanics, September 1956.
12. Argyris, J. H., "Energy Theorems and Structural Analysis," Butterworth's Scientific Publications, London, England, 1960.
13. Falby, W. E., and Zalesak, J., Comparison of Matrix Force and Direct Stiffness Methods of Redundant Structure Analysis, Grumman Advanced Development Report No. ADR 02-11-65.1, January 1965.

14. Griffith, G. E., Experimental Investigation of the Effects of Plastic Flow in a Tension Panel with a Circular Hole, NACA TN No. 1705, September 1948.
15. Jones, I. W., Some Refinements to Wing Redundant Structure Analysis Methods, Grumman Advanced Development Report No. ADR 04-03b-61.3.
16. Mendelson, A., and Manson, S. S., Practical Solutions of Plastic Deformation Problems in Elastic-Plastic Range, NACA TN 4088, September 1959.
17. Mentel, T. J., On Evaluation of Matrix Methods for Nonlinear Biaxial Stress Analysis, Grumman Advanced Development Report No. ADR 02-11-64.2, June 1964.
18. Millenson, M. B., and Manson, S. S., Determination of Stresses in Gas Turbine Disks Subjected to Plastic Flow and Creep, NACA Report No. 906, 1948.
19. Lansing, W., Jensen, W. R., and Falby, W. E., Matrix Analysis Methods for Inelastic Structures, Grumman Advanced Development Report No. ADR 02-11-65.4, November 1965. Presented at conference on "Matrix Methods in Structural Mechanics," October 26-28, 1965 at the Air Force Institute of Technology, Wright-Patterson Air Force Base, Dayton, Ohio.
20. Denke, P. H., "A Matrix Method of Structural Analysis," Proceedings of the Second U. S. National Congress of Applied Mechanics, June 1954.

A number of the references were traced by a machine search of NASA and Department of Defense holding under the following headings:

- 1) Anisotropic plasticity of metals
- 2) Anisotropic creep of metals
- 3) Bauschinger effect of metals
- 4) Cyclic loading of metals

UNCLASSIFIED

Security Classification

DOCUMENT CONTROL DATA - R&D		
(Security classification of title, body of abstract and indexing annotation must be entered when the overall report is classified)		
1. ORIGINATING ACTIVITY (Corporate author) Grumman Aircraft Engineering Corporation South Oyster Bay Road Bethpage, Long Island, New York		2a. REPORT SECURITY CLASSIFICATION Unclassified
		2b. GROUP
3. REPORT TITLE (U) MATRIX ANALYSIS METHODS FOR ANISOTROPIC INELASTIC STRUCTURES		
4. DESCRIPTIVE NOTES (Type of report and inclusive dates) Final technical report on work accomplished from January 1965 to October 1965		
5. AUTHOR(S) (Last name, first name, initial) Jensen, W. R.; Falby, W. E.; Prince, N.		
6. REPORT DATE April 1966	7a. TOTAL NO. OF PAGES 124	7b. NO. OF REFS 17
8a. CONTRACT OR GRANT NO. AF 33(615)-2260	9a. ORIGINATOR'S REPORT NUMBER(S) ADR 02-11-65-5	
8b. PROJECT NO. 1467		
8c. Task No. 146701	9b. OTHER REPORT NO(S) (Any other numbers that may be assigned this report) AFFDL-TR-65-220	
10. AVAILABILITY/LIMITATION NOTICES This document is subject to special export controls and each transmittal to foreign governments or foreign nationals may be made only with prior approval of the AF Flight Dynamics Laboratory, FDTR, Wright-Patterson AFB, Ohio 45433.		
11. SUPPLEMENTARY NOTES	12. SPONSORING MILITARY ACTIVITY Air Force Flight Dynamics Laboratory Research and Technology Division Air Force Systems Command Wright-Patterson Air Force Base, Ohio 45433	
13. ABSTRACT Most aerospace structural materials exhibit some degree of anisotropic strain hardening. A measure of anisotropy is introduced into structural elements by such fabrication processes as drawing, cold rolling and extrusion. During the past few years, several methods have appeared in the literature for introducing inelastic isotropic material behavior effects into existing matrix analysis routines. A review is presented of one of these methods. It is essentially a step-by-step calculation procedure, and corresponds to the flow theory of plasticity. The method has been extended to include the effects of anisotropic material and is formulated as a standard initial strain influence coefficient problem. Several analyses of an aluminum alloy (2024-T4) shear lag structure which has been tested previously for the Air Force are carried out first assuming isotropic material properties and then anisotropic properties. The resulting correlation between test results and that predicted by isotropic theory is reasonably good. An analysis of a 1100F aluminum shear lag structure, carried out by the incremental method, gave reasonably good agreement. However, the anisotropic creep capability was not checked for want of test data. The approach is a reasonably good phenomenological model of a complex physical problem. The digital computer program submitted is suited for inclusion of other material nonlinearity.		

DD FORM 1 JAN 64 1473

UNCLASSIFIED  
Security Classification

UNCLASSIFIED

Security Classification

14. KEY WORDS	LINK A		LINK B		LINK C	
	ROLE	WT	ROLE	WT	ROLE	WT
Anisotropic Plasticity of Metals Anisotropic Creep of Metals Matrix Structural Analysis						

**INSTRUCTIONS**

**1. ORIGINATING ACTIVITY:** Enter the name and address of the contractor, subcontractor, grantee, Department of Defense activity or other organization (*corporate author*) issuing the report.

**2a. REPORT SECURITY CLASSIFICATION:** Enter the overall security classification of the report. Indicate whether "Restricted Data" is included. Marking is to be in accordance with appropriate security regulations.

**2b. GROUP:** Automatic downgrading is specified in DoD Directive 5200.10 and Armed Forces Industrial Manual. Enter the group number. Also, when applicable, show that optional markings have been used for Group 3 and Group 4 as authorized.

**3. REPORT TITLE:** Enter the complete report title in all capital letters. Titles in all cases should be unclassified. If a meaningful title cannot be selected without classification, show title classification in all capitals in parenthesis immediately following the title.

**4. DESCRIPTIVE NOTES:** If appropriate, enter the type of report, e.g., interim, progress, summary, annual, or final. Give the inclusive dates when a specific reporting period is covered.

**5. AUTHOR(S):** Enter the name(s) of author(s) as shown on or in the report. Enter last name, first name, middle initial. If military, show rank and branch of service. The name of the principal author is an absolute minimum requirement.

**6. REPORT DATE:** Enter the date of the report as day, month, year; or month, year. If more than one date appears on the report, use date of publication.

**7a. TOTAL NUMBER OF PAGES:** The total page count should follow normal pagination procedures, i.e., enter the number of pages containing information.

**7b. NUMBER OF REFERENCES:** Enter the total number of references cited in the report.

**8a. CONTRACT OR GRANT NUMBER:** If appropriate, enter the applicable number of the contract or grant under which the report was written.

**8b, 8c, & 8d. PROJECT NUMBER:** Enter the appropriate military department identification, such as project number, subproject number, system numbers, task number, etc.

**9a. ORIGINATOR'S REPORT NUMBER(S):** Enter the official report number by which the document will be identified and controlled by the originating activity. This number must be unique to this report.

**9b. OTHER REPORT NUMBER(S):** If the report has been assigned any other report numbers (either by the originator or by the sponsor), also enter this number(s).

**10. AVAILABILITY/LIMITATION NOTICES:** Enter any limitations on further dissemination of the report, other than those imposed by security classification, using standard statements such as:

- (1) "Qualified requesters may obtain copies of this report from DDC."
- (2) "Foreign announcement and dissemination of this report by DDC is not authorized."
- (3) "U. S. Government agencies may obtain copies of this report directly from DDC. Other qualified DDC users shall request through \_\_\_\_\_."
- (4) "U. S. military agencies may obtain copies of this report directly from DDC. Other qualified users shall request through \_\_\_\_\_."
- (5) "All distribution of this report is controlled. Qualified DDC users shall request through \_\_\_\_\_."

If the report has been furnished to the Office of Technical Services, Department of Commerce, for sale to the public, indicate this fact and enter the price, if known.

**11. SUPPLEMENTARY NOTES:** Use for additional explanatory notes.

**12. SPONSORING MILITARY ACTIVITY:** Enter the name of the departmental project office or laboratory sponsoring (paying for) the research and development. Include address.

**13. ABSTRACT:** Enter an abstract giving a brief and factual summary of the document indicative of the report, even though it may also appear elsewhere in the body of the technical report. If additional space is required, a continuation sheet shall be attached.

It is highly desirable that the abstract of classified reports be unclassified. Each paragraph of the abstract shall end with an indication of the military security classification of the information in the paragraph, represented as (TS), (S), (C), or (U).

There is no limitation on the length of the abstract. However, the suggested length is from 150 to 225 words.

**14. KEY WORDS:** Key words are technically meaningful terms or short phrases that characterize a report and may be used as index entries for cataloging the report. Key words must be selected so that no security classification is required. Identifiers, such as equipment model designation, trade name, military project code name, geographic location, may be used as key words but will be followed by an indication of technical context. The assignment of links, rules, and weights is optional.

DD FORM 581

UNCLASSIFIED

Security Classification



END

DATE  
FILMED

11 — 66